



**Poznan University of Medical Sciences
Poland**

JMS *Journal of Medical Science*

previously *Nowiny Lekarskie*

Founded in 1889

2019
Vol. 88, No. 2

QUARTERLY

Indexed in:
Polish Medical Bibliography, Index Copernicus,
Ministry of Science and Higher Education, Ebsco, Google Scholar

eISSN 2353-9801
ISSN 2353-9798

www.jms.ump.edu.pl

EDITOR-IN-CHIEF

Jarosław Walkowiak

EDITORIAL BOARD

David H. Adamkin (USA)
Adrian Baranchuk (Canada)
Grzegorz Bręborowicz (Poland)
Paolo Castiglioni (Italy)
Wolfgang Dick (Germany)
Leon Drobnik (Poland)
Janusz Gadzinowski (Poland)
Michael Gekle (Germany)
Przemysław Guzik (Poland)
Karl-Heinz Herzig (Germany)
Mihai Ionac (Romania)
Lucian Petru Jiga (Germany)
Berthold Koletzko (USA)
Stan Kutcher (Canada)
Oded Langer (USA)
Tadeusz Maliński (USA)
Leszek Paradowski (Poland)
Antoni Pruszewicz (Poland)
Georg Schmidt (Germany)
Mitsuko Seki (Japan)
Ewa Stępień (Poland)
Jerzy Szaflarski (USA)
Bruno Szczygieł (Poland)
Kai Taeger (Germany)
Marcos A. Sanchez-Gonzalez (USA)
Krzysztof Wiktorowicz (Poland)

ASSOCIATE EDITORS

Agnieszka Bienert
Maria Iskra
Ewa Mojs
Adrianna Mostowska

SECTION EDITORS

Jaromir Budzianowski — Pharmaceutical Sciences
Paweł Jagodziński — Basic Sciences
Joanna Twarowska-Hauser — Clinical Sciences

LANGUAGE EDITORS

Margarita Lianeri (Canada)
Jacek Żywiczka (Poland)

STATISTICAL EDITOR

Magdalena Roszak (Poland)

SECRETARIAT ADDRESS

27/33 Szpitalna Street
60-572 Poznań, Poland
phone: +48 618491432, fax: +48 618472685
e-mail: jms@ump.edu.pl
www.jms.ump.edu.pl

DISTRIBUTION AND SUBSCRIPTIONS

70 Bukowska Street, 60-812 Poznań, Poland
phone/fax: +48 618547414
e-mail: sprzedazwydawnictw@ump.edu.pl

PUBLISHER

Poznan University of Medical Sciences

© 2019 by respective Author(s). Production and hosting by
Journal of Medical Science (JMS)

This is an open access journal distributed under the terms and
conditions of the Creative Commons Attribution (CC BY-NC)
licence

eISSN 2353-9801

ISSN 2353-9798

Publishing Manager: Grażyna Dromirecka

Technical Editor: Bartłomiej Wąsiel



WYDAWNICTWO NAUKOWE
UNIWERSYTETU MEDYCZNEGO
IM. KAROLA MARCINKOWSKIEGO
W POZNANIU

60-812 Poznań, ul. Bukowska 70
tel./fax: +48 61 854 71 51
www.wydawnictwo.ump.edu.pl

Ark. wyd. 6,9. Ark. druk. 8,3.
Zam. nr 153/19.

The Editorial Board kindly informs that since 2014 *Nowiny Lekarskie* has been renamed to *Journal of Medical Science*.

The renaming was caused by using English as the language of publications and by a wide range of other organisational changes. They were necessary to follow dynamic transformations on the publishing market. The Editors also wanted to improve the factual and publishing standard of the journal. We wish to assure our readers that we will continue the good tradition of *Nowiny Lekarskie*.

You are welcome to publish your basic, medical and pharmaceutical science articles in *Journal of Medical Science*.

Ethical guidelines

The Journal of Medical Science applies the ethical principles and procedures recommended by COPE (Committee on Conduct Ethics), contained in the Code of Conduct and Best Practice Guidelines for Journal Editors, Peer Reviewers and Authors available on the COPE website: <https://publicationethics.org/resources/guidelines>

CONTENTS

ORIGINAL PAPER

Milud Shadi, Piotr Janusz, Paweł Koczewski, Michał Walczak, Joanna Kraśny, Tomasz Kotwicki
Skin necrosis after SUPERknee procedure – typical versus modified surgical approach 75

Mirosława Wieczorek-Filipiak, Sławomira Drzymała-Czyż, Dariusz Walkowiak, Jarosław Szydłowski, Anna Miśkiewicz-Chotnicka, Zuzanna Szajstek, Jerzy A. Moczko, Jarosław Walkowiak
Acid steatocrit in the first 2 years of life: diagnostic accuracy and reference limits 82

Hubert Kardach, Aneta Olszewska, Ewa Firlej, Agnieszka Bogdanowicz, Ewelina Golusińska-Kardach, Anna Szponar-Żurowska, Barbara Biedziak
Force decay of intermaxillary orthodontic elastics: in vitro study 91

Małgorzata Dobrzyńska, Ilona Górna, Grzegorz Kosewski, Magdalena Kowalówka, Izabela Bolesławska, Anna Morawska, Juliusz Przysławski
The influence of the shift work system on dietary factors contributing to the development of cardiovascular disease 96

REVIEW PAPERS

Andrzej Breborowicz, Kazuo Umezawa
Causes and mechanisms of peritoneal fibrosis and possible application of NF- κ B inhibitor for prevention and treatment 102

Piotr Szczechowiak, Tomasz Piorunek
Spirometry in selected clinical situations. 112

THOUSAND WORDS ABOUT...

Jacek Tarchalski, Tomasz Piorunek, Przemysław Guzik
A thousand words about the cardiopulmonary exercise test in respiratory system diseases. 117

Rafał Dankowski, Marek Leszniewski, Małgorzata Pyda, Andrzej Szyszka
A thousand words about the imaging in cardiac amyloidosis 123

THE RATIONALE, DESIGN AND METHODS OF NEW STUDIES

*Eliza Matuszewska, Paweł Dereziński, Agnieszka Klupczyńska, Agata Światły-Błaszczewicz, Szymon Plewa,
Jan Lubawy, Arkadiusz Urbański, Grzegorz Rosiński, Zenon J. Kokot, Jan Matysiak*

[Characterization of the selected honeybee products based on omics techniques](#) 129

[Instructions for Authors](#) 133



ORIGINAL PAPER

DOI: <https://doi.org/10.20883/jms.337>

Skin necrosis after SUPERknee procedure – typical versus modified surgical approach

Milud Shadi^{1,a}, Piotr Janusz^{2,b}, Paweł Koczewski^{3,c}, Michał Walczak^{3,d}, Joanna Kraśny^{3,e}, Tomasz Kotwicki^{1,f}

¹ Department of Spine Disorders and Pediatric Orthopedics, Poznan University of Medical Sciences, Poland

² Spine Disorders Unit, Department of Spine Disorders and Pediatric Orthopedics, Poznan University of Medical Sciences, Poland

³ Department of Pediatric Orthopedics and Traumatology, Poznan University of Medical Sciences, Poland

^a <https://orcid.org/0000-0002-8751-0243>

^b <https://orcid.org/0000-0001-5702-4933>

^c <https://orcid.org/0000-0001-8063-4000>

^d <https://orcid.org/0000-0001-5843-2680>

^e <https://orcid.org/0000-0003-2419-1166>

^f <https://orcid.org/0000-0003-0810-9361>

ABSTRACT

Introduction. SUPERknee procedure (SK) is a treatment for complex knee instability in children with congenital deformations. Due to wide surgical approach and long time of surgery (ST) the skin around the knee is in risk of ischemic necrosis (SN) or healing complications (HC).

Aim. The purpose of the study is to compare incidence of SN in SK using typical and modified approach.

Material and Methods. Sixteen patients underwent SK since 2015 till 2016, in mean age 8.1 (4.3–12.7) y.o. In 8 cases SK and in 8 SK combined with SUPERhip (SK+SH) was performed. In 6 patients (3 SK and 3 SK+SH) the approach was performed from one incision (OIA). In 10 patients (5 SK and 5 SK+SH) a modified approach was performed, involving additional skin incision (DIA). The occurrence of SN, ST and risk factors of HC were evaluated.

Results. SN appeared in 2 cases treated with OIA (33%). There was no SN in DIA (0%). With this number of patients the difference was below level of significance, $p = 0.1250$, $OR = 11.7$. In one patient treated with SK+SH area of SN was 17.5 cm². In the other patient treated with SK 35 cm². Mean ST in SK was 3.4h (2.5–4.0) and in SK+SH 4.6h (4.0–5.5). ST of the surgery with OIA was 4.1h (2.5–5.5) and in DIA 3.7h (3.0–4.5), $p = 0.4746$. No additional risk factor relevant to SN was found.

Keywords: SUPERknee, SUPERhip, super knee, super hip, healing complications, skin necrosis.

Introduction

Congenital lower limb deficiencies (CLLD) are heterogeneous group of diseases characterizing a wide spectrum of pathology, ranging from mild to severe limb deformations. In this group the most common are: congenital femoral deficiency (CFD), fibular hemimelia (FH) and tibial hemimelia (TH) [1]. Although, in each disease from CLLD the main problem is situated in different localization of the lower limb and requires different ortho-

pedic solutions (eg in CFD the main problem is a hip deformation and in FH the main problems are foot, ankle and cruise deformations), in most cases whole limb is involved with various severity. There are similarities in CLLD and all of them need complex treatment with many stages and many surgical procedures [2–4]. One of the most important common feature in all types of CLLD is the lower limbs length discrepancy of various severity accompanied by wide range of axial deformity [1, 3, 5, 6]. The goal of the treatment of

children born with congenital CLLD is to achieve an optimal function in adult life and as little musculoskeletal pain and complaints, including cosmetic aspects, as possible [7]. It in this purpose normal alignment with equal limb length and a normal gait pattern with full weight-bearing is required [8].

Another typical finding in CLLD is instability of the knee. Depending on the severity of the deficiency, the instability can be detected in early infancy or later during life, sometimes without clinical significance. However, instability can appear during deformity correction and bone-lengthening procedures, leading to flexion contracture or subluxation of the knee and appears to be one of the biggest challenges in deformity correction and lengthening [1, 7]. Prevention of subluxation during lengthening in patients with congenital knee instability can be achieved with bridging of the knee with monolateral or circular fixators. Intensive physical therapy and bracing may prevent knee subluxation during lengthening using intramedullary nails. Knee stability as well as early detection and treatment of knee subluxation have the highest priority in lengthening procedures in all patients with CFD and/or FH [7].

When analyzing the knee deformation in CLLD, not only the stability of the knee must be taken into consideration, but also the patella alignment and the joint contracture [2]. The complex reconstructive procedure for children with significant instability of the knee in course of CLLD called SUPERknee (SK) was introduced by D. Paley [2]. According to Paley SUPER is an acronym for Systematic Utilitarian Procedure for Extremity Reconstruction. This procedure has three goals: reconstruct ACL/PCL, realign patella and correct flexion contracture. In case of CFD may be performed with or independent of the complex hip reconstruction SUPERhip (SH), as well as in FH with distal part of the lower limb reconstruction [3, 5]. In CFD the instability pattern is different than in an isolated tear of ACL and there is more of a rotary instability. Therefore, according to Paley, a purely intra-articular ligament reconstruction is insufficient and can lead to recurrent instability. Thus, the combination of extra- and intra-articular ACL ligament reconstruction is ideal and it can now be safely done as young as 2 years of age [5].

SK is a complex procedure combining two or more of the following five procedures: (1) the Langenskiöld procedure for congenital dislocation of the patella [9]; (2) the MacIntosh procedure for ACL deficiency including extra and intra-articular ACL reconstruction using the fascia lata [10]; (3) the Grammont procedure for recurrent dislocation of the patella [11]; (4) as the reverse MacIntosh to prevent external rotatory instability and to act as an extra-articular posterior cruciate ligament introduced by Paley [10]; and (5) the Paley anterior approach to posterior capsulotomy of knee [2]. The procedure each time is customized and not all steps are needed in each case.

The surgical approach proposed for this surgery was described as a long S-shaped distal to the tibial tuberosity distally and midlateral proximally which can be extension of the SUPERhip surgical approach or performed as isolated incision. It was indicated to perform additional medial incision when capsulotomy is needed [2, 12].

Taking into consideration of benefits of SK procedure we have used it in our Department since 2015 as a preparatory step to the thigh lengthening in children with CLLD. However, when we have used described surgical approach with the single skin incision, in some cases we have revealed skin necrosis at the level of lateral area of the knee. We could not find in the literature a single publication concerning this topic in aspect of SK procedure. Thus, we have analyzed influence of the type of the surgical approach and risk factors affecting the wound healing on the occurrence of the skin necrosis in patients with CLLD.

Material and Methods

All patients treated in our clinic with SK procedure since March 2015 till December 2016 were included into the study. The criterion for the SK procedure was the knee instability due to the congenital limb deficiency (CFD, FH). SK was performed either as a single procedure or in combination with SH procedure. Two types of skin incisions for surgical approach were used: (1) single skin incision surgical approach (OIA) started at the lateral aspect of the thigh and extended laterally around the patella up to the medial part of

the tibial tuberosity (**Figure 1**) or (2) double skin incisions surgical approach (DIA) with additional incision at the medial aspect of the knee served to attach the PCL graft – **Figure 2**.

All patients have been evaluated before surgery, on the first day after surgery the 2, 6, 12

weeks after surgery, 6, 12 and 24 months after surgery. In case of the wound healing problems, the evaluation was performed weekly until the skin healed. The wound healing complications and the incidence of the skin necrosis, the necrosis area, the type of the surgery and the time of

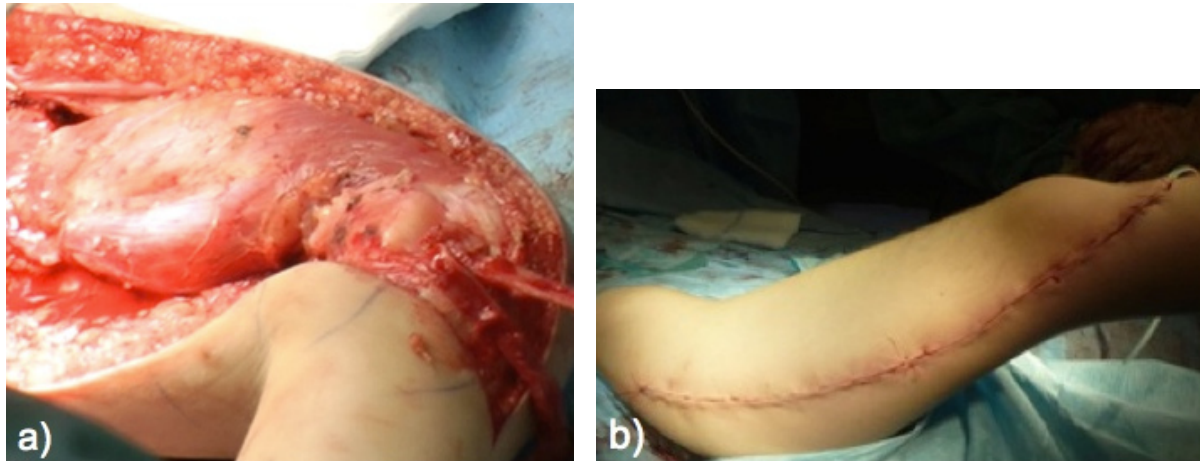


Figure 1. Single incision surgical approach for combination of SUPERhip with SUPERknee surgery, a) during tissues dissection, b) after skin sutured

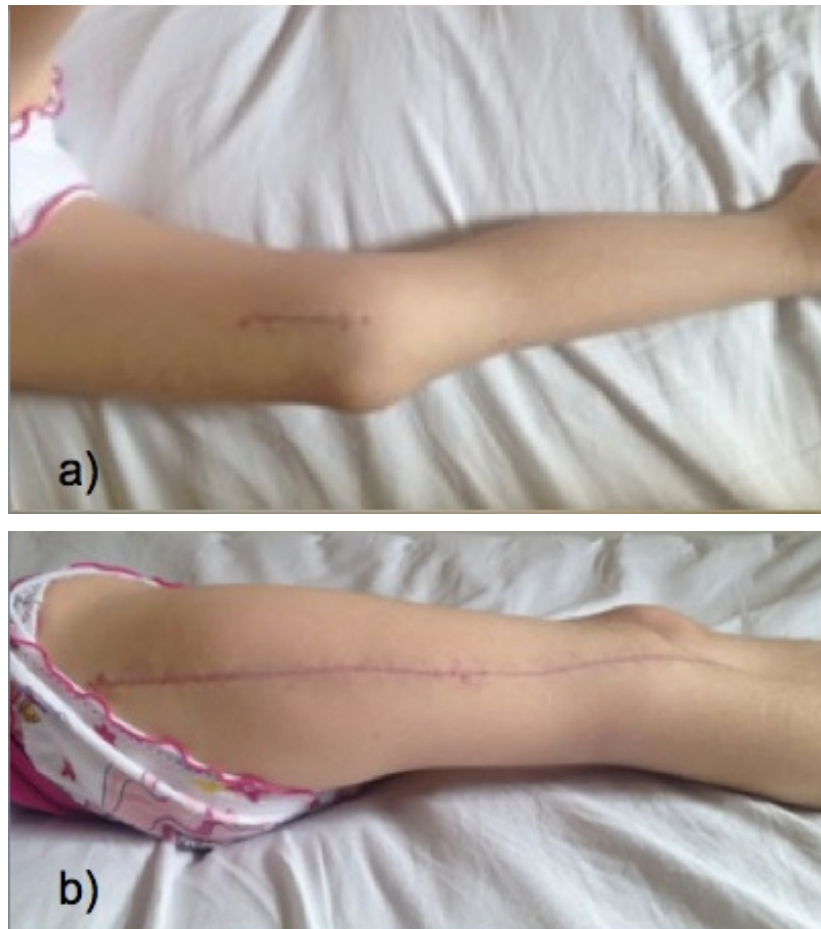


Figure 2. Double incisions surgical approach for SUPERknee surgery: a) lateral, b) medial

the surgery (ST) were evaluated. From the medical history previously described potential risk factors for the wound healing such as: diabetes, cachexia, immunodeficiency, immunosuppressive therapy, poor nutrition, diverticulosis, infection elsewhere, obesity, smoking, renal failure, hypothyroidism, alcohol abuse and previous surgeries at the area of present treatment were established [13].

Statistical analysis

For each parameter, the mean values, standard deviation and range were calculated. The normal distribution of data was analyzed with the Kruskal-Wallis test. The unpaired t-test was used to compare means between the patients with single vs. double incision surgical approach. The nonparametric parameter distribution was compared using Fisher's exact test. A p-level of 0.05 was considered significant. The data were analyzed using GraphPad InStat statistical software (Graph Pad Software, San Diego, CA, USA).

Results

Sixteen patients were enrolled: 8 boys and 8 girls in the mean age at the time of surgery 8.1 years old (SD \pm 2.6, range: 4.3–12.7). The diagnoses were as follow: 9 patients with CFD, 3 patients with FH and 4 patients with combination of CFD and FH. In 6 patients (3 SK and 3 SK+SH) OIA was performed. In 10 patients (5 SK and 5 SK+SH) DIA was performed. The mean follow-up was 30.2 months (SD \pm 8.1, range (26–41)).

The wound healing problems with the skin necrosis appeared in 2 patients treated with OIA (33%). There was no wound healing problems in DIA (0%), $p = 0.1250$, OR = 11.7 – **Figure 3**.

In both cases the skin necrosis was situated at the anterolateral aspect of the knee. The first patient underwent SK+SH, the area of the skin necrosis after surgery was 17.5 cm². In this case surgery time was 4.5 h. The second patient underwent SK the area of the skin necrosis after surgery was 35 cm². In this case surgery time was 3.5h (**Figure 4**). Both patients healed with the skin scar in 4 months.

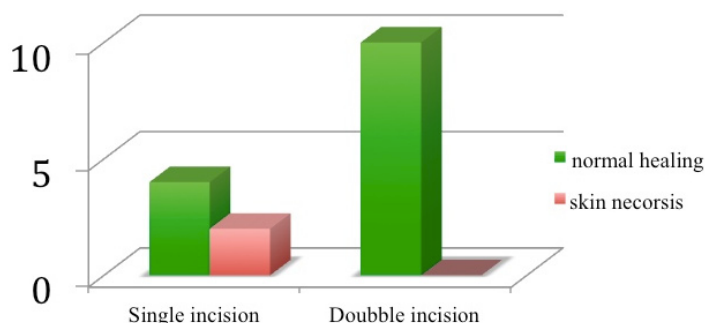


Figure 3. Graph presenting number of the skin necrosis for surgeries performed with single incision surgical approach and double incisions surgical approach

Table 1. The time of the surgery for patients with the skin necrosis and the mean surgery time for all patients

	Surgery time of surgery for the patient with skin necrosis	Mean time of surgery for all patients
SUPERknee procedure	3.5h (n = 1)	3.4h (n = 7)
Combination of SUPERknee with SUPERhip procedure	4.5h (n = 1)	4.6h (n = 7)

Table 2. Number of the patients with the knee surgeries prior to SUPERknee operation

	Prior surgeries at the knee area		No prior surgeries at the knee area	
	Single incision surgical approach	Double inactions surgical approach	Single incision surgical approach	Double inactions surgical approach
Patients with skin necrosis	1	0	1	0
Patients with normal healing wounds	0	3	4	7



Figure 4. Patient treated with single incision surgical approach at 2 week (a), 6 weeks (b) and 12 months (c) after super knee surgery

The mean surgery time was in SK 3.4h (SD \pm 0.6, range: 2.5–4.0) and in SK+SH 4.6h (SD \pm 0.5 range: 4.0–5.5). The surgery time in cases with skin necrosis was similar to the mean surgery time for each group – **Table 1**.

There was no difference in the surgery time between OIA and DIA. The mean surgery time was 4.1h (SD \pm 1.0, range: 2.5–5.5) in OIA and 3.7h (SD \pm 0.6 range: 3.0–4.5) in DIA, $p = 0.4746$.

The prior knee surgeries with the skin scars was present in one patient with skin necrosis (50% of all wound healing problems) when one incision was applied and in 3 patients with normal wound healing, however, all of them have DIA – **Table 2**.

No patient revealed additional disease or risk factor relevant to the wound healing process. No incidence of: diabetes, cachexia, immunodeficiency, immunosuppressive therapy, poor nutrition, diverticulosis, infection elsewhere, obesity, smoking, renal failure, hypothyroidism and alcohol abuse in both groups was noted.

Discussion

The complex method of ACL and PCL reconstruction and improvement stability in CLLD proposed

by Paley is nowadays one of the most promising procedures for children with CFD, FH and TH. This procedure, together with external fixator bridging the knee, allowing the knee motion preservation and accompanied by intensive physiotherapy, provides safe possibility of the femur lengthening with good functional result. Until use this combination, a lengthening of the femur in patents with the knee instability had great burden of the potential risk of knee subluxation [1].

Although, this method is very promising, it is technically demanding and can be associated with severe complications. One of the complications is early wound healing problem. In this method large approach with deep and wide skin dissection is necessary. Even if the surgery is limited only to ACL and PCL reconstruction, without additional steps, the skin and the subcutaneous layer dissection is still very extensive. Such a large approach is needed for a proper graft positioning according to the description of the procedure: there have to be access to posterior capsule, lateral and anterior aspect of the knee as well as medial part of the join up to the intermuscular septum [2]. Especially the PCL attachment to the intermuscular septum at the medial aspect of the knee requires skin dissection from the lateral through the anterior to the medial aspect

of the knee creates large the skin flap, enhance risk of destruction of the skin blood supply and increase chance of the skin necrosis in this area [13, 14].

The early healing problem with skin necrosis may lead to the joint infection and the sever scars at the level of knee joint. Except obvious adverse cosmetic effect and skin sensation disturbance, may cause the knee joint contractures and secondary deformities (**Figure 4**) [13–15]. In our group of patents we deal with the soft tissues very gently. We paid attention to keep the skin flap as thick as possible, we kept the exposed tissues moist, we tried not to pull to hard tissues with retractors and we used a wound drainage. All this means are described as helpful to decrease risk of skin necrosis [13]. Nevertheless, we have observed two cases of the sever wound healing problem. Thus, when we evaluated our previous cases we observed that patients who needed additional medial incisions due to capsulotomy or 8-plate implantation have better wound healing. The second medial incision allows us to attach properly PCL graft to the intramuscular septum and decrease skin flap dissection at the antero-medial aspect of the knee. According the studies concerning the wound healing, careful attention should be paid to limiting the size of skin flaps and keeping them thick to preserve the skin blood supply [13, 14]. The blood supply to the skin over the knee joint is fasciocutaneous and is more robust on the medial side [16] and additional small medial incision may reduce devascularization of the skin flap. We are aware that with this number of patients the difference was below level of statistical significance, $p = 0.1250$, however, due to severity of this complication we perform all SK surgeries with the additional medial skin incision and we do not have new cases of wound healing problem.

Another issue which is associated with the wound healing problems is prolonged time of the surgery [13], however the surgery time in cases with skin necrosis was similar to mean time of each type of surgery in our group (**Table 1**).

In search of the additional risk of the wound healing complication, due to paucity of literature concerning SK procedure, we based our possible risk factors on the literature concerning the

wound healing problem after total knee arthroplasty (TKA). It was motivated by similar area of the surgery and great number of publications concerning the surgical approach complication in TKA [13, 14]. Unfortunately, most of the risk factors are not suitable for the pediatric patients (eg alcohol abuse or smoking) another are rare in this group (eg diverticulosis or hypothyroidism). Thus, probably this was the reason why we could not find many of them in our study.

Another important risk factor in the wound healing problems are skin scars after previous surgeries at the knee area [13, 14]. In our study the number of patients is too small to demonstrate statistically significant difference, however in our group prior surgeries in single incision approach were had greater impact than in double incision approach.

The wound healing problem was not mentioned by the author of the procedure. However in early technique description the additional medial incision was suggested when the knee posterior capsulotomy is needed [2, 12]. Whereas, in the most recent publication there is suggestion that, if performed with a SH procedure, the incision is a distal extension of the SH incision. If performed as an isolated procedure, it can be done through one midline anterior incision or one medial and one lateral incision [5]. In our opinion the second incision is beneficial and can be used in each case of SK for PCL graft placement.

The strong site of this study is the fact that this is a first study concerning this problem. The SK procedure address important problem of the knee instability in patients with CLLD. The popularity of this technique increases and more surgeons use it in practice. Thus, the study may help other surgeons avoiding significant complications with wound healing in SK procedure.

One of the limitations of this study is small sample size, however, these procedures are not routinely performed surgeries. On the one hand further evaluation with the larger sample size could give some additional results, on the other it is ethically controversial to use the single incision approach when the risk of the skin necrosis is known. Another limitation is that is single center study. It would be beneficial to compare our observations with patients from other hospitals.

Conclusions

The double skin incision surgical approach for the SUPERknee procedure may decrease incidence of the wound healing complications and the skin necrosis. It does not extend the time of surgery. It should be considered in all cases, especially in patients with previous surgeries in the knee area and with additional risk factors.

Acknowledgements

Conflict of interest statement

The authors declare no conflict of interest.

Funding sources

There are no sources of funding to declare.

Abbreviations: CLLD, congenital lower limb deficiency; CFD, congenital femoral deficiency; FH, fibular hemimelia; TH, tibial hemimelia; SUPER, Systematic Utilitarian Procedure for Extremity Reconstruction; SK, SUPERknee; SH, SUPERhip; OIA, single incision surgical approach; DIA, double skin incisions surgical approach; ST, time of the surgery.

References

1. Mindler GT, Radler C, Ganger R. The unstable knee in congenital limb deficiency. *Journal of children's orthopaedics*. 2016;10(6):521–8.
2. Paley DGF. Lengthening Reconstruction Surgery for Congenital Femoral Deficiency. In: Kocaoğlu MTH, Eralp L, editor. *Advanced Techniques in Limb Reconstruction Surgery*. Berlin, Heidelberg: Springer; 2015.
3. Paley D. Surgical reconstruction for fibular hemimelia. *Journal of children's orthopaedics*. 2016;10(6):557–83.
4. Prince DE, Herzenberg JE, Standard SC, Paley D. Lengthening With External Fixation Is Effective in Congenital Femoral Deficiency. *Clinical orthopaedics and related research*. 2015;473(10):3261–71.
5. Paley DCDY, Prince DE. Congenital Femoral Deficiency Reconstruction and Lengthening Surgery. In: S S, editor. *Pediatric Lower Limb Deformities: Principles and Techniques of Management*. Springer, Cham; 2016. p. 361–425.
6. Paley D. Tibial hemimelia: new classification and reconstructive options. *Journal of children's orthopaedics*. 2016;10(6):529–55.
7. Kaastad TS, Tveter AT, Steen H, Holm I. Physical function and health-related quality of life in young adults with unilateral congenital lower-limb deficiencies. *Journal of children's orthopaedics*. 2017;11(5):348–57.
8. Hamdy RC, Makhdom AM, Saran N, Birch J. Congenital fibular deficiency. *The Journal of the American Academy of Orthopaedic Surgeons*. 2014;22(4):246–55.
9. Langenskiöld A, Ritsila V. Congenital dislocation of the patella and its operative treatment. *Journal of pediatric orthopedics*. 1992;12(3):315–23.
10. Amirault JD, Cameron JC, MacIntosh DL, Marks P. Chronic anterior cruciate ligament deficiency. Long-term results of MacIntosh's lateral substitution reconstruction. *The Journal of bone and joint surgery British volume*. 1988;70(4):622–4.
11. Grammont PM, Latune D, Lammaire IP. Treatment of subluxation and dislocation of the patella in the child. Elmslie technic with movable soft tissue pedicle (8 year review). *Der Orthopade*. 1985;14(4):229–38.
12. Paley D SSC. Lengthening Reconstruction Surgery: for Congenital Femoral Deficiency. In: S. Robert Rozbruch SI, editor. *Limb Lengthening and Reconstruction Surgery*. 1st ed. Boca Raton CRC Press 2006
13. Vince K, Chivas D, Droll KP. Wound complications after total knee arthroplasty. *The Journal of arthroplasty*. 2007;22(4 Suppl 1):39–44.
14. Jones RE, Russell RD, Huo MH. Wound healing in total joint replacement. *The bone & joint journal*. 2013;95-B(11 Suppl A):144–7.
15. Pujol N, Boisrenoult P, Beaufils P. Post-traumatic knee stiffness: surgical techniques. *OTSR*. 2015;101(Suppl 1):S179–86.
16. Johnson DP, Eastwood DM, Bader DL. Biomechanical factors in wound healing following knee arthroplasty. *Journal of medical engineering & technology*. 1991;15(1):8–14.

Acceptance for editing: 2019-05-09
Acceptance for publication: 2019-06-29

Correspondence address:

Janusz Piotr
Spine Disorders Unit, Department of Spine Disorders
and Pediatric Orthopedics
Poznan University of Medical Sciences
135 28 Czerwca 1956 r. Street, 61-545 Poznań, Poland
phone: +48 618310157
e-mail: mdpjanusz@gmail.com



ORIGINAL PAPER

DOI: <https://doi.org/10.20883/jms.320>

Acid steatocrit in the first 2 years of life: diagnostic accuracy and reference limits

Mirosława Wieczorek-Filipiak^{1,a}, Sławomira Drzymała-Czyż^{1,b}, Dariusz Walkowiak^{2,c}, Jarosław Szydłowski^{3,d}, Anna Miśkiewicz-Chotnicka^{1,e}, Zuzanna Szajstek¹, Jerzy A. Moczko^{4,f}, Jarosław Walkowiak^{1,g}

¹ Department of Pediatric Gastroenterology and Metabolic Diseases, Poznan University of Medical Sciences, Poland

² Department of Organization and Management in Health Care, Poznan University of Medical Sciences, Poland

³ Department of Paediatric Otolaryngology, Poznan University of Medical Sciences, Poland

⁴ Department of Computer Science and Statistics, Poznań University of Medical Sciences, Poland

^a  <https://orcid.org/0000-0002-8828-1550>

^b  <https://orcid.org/0000-0001-8291-5439>

^c  <https://orcid.org/0000-0001-8874-2401>

^d  <https://orcid.org/0000-0002-8447-788X>

^e  <https://orcid.org/0000-0001-5073-2435>

^f  <https://orcid.org/0000-0002-4164-6196>

^g  <https://orcid.org/0000-0001-5813-5707>

ABSTRACT

Introduction. The measurement of acid steatocrit (AS) is an established method to assess faecal fat balance. However, data regarding AS in healthy infants and toddlers are sparse.

Aim. This study aimed to determine the range of normal values for AS in the first two years of life and evaluate the correlations with other faecal fat balance tests.

Material and Methods. AS (%) was assessed by 72-hour stool collection in 160 children aged 1–24 months (8 groups of 20: aged 1–3, 4–6 months, etc.).

Results. AS was higher in infants < 6 months than in those aged 7–12, 13–18 and 19–24 months ($p < 0.05$, $p < 0.001$ and $p < 0.001$, respectively). The correlations between AS and age and faecal fat concentration (FFC) were statistically significant, but moderate or weak ($r = -0.48$, $p < 0.0001$; $r = 0.28$, $p < 0.001$, respectively). A 90th/95th percentile nomogram of AS was created based on these results, with values ranging from 23.6/23.9% at 1 month to 12.1/12.9% at 24 months.

Conclusions. Healthy infants have a significantly higher AS than older children. For this reason, we propose an upper limits nomogram, providing detailed reference values for infants and children in their first two years of life. However, it should be noted that AS does not reflect adequately FFE and FFC in this population.

Keywords: exocrine pancreatic function, healthy children, reference intervals, fecal free fatty acids.

Introduction

Fat excretion and concentration in the 72-hour stool collection by the titrimetric Van de Kamer method is considered the gold standard for the diagnosis of fat malabsorption [1–4]. Although it is a non-invasive, simple and inexpensive test, it is also time-consuming, difficult to perform,

especially in infants using diapers, and undesirable for patients and laboratory personnel [3, 5, 6]. Furthermore, this method requires proper training of the patient to improve the reliability of the test. For this reason, other methods have been investigated.

An alternative test is the measurement of acid steatocrit (AS), which was first described by Tran

et al. [7] in 1994 as a simple screening test for steatorrhea. This method remains not only facile (no 3-day collection) but is also cost-effective. AS is considered very reliable as it correlates well with the coefficient of fat absorption (CFA) and faecal fat excretion (FFE) in defining significant steatorrhea in alcoholic chronic pancreatitis [8, 9]. However, it is not standardised, possibly influenced by dietary fat intake, and unhelpful in patients with mild steatorrhea [2, 10]. It should also be emphasised that despite evidence of the clinical usefulness of AS in cystic fibrosis, chronic pancreatitis, small bowel disease and untreated coeliac disease, data on normal AS in healthy infants and toddlers are sparse [2, 4, 9, 11, 12].

Since the gastrointestinal tract is immature in infants and young children, it may be expected that not only FFE and faecal fat concentration (FFC) but also AS will be higher than in older subjects [13, 14]. Therefore, the aims of the present study were to determine the range of normal AS values in the first two years of life and to evaluate the correlations with other faecal tests assessing fat loss.

Material and Methods

Patients

One hundred and sixty infants and toddlers (82 boys, 78 girls; aged 4 weeks–24 months) were recruited for the purpose of the study, all of whom had normal pancreatic status determined using the faecal elastase-1 concentration as described previously [15]. In all patients, FFC and FFE were defined as described earlier [15]. The children were divided into 8 groups of 20 aged 1–3 months, 4–6 months, etc. The exclusion criteria were prematurity and the presence of comorbidities (e.g., chronic gastrointestinal diseases, inflammatory processes or other). The inclusion criteria were age \leq 24 months and agreement

to participate in the study. The anthropometric parameters describing the healthy subjects are presented in **Table 1**.

Methods

A 72-hour stool collection was performed on all children. Faecal samples were weighed and homogenised before analysis using the method of Tran et al. [7] to determine AS. After centrifugation, the individual layers were measured and the percentage AS was calculated using the formula:

$$\text{AS (\%)} = \frac{\text{Fatty layer length}}{\text{Fatty layer length} + \text{Solid layer length}}$$

The flow chart showing the accuracy of AS compared with other faecal fat tests was prepared based on STARD 2015 guidelines for reporting diagnostic accuracy studies [16]. Abnormal values were assumed in flow chart A: AS higher than 20%, FFE higher than 5 g/day and FFC higher than 5% (AS values lower than 10% were considered normal). In flow chart B every result higher than the 90th percentile was considered as abnormal.

Statistical methods

The study size was calculated using G*Power v. 3 (University of Dusseldorf, Dusseldorf, Germany). The unpaired comparisons between subgroups of size not smaller than 17 were determined to be sufficient assuming power of the test at 80% and a 5% significance level.

GraphPad Prism 5.01 software (GraphPad Software, Inc., La Jolla, CA, USA) was used for statistical analysis. AS values are given as medians and 1st–3rd quartiles. Differences between groups were evaluated by the Kruskal-Wallis test with *post-hoc* testing (Dunn's multiple comparison test). The influence of FFC, FFE, faecal elastase-1

Table 1. Basic anthropometric data of the studied healthy infants and young children. The number of children in each group was 20

	Age (months)								p
	1–3	4–6	7–9	10–12	13–15	16–18	19–21	22–24	
	Median values [1 st –3 rd quartiles]								
Z-score for body weight	-0.03 [-0.46–1.04]	-0.05 [-0.90–0.85]	0.14 [-0.49–0.55]	0.09 [-0.44–0.65]	-0.14 [-0.73–0.47]	0.08 [-0.35–0.89]	0.02 [-0.92–0.53]	0.01 [-0.61–0.43]	Ns.
Sex ratio (male/female)	8 / 12	10 / 10	10 / 10	10 / 10	7 / 13	11 / 9	14 / 6	12 / 8	Ns.

concentration, age, sex, Z-score for body mass on AS value was assessed using multiple linear logistic regression. Correlations were evaluated using the Pearson test and p -values < 0.05 were considered statistically significant.

For the graphical presentation of AS, results were smoothed by the least squares weighted distances method (Stata/SE 15.0 64 bit for Windows, College Station, USA). To determine the reference values for AS, the 90/95th percentile was calculated and estimated on the nomogram according to the respective percentile for each age group.

Ethical considerations

The study protocol was approved by the Ethical Committee of the Poznań University of Medical Sciences, Poland (decision no. 1275/05). Written informed consent was obtained from all the subjects' parents. The study was carried out in accordance with the revised Declaration of Helsinki.

Results

Differences in AS between younger and older age groups were found and are presented in **Table 2**. AS values in the first 6 months were

higher ($p < 0.05$, $p < 0.001$ and $p < 0.001$, respectively) than in children aged 7–12, 13–18 and 19–24 months (median [1st–3rd quartile], 14.6% [12.1–18.0], 11.7% [9.2–14.0], 9.9% [6.8–12.5], 9.8% [6.9–12.0], respectively) and in the first year of life higher than in the second year (13.3% [10.7–15.5] vs 9.9% [6.8–12.2]; $p < 0.0001$) (**Figure 1**). The dependence of AS values on age smoothed using the LOWESS method is shown in **Figure 2**.

The relationship between AS and age and FFC/FFE is depicted in **Figure 3**. The correlations between AS and age as well as FFC were statistically significant but moderate or weak ($r = -0.4788$, $p < 0.0001$; $r = 0.2812$, $p < 0.001$; respectively). There were no correlations between AS and faecal elastase-1 or FFE.

In multiple regression analysis, values of AS were predicted by age (p model < 0.000001 , $p = 0.000042$, $b = -0.25453$).

All infants aged 1–3 months, 75% of those aged 4–6 and 7–9 months, and 55% of those aged 10–12 months had higher AS than normal values proposed for older children ($< 10\%$) [2]. For this reason, a nomogram representing 90th/95th percentiles of AS was generated (**Table 3**). The reference percentile curves for AS are shown in **Figure 4 AB**.

A flow diagram according to the STARD initiative describing the accuracy of AS to determine FFE and FFC was also created (**Figure 5 AB**).

Table 2. Acid steatocrit in healthy infants and young children. The number of subjects in each group was 20

Fecal test	Age (months)							
	1–3	4–6	7–9	10–12	13–15	16–18	19–21	22–24
	Median values [1 st –3 rd quartiles]							
Acid steatocrit (%)	15.5 ^{abcde} [13.7–18.7]	13.2 ^f [10.6–15.7]	13.0 [11.0–14.3]	10.8 ^a [8.1–13.7]	9.9 ^b [6.9–12.2]	9.3 ^c [6.9–13.1]	10.4 ^d [8.4–12.6]	8.7 ^{ef} [6.2–10.8]

^a $p < 0.05$, ^{b,c} $p < 0.01$, ^{d,f} $p < 0.05$, ^e $p < 0.001$

Table 3. Nomogram for the assessment of acid steatocrit (AS) in the first two years of life. The 90th and 95th percentiles are shown. Smoothing for AS was performed using the method of least squares weighted distances

Age (months)	1	2	3	4	5	6	7	8	9	10	11	12	13	14	15	16	17	18	19	20	21	22	23	24
P90 th AS (%)	23.6	21.7	20.9	20.0	19.4	18.3	17.7	16.4	16.2	15.9	15.6	15.4	15.1	15.1	15.2	15.3	15.4	15.2	14.9	14.2	13.6	13.2	12.6	12.1
P95 th AS (%)	23.9	23.2	22.8	22.2	21.5	20.6	19.8	19.2	19.0	19.0	19.7	18.0	17.3	16.7	16.2	16.0	15.9	15.7	15.3	14.6	14.2	13.8	13.3	12.9

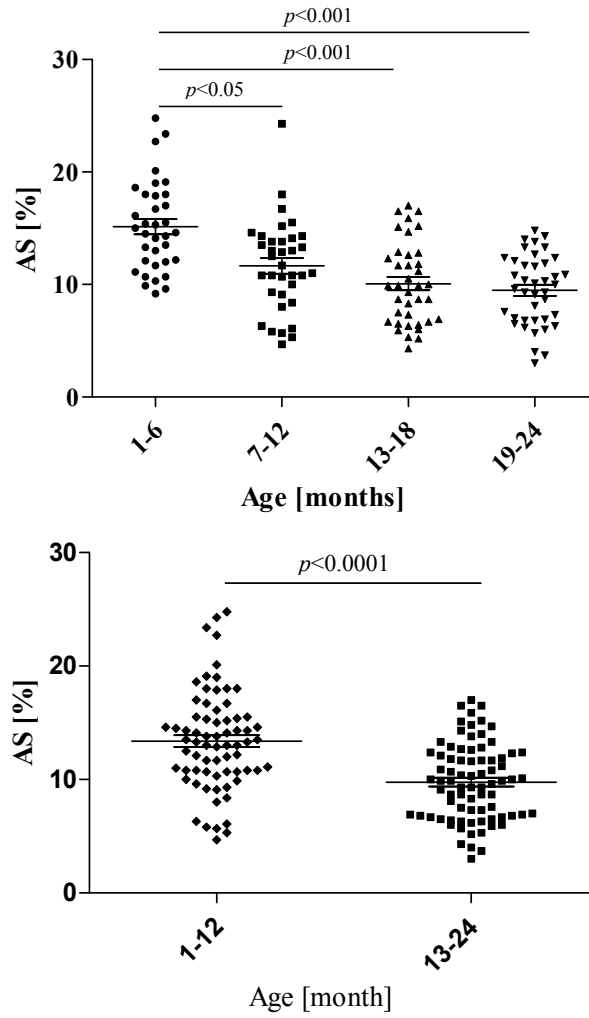


Figure 1. Acid steatocrit (AS; %) value in healthy infants and young children in different age subgroups

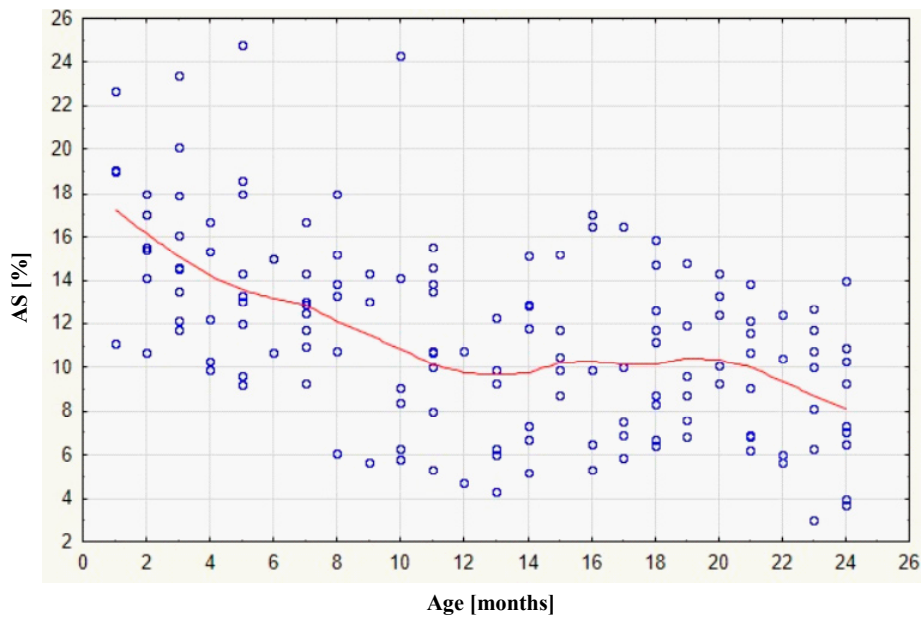


Figure 2. The dependence of acid steatocrit (AS; %) on age smoothed using the LOWESS method (bandwidth = 0.8)

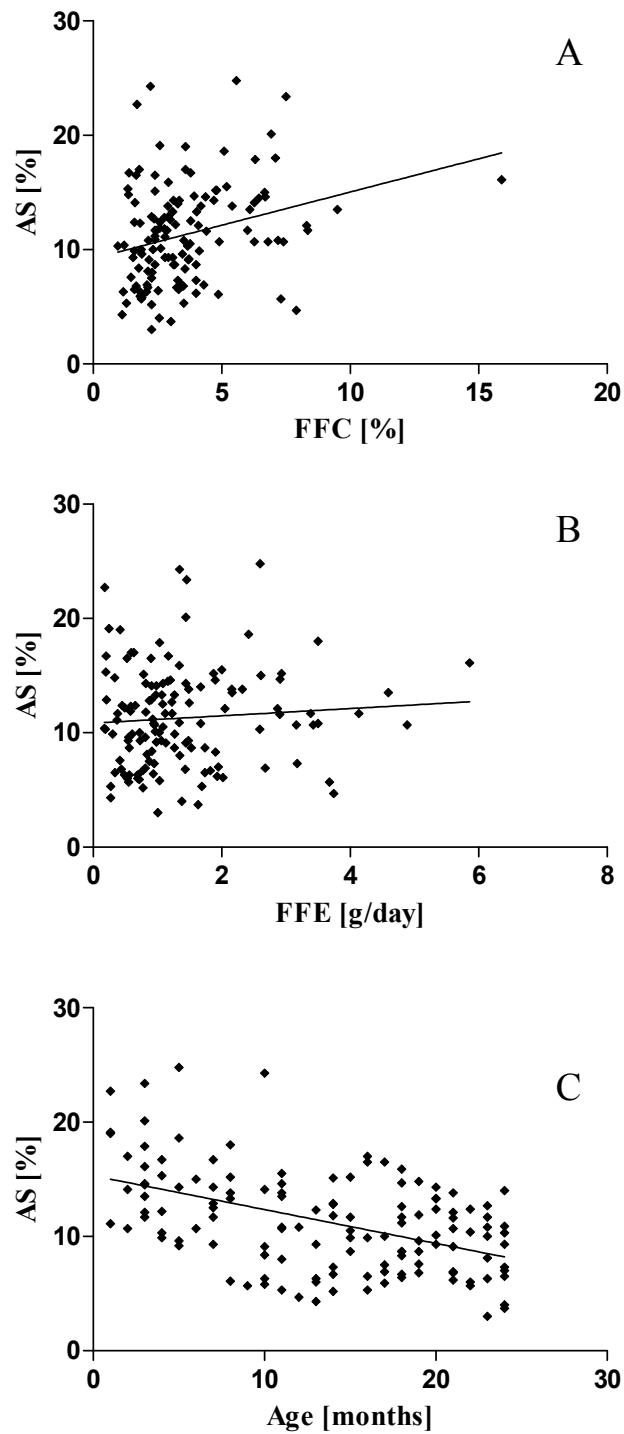


Figure 3. Correlation of acid steatocrit value (AS; %) and fecal fat concentration (FFC; $p < 0.001$, $r = 0.2812$), fecal fat excretion (FFE; $p = 0.3790$) and age of children ($p < 0.0001$, $r = -0.4788$)

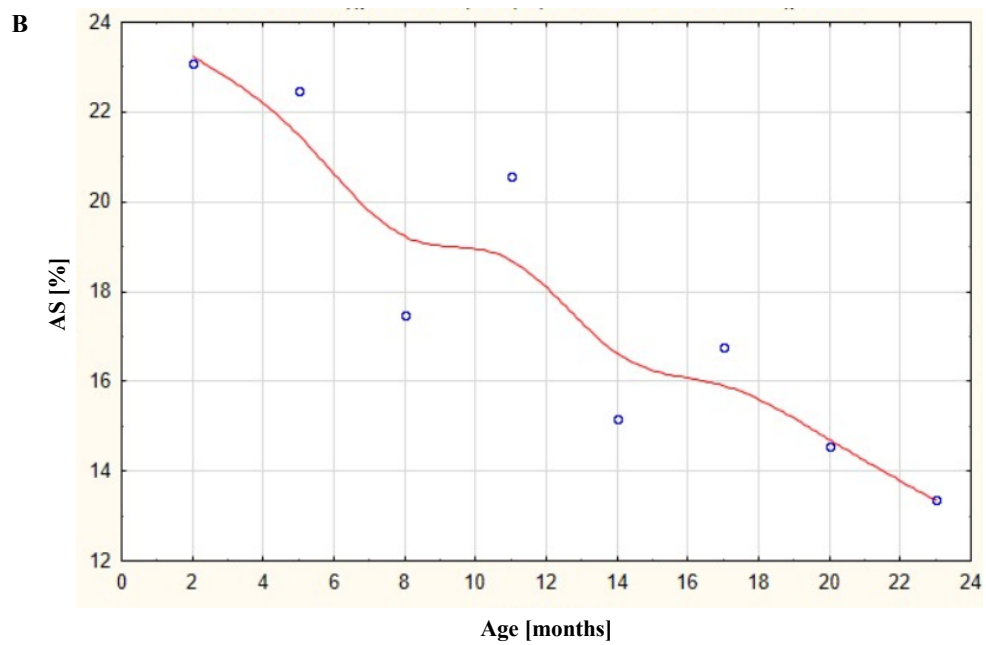
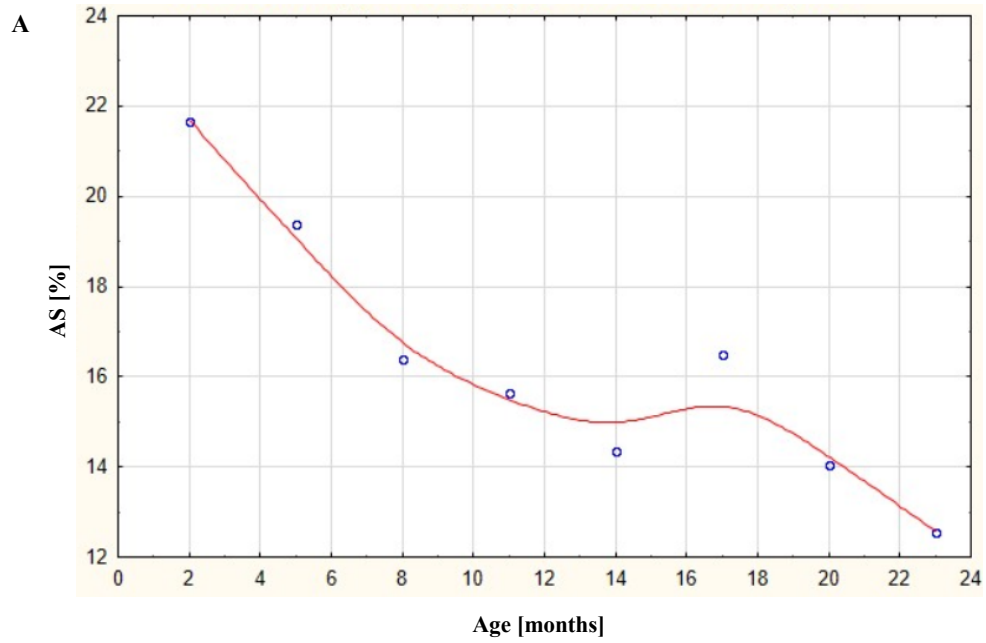


Figure 4. The reference 90th (A) and 95th (B) percentile curves generated for acid steatocrit (AS) smoothed by the least squares weighted distances method

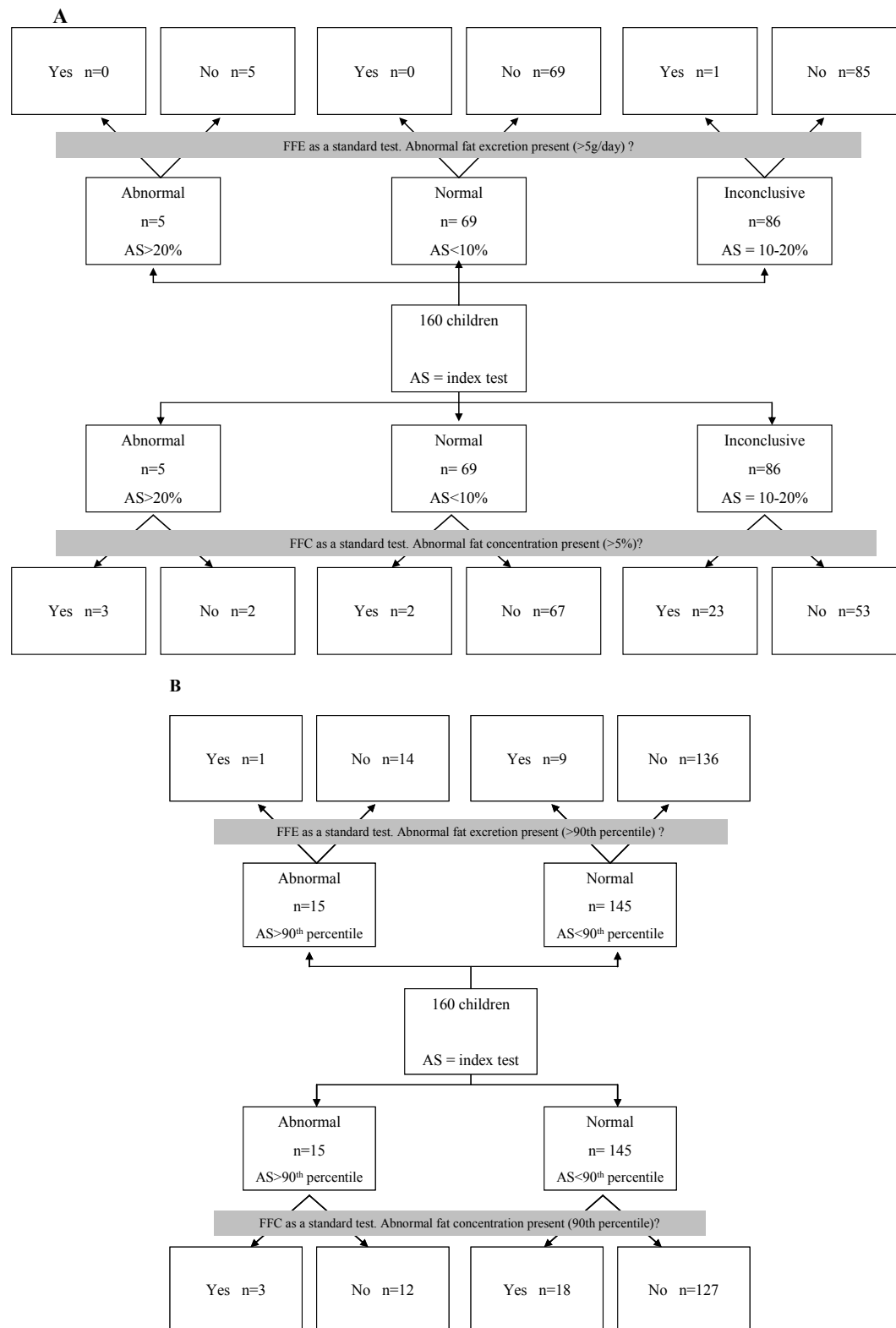


Figure 5. Flow diagram of diagnostic accuracy of acid steatocrit (AS) and stool collection (fecal fat excretion (FFE) & fecal fat concentration (FFC))

Discussion

This study provides new AS reference values and evaluated the applicability of AS in the first two years of life. The preceding literature described AS only in the context of significant steatorrhea in patients with gastrointestinal diseases compared to healthy subjects. However, the produced data could not be reliably extrapolated to healthy infants because the studies involved small groups of children with a large age range (in none of the manuscripts the infants were delineated as an individual subgroup). This is the first study to propose reference intervals based on a large number of healthy infants and toddlers. Nonetheless, this study is limited as the effects of diet (breast-fed vs non-breast-fed infants) on the obtained results were not taken into consideration.

AS has been described as a reliable tool in screening for steatorrhea in a paediatric population [17]. A few studies [7, 9, 17, 18] documented its high correlation with FFE and/or FFC in cystic fibrosis or chronic pancreatitis patients. Although three of these articles described healthy subjects as a control group, these results cannot be used for creating reference values. The first study included only 6 children aged from 3 to 12 years (mean age of 5.8 years) [7], showing a high correlation between faecal fat content and AS (0.81) and a lower AS value in healthy children (3.8%) as compared with cystic fibrosis patients (26.9%), but infants and toddlers were not included in the study. In the second study, Amann *et al.* [9] only analysed stool samples from 15 healthy adults. In the third study, the median AS [10th–90th percentile] in 29 healthy children was 7.2% [3.0%–15%] [17], but interpretation of the results is difficult due to the broad age range (0.6–16 years). All subjects were analysed as one group, therefore no age-related differences in FFE could be analysed.

Van de Neucker *et al.* [11] compared AS values in healthy children with those of sick children without (asthma patients) or with gastrointestinal involvement (patients with cystic fibrosis, untreated coeliac disease, various gastrointestinal problems). The control group comprised 25 boys and 25 girls with a mean age of 3.9 years (the youngest infant was 6 months-old) and their median AS was 3.3% [5th–90th percentile: 0–21.0%]. It should be emphasised that very

high AS up to 44.8% were also found, however no analysis of the influence of age on AS values was performed. It is worth noting that in the present study, the obtained results were also higher than the earlier suggested cut-off level of 10% (median AS for all children up to 1 years was 13.3%; maximum was 24.8%) [2, 3].

The evaluation of the applicability of AS in cystic fibrosis patients without or with mild steatorrhea (< 10 g/day) was the main goal of our previous study [2]. In the 72-hour stool collection, there were rather weak or moderate correlations between AS and FFE/FFC ($r = 0.394$, $p < 0.005$; $r = 0.454$, $p < 0.001$, respectively). Using two cut-off values for normal AS (10%) and abnormal AS (20%), the sensitivity, specificity, negative, and positive predictive values in the determination of abnormal FFC and FFE were not satisfactory. Therefore, it was concluded that AS has a limited practical value in patients without or with only mild steatorrhea. Undoubtedly, healthy infants are an interesting group for similar analysis. The limited usefulness of AS was reflected in the results obtained in the present study (flow chart), with no regard to the cut-off level values of AS and FFC/FFE (Figure 5). Overall, AS does not seem to be useful in subjects other than those with severe steatorrhea.

In conclusion, healthy infants have a significantly higher AS than older children. For this reason, we propose an upper limits nomogram, providing detailed reference values for infants and children in their first two years of life. However, it should be noted that AS does not reflect adequately FFE and FFC in this population.

Acknowledgements

Conflict of interest statement

The authors declare no conflict of interest.

Funding sources

The study was supported by the grants from the Poznań University of Medical Sciences (No 502–01–1103603–07588).

Author Contributions

Conceptualization – MWF, SDC & JW; design of the work – MWF, SDC, DW, JSz, AMC & JW; acquisition of data – MWF, SDC, JSz, ZS; analysis and interpretation – MWF, SDC, DW, JAM & JW; data visualization – MWF, SDC, JAM; writing – original draft preparation – MWF, SDC & JW; writing – review & editing – DW, JSz, ZS, AMC; funding acquisition – JW.

References

1. Van De Kamer JH, Ten Bokkel Huinink H, Weyers HA. Rapid method for the determination of fat in feces. *J Biol Chem.* 1949 Jan;177(1):347–355.
2. Walkowiak J, Lisowska A, Blask-Osipa A, Drzymała-Czyż S, Sobkowiak P, Cichy W, et al. Acid steatocrit determination is not helpful in cystic fibrosis patients without or with mild steatorrhea. *Pediatr Pulmonol.* 2010 Mar;45(3):249–254.
3. Walkowiak J, Nousia-Arvanitakis S, Henker J, Stern M, Sinaasappel M, Dodge JA. Indirect pancreatic function tests in children. *J Pediatr Gastroenterol Nutr.* 2005 Feb;40(2):107–114.
4. Girish BN, Rajesh G, Vaidyanathan K, Balakrishnan V. Fecal elastase I and acid steatocrit estimation in chronic pancreatitis. *Indian J Gastroenterol.* 2009 Dec;28(6):201–205.
5. Cohen JR, Schall JI, Ittenbach RF, Zemel BS, Stallings VA. Fecal elastase: pancreatic status verification and influence on nutritional status in children with cystic fibrosis. *J Pediatr Gastroenterol Nutr.* 2005 Apr;40(4):438–444.
6. Weintraub A, Blau H, Mussaffi H, Picard E, Bentur L, Kerem E, et al. Exocrine pancreatic function testing in patients with cystic fibrosis and pancreatic sufficiency: a correlation study. *J Pediatr Gastroenterol Nutr.* 2009 Mar;48(3):306–310.
7. Tran M, Forget P, Van den Neucker A, Strik J, van Kreel B, Kuijten R. The acid steatocrit: a much improved method. *J Pediatr Gastroenterol Nutr.* 1994 Oct;19(3):299–303.
8. Kamath MG, Pai CG, Kamath A, Kurien A. Comparing acid steatocrit and faecal elastase estimations for use in M-ANNHEIM staging for pancreatitis. *World J Gastroenterol.* 2017 Mar;23(12):2217–2222.
9. Amann ST, Josephson SA, Toskes PP. Acid steatocrit: a simple, rapid gravimetric method to determine steatorrhea. *Am J Gastroenterol.* 1997 Dec;92(12):2280–2284.
10. Sperti C, Moletta L. Staging chronic pancreatitis with exocrine function tests: Are we better? *World J Gastroenterol.* 2017 Oct;23(38):6927–6930.
11. Van den Neucker AM, Kerkvliet EM, Theunissen PM, Forget PP. Acid steatocrit: a reliable screening tool for steatorrhea. *Acta Paediatr.* 2001 Aug;90(8):873–875.
12. Catapani WR, da Silva AN, de Morais MB, Fagundes Neto U. Clinical usefulness of acid steatocrit in pediatric practice. *Arq Gastroenterol.* 1999 Apr-Jun;36(2):105–108.
13. Lebenthal E, Lee PC. Development of functional responses in human exocrine pancreas. *Pediatrics.* 1980 Oct;66(4):556–560.
14. McClean P, Weaver LT. Ontogeny of human pancreatic exocrine function. *Arch Dis Child.* 1993 Jan;68(1):62–65.
15. Wieczorek-Filipiak M, Drzymała-Czyż S, Szczepanik M, Miśkiewicz-Chotnicka A, Wenska-Chyży E, Moczko JA, et al. Fecal elastase-1 in healthy children up to 2 years of age: a cross-sectional study. *Dev Period Med.* 2018;22(2):123–127.
16. Cohen JF, Korevaar DA, Altman DG, Bruns DE, Gatsonis CA, Hoof L, et al. STARD 2015 guidelines for reporting diagnostic accuracy studies: explanation and elaboration. *BMJ Open.* 2016 Nov;6(11):e012799.
17. Van den Neucker AM, Forget P-P, van Kreel B. Lipid, nitrogen, water and energy content of a single stool sample in healthy children and children with cystic fibrosis. *Eur J Pediatr.* 2003 Nov;162(11):764–766.
18. Wagner MH, Bowser EK, Sherman JM, Francisco MP, Theriaque D, Novak DA. Comparison of steatocrit and fat absorption in persons with cystic fibrosis. *J Pediatr Gastroenterol Nutr.* 2002 Aug;35(2):202–205.

Acceptance for editing: 2019-03-12
Acceptance for publication: 2019-06-29

Correspondence address:

Jarosław Walkowiak
Department of Pediatric Gastroenterology
and Metabolic Diseases
Poznan University of Medical Sciences
27/33 Szpitalna Street, 60–572 Poznań, Poland
phone: +48 618491432
e-mail: jarwalk@ump.edu.pl



ORIGINAL PAPER

DOI: <https://doi.org/10.20883/jms.316>

Force decay of intermaxillary orthodontic elastics: in vitro study

Hubert Kardach^{1, a}, Aneta Olszewska^{1, b}, Ewa Firlej^{1, c}, Agnieszka Bogdanowicz^{1, d}, Ewelina Golusińska-Kardach^{2, e}, Anna Szponar-Żurowska^{1, f}, Barbara Biedziak^{1, h}

¹ Division of Facial Malformation, Department of Dental Surgery, Poznan University of Medical Sciences, Poland

² Department of Dental Surgery, Poznan University of Medical Sciences, Poland

^a <https://orcid.org/0000-0002-6204-4266>

^b <https://orcid.org/0000-0003-1286-6779>

^c <https://orcid.org/0000-0002-4070-1210>

^d <https://orcid.org/0000-0001-8364-1935>

^e <https://orcid.org/0000-0002-9520-2670>

^f <https://orcid.org/0000-0002-9226-1704>

^g <https://orcid.org/0000-0002-6150-9957>

^h <https://orcid.org/0000-0002-6150-9957>

ABSTRACT

Introduction. Orthodontic elastics are widely used in orthodontic treatment. It's been proved that they have advantages such as low cost, ease of use, but also disadvantages, mainly force decay in time and increased entrapment of biofilm. Amount of the force is of extreme significance. This force can be altered by physical or chemical factors.

Material and Methods. Latex elastics in 3 different diameters were selected for this study. Each elastic was stretched and placed on hooks that are at specified distances that equal 3 times the diameter of each elastic. The forces produced by stretching was measured using tension gauge and the measurement were taken at specific time intervals of 0h, 3h, 12h, 24h. The same process was repeated for elastics in dry and artificial environment.

Results. Elastics in the dry environment showed progressive force decay cause by stretching over time. Just after 3 hours force decay between 6,07% and 8,75% was observed. The biggest loss of force between 13,61 – 16,13 % was measured after 24 hours. Compared to the dry environment, an even more significant force decay was observed in the artificial saliva. After first 3 hours force loss was between 4,99% – 9,22%. The biggest force decay was observed after 24 hours and it was 5 % higher compared to dry environment.

Conclusions. 1) The artificial saliva environment and time of exposure to it, have a negative effect on the properties of elastomeric. 2) To maintain the effective orthodontic strength of elastics, they should be replaced every 12 hours.

Keywords: force decay, orthodontic elastics, artificial saliva, elastomeric.

Introduction

As technology evolves, orthodontic elastics are being increasingly used in orthodontics when treating with the use of permanent braces. They are the source of force necessary in the biomechanics of tooth movement [1]. The idea for using elastic material started in mid 1960s [2]. In 1970 Andreasen and Bishara conducted first research

on elastomeric chains. In the years that followed, more researchers have provided benefits of elastic material used in orthodontics, involving elastomeric chains and intraoral elastics, such as ease of use, low cost [3–5]. However, there are disadvantages, mainly degradation of elastic material that result in force decay in time and increased entrapment of biofilm [6–7].

The amount of orthodontic force depends on the type and size of the elastics used. The two types of elastics that are used to achieve this effect are the latex and non-latex types. Both ensure biocompatibility with the mucosa, and patient comfort. The non-latex are made of synthetic material (polyurethane) and are used in patients who are allergic to latex [8–9].

Orthodontic elastics have two defining parameters: their diameter (1/8", 3/16", 1/4", 5/16", 3/8") and the force they generate (2.5 oz, 3.5 oz, 4.5 oz, 6.5 oz). Elastics as the source of orthodontic power can be applied in orthopedic treatment e.g. extraorally in combination with a facial mask or they can be applied intraorally – stretched between the upper and lower aligners [10]. The amount of force applied is of extreme significance to the success of the treatment. This force can be altered by physical or chemical factors. Laboratory research assessing the properties of latex and non-latex elastics has shown that force decay is more significant in the non-latex [11–12].

Aim

The aim of this study was to assess the changes in force produced by orthodontic elastics in the oral cavity environment.

Material and Methods

The latex elastics chosen for the study came from one manufacturer (American Orthodontics) and in three different diameters (3/16", 4/16", 5/16"), all generating the same force (4.5 oz). According to the manufacturer, at three times the inner lumen stretch, the elastomer should produce a force of 4.5 oz. All the elastics used in the study were delivered on the same day, checked for use by dates and stored according to the instruction manual. 500 elastics of each size were submitted to the presellection process of the study. Torn or deformed pieces were discarded. This process was repeated for each of the diameters. 50 elastics of each diameter (3/16", 4/16", 5/16") were selected for the study in which the force they generate at different time intervals (0.3h, 12h, 24h) and in two different environments (dry and with artificial saliva) was observed. To observe

the behavior of elastomers in vitro in the environment of the oral cavity, an artificial saliva solution has been prepared according to the data in **Table 1** [13].

Table 1. Artificial saliva components

Chemical component	g/l
NaCl	0,7
KCl	1,2
KH ₂ PO ₄	0,2
NaHCO ₃	1,5
Na ₂ HPO ₄	0,26
KSCN	0,33

In order to carry out the study, plexiglass tiles with metal hooks placed at set distances (14.4 mm, 19.2 mm, 23.7 mm) that equal three times the diameter of each elastic were prepared. The elastics remained stretched on those hooks for the entirety of the study. The force produced by stretching the elastic three times, was measured in g/pound using a Haag-Streit Diagnostics Correx 250 g tension gauge (**Figure 1**) and the measurements were taken at specific time intervals of 0h, 3h, 12h, 24h – separately for each size of elastic. All those measurements were recorded by the same researcher. The same process was repeat-



Figure 1. Correx tension gauge

ed for the elastics submerged in room-temperature artificial saliva.

The results were analyzed using the Mann-Whitney test in order to assess the statistical differences between the effect of force produced by each size of the elastics in both dry and artificial saliva environments. The Dunn test was used to compare paired results (0–3h, 0–12h, 0–24h, 3–12h, 3–24h, 12–24h). The statistical significance threshold was set at $p = 0.05$.

Results

The average amount of force generated by orthodontic elastics in the dry and artificial saliva environments at different time intervals is presented in **Table 2**. The force decay of orthodontic elastics expressed in % at given time intervals ($t_1 = 0-3h$, $t_2 = 0-12h$, $t_3 = 0-24h$) is pictured in **Figures 2, 3 and 4**.

The elastics in the dry environment showed progressive force decay caused by stretching over time and the differences were statistically significant. Just after 3 hours of stretching, a force decay between 6,07% and 8,75% was observed. After 12 hours the force decay was at 11,39–11,94%. The biggest force decay of 13,61–16,13% was observed after 24 hours.

Compared to the dry environment, an even more significant force decay caused by stretching over time was observed in the artificial saliva environment. In the first three hours of stretching the force decay was at 4,99–9,22%. After 12 hours the force decay was at 10,60–14,64%. The biggest force decay was observed after 24 hours and it was 5% higher than in the elastics placed in the dry environment.

While conducting the study, it has been observed that the oral cavity environment and particularly the saliva solution, influence the mechanical properties of the elastic elements

Table 2. Elastics mean force values (g/pound + SD)

		t=0	SD	t=3	SD	t=12	SD	t=24	SD
Dry environment	3/16	122	10,35	114,6	8,32	108,1	9,94	102,5	6,80
	4/16	121,2	6,82	110,6	7,60	107	6,14	104,7	6,58
	5/16	114,7	7,38	105,7	8,86	101	8,33	96,2	6,19
Artificial saliva	3/16	114,2	9,60	108,5	8,10	102,1	7,36	92,4	6,72
	4/16	116,1	7,65	105,4	8,32	99,1	7,54	91	5,62
	5/16	104,1	9,73	98,7	8,13	91,5	9,22	86,7	5,94

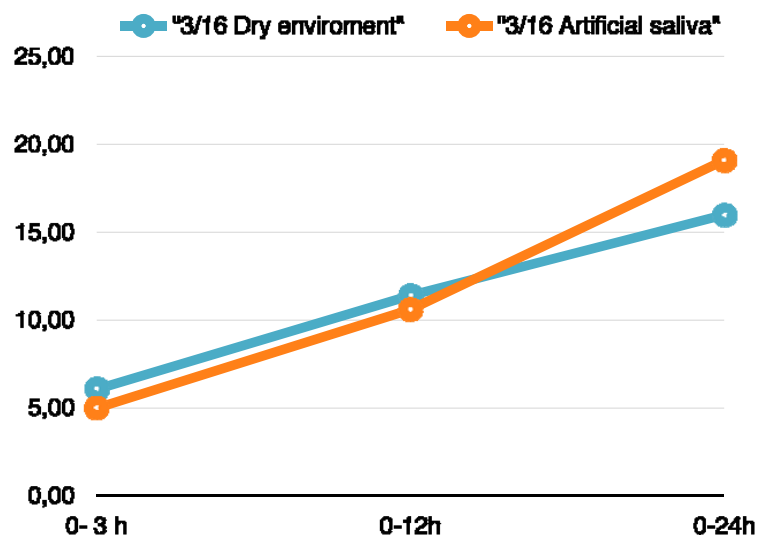


Figure 2. Force decay percentage comparison of 3/16 elastics in two environments

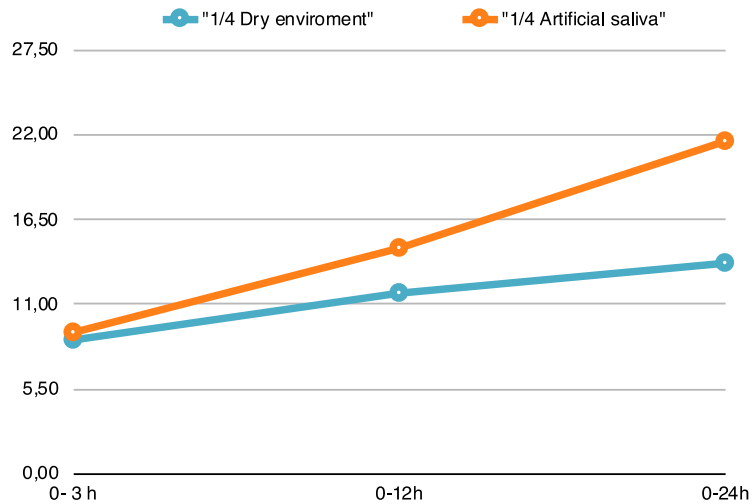


Figure 3. Force decay percentage comparison of 1/4 elastics in two environments

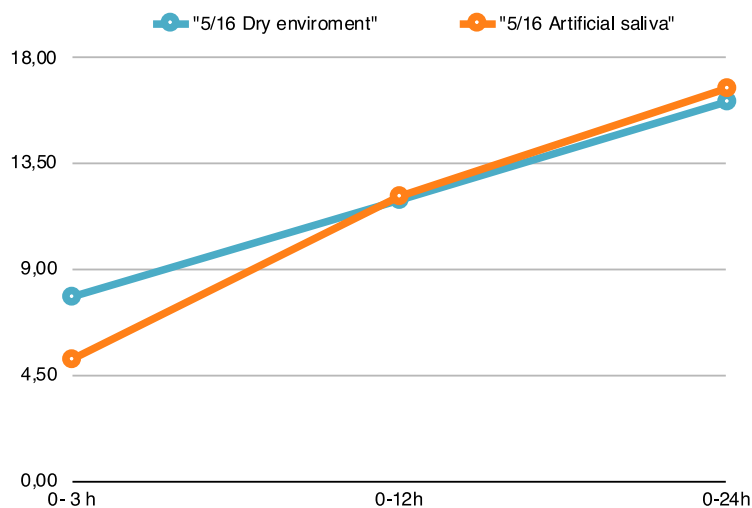


Figure 4. Force decay percentage comparison of 5/16 elastics in two environments

used in orthodontics. Kumar et al. came to similar conclusions when studying force decay of another type of orthodontic elastic elements – elastomeric chains. The researchers have observed a force decay of almost 50% after exposure to tea solutions and a 22% force decay after exposure to Coca-Cola [14]. In their in vivo study of mechanical properties of orthodontic elastics, Pithon et al. have compared force decay of latex and non-latex elastics. After 12 hours of usage by the patient, the 1/4" and 5/16" non-latex elastics have produced more orthodontic force than their latex counterparts. After 24 hours of wear, the 1/8" diameter latex elastics recorded the smallest force decay of those observed [15].

During orthodontic treatment, the elastic elements are exposed to the influence of many different factors such as solutions, individual

composition of a patient's saliva which includes a changing pH, dental hygiene treatments, various types and temperatures of ingested food, or the muscle force of the stomatognathic system during speaking and chewing. When analysing the force required in the biomechanics of orthodontic treatment, it is necessary to take into account the physical, mechanical and chemical factors that influence the elastic elements.

Conclusions

1. The orthodontic elastics have shown a progressive force decay.
2. The artificial saliva environment and time of exposure to it, have a negative effect on the properties of elastomers.

3. To maintain the effective orthodontic strength of elastics, they should be replaced every 12 hours

Acknowledgements

Conflict of interest statement

The authors declare no conflict of interest.

Funding sources

There are no sources of funding to declare.

Author contributions

HK, BB – conception and design, data analysis, interpretation; HK, AO, EF, AB – article drafting or critical advice; HK, BB – final approval.

References

1. Lacerda Dos Santos R, Pithon MM, Romanos MT. The influence of pH levels on mechanical and biological properties of nonlatex and latex elastics. *The Angle Orthodontist*. 2012;82:709–714.
2. Stoner MM. Extraction treatment. In: Graber TM, editor. *Orthodontic concepts and techniques*, volume 1. Philadelphia: W. B. Saunders; 1969.
3. Andreasen GF, Bishara SE. Comparison of elastik chains with elastics involved with intra-arch molar to molar forces. *Angle Orthod*. 1970;40:151–8.
4. Bishara SE, Andreasen GF. A comparison of time related forces between plastic elastiks and latex elastics. *Angle Orthod*. 1970;40: 319–28.
5. Buchmann N, Senn C, Ball J, Brauchli L. Influence of initial strain on the force decay of currently available elastic chains over time. *Angle Orthod*. 2012;82:529–35.
6. Ash JL, Nikolai RJ. Relaxation of orthodontic elastomeric chains and modules in vitro and in vivo. *J Dent Res*. 1978;57:685–90.
7. de Souza RA, de Araujo Magnani MB, Nouer DF, da Silva CO, Klein MI, Sallum EA, et al. Periodontal and microbiologic evaluation of 2 methods of archwire ligation: Ligature wires and elastomeric rings. *Am J Orthod Dentofacial Orthop*. 2008;134: 506–12.
8. Sauget PS, Stewart KT, Katona TR. The effect of pH levels on nonlatex vs latex interarch elastics. *The Angle Orthodontist*. 2011;81:1070–1074.
9. Beattie S, Monaghan P. An in vitro study simulating effects of daily diet and patient elastic band change compliance on orthodontic latex elastics. *The Angle Orthodontist*. 2004;74:234–239.
10. Pithon MM, Souza RF, Freitas LMA et al. Mechanical properties intermaxillary latex and latex-free elastics. *Journal of the World Federation of Orthodontists*. 2013;2:15–18.
11. Loriato LB, Machado AW, Pacheco W. Clinical and biomechanical aspects of elastics in Orthodontics. *Dental Press Journal of Orthodontics*. 2006;5:43–55.
12. Fernandes DJ, Fernandes GM, Artese F et al. Force extension relaxation of medium force orthodontic latex elastics. *The Angle Orthodontist*. 2011;81:812–819.
13. Loch J, Krawiec H. Zachowanie korozyjne stopów kobaltu w roztworze sztucznej śliny. *Archives of Foundry Engineering*. 2013;13:101–106.
14. Kumar K, Shetty S, Krithika MJ, et al. Effect of commonly used beverage, soft drink, and mouthwash on force delivered by elastomeric chain: a comparative in vitro study. *Journal of International Oral Health*. 2014;3:7–10.
15. Pithon MM, Mendes JL, da Silva CA et al. Force decay of latex and non-latex intermaxillary elastics: a clinical study. *European Journal of Orthodontics*. 2016;1:39–43.

Acceptance for editing: 2019-05-09
Acceptance for publication: 2019-06-29

Correspondence address:

Hubert Kardach
Division of Facial Malformation
Department of Dental Surgery
Poznan University of Medical Sciences
70 Bukowska Street, 60-812 Poznań, Poland
e-mail: hkardach@ump.edu.pl



ORIGINAL PAPER

DOI: <https://doi.org/10.20883/jms.324>

The influence of the shift work system on dietary factors contributing to the development of cardiovascular disease

Małgorzata Dobrzyńska^a, Ilona Górna^b, Grzegorz Kosewski^c, Magdalena Kowalówka^d, Izabela Bolesławska^e, Anna Morawska^e, Juliusz Przysławski^f

Department of Bromatology, Poznan University of Medical Sciences, Poland

^a <https://orcid.org/0000-0001-9589-522X>

^b <https://orcid.org/0000-0002-9652-0785>

^c <https://orcid.org/0000-0002-6380-7704>

^d <https://orcid.org/0000-0002-6484-5462>

^e <https://orcid.org/0000-0001-6780-3105>

^f <https://orcid.org/0000-0002-6957-0509>

^g <https://orcid.org/0000-0001-9205-2817>

ABSTRACT

Aim. The aim of this study was to assess eating behavior in the groups of women who are working on different, unchanged shifts as well as identifying differences in the consumption of nutrients that may increase the risk of cardiovascular disease.

Material and Methods. The study was carried out among 300 randomly selected women working in a permanent shift (morning, afternoon, night). In the study, the assessment of the daily intake was carried out using 24-h dietary recall. Anthropometric measurements were carried out to assess the nutritional status. The interview regarding the food consumption was complemented by dietary questionnaire about selected lifestyle parameters contributing to the development of cardiovascular disease and the type of their work.

Results. The body mass index (BMI) in all groups was within the adequate values. The analysis of waist to hip ratio (WHR) showed that in the morning and night shift, was exceeded the adequate values recommended in the prevention of cardiovascular disease (WHR = 0.83 ± 0.1 in both groups). The analysis of the daily food rations of women revealed disparities regarding nutritional recommendations. Statistically significant differences in protein and saccharose intake were observed ($p > 0.05$). The average vitamin D content in the daily food rations of women was insufficient (average $1.4 \mu\text{g}$ per day); however, it was not statistically significant.

Conclusions. The shift work system was influence on eating behaviors in study women. In particular in women which were worked on the night shift, which may contribute to the development of cardiovascular disease in the future.

Keywords: work system; nutritional status; dietary intake; dietary habits; cardiovascular disease; vitamin D.

Introduction

Cardiovascular disease is the most common cause of death in the world and contribute a significant epidemiological issue. Modern lifestyle can create a number of circumstances that aid inappropriate nutrition and inadequate health

habits, which may contribute to the development of cardiovascular disease. Fast pace of life, shift work system and the duties related to it result in reduced time to prepare home-cooked meals and favour the consumption of ready-made meals, highly-processed or fast-food products, becoming at the same time one of the most signifi-

cant risk factors for the development of disease of affluence [1, 2]. On the other hand, fashion for slimness among women leads to reduction of the energy value of food rations, which may also contribute to the development of cardiovascular disease [3, 4]. Moreover, inadequate health habits may be caused by the shift work system. An irregular sleep-wake rhythm and the long-term reduction of sleep contribute to a change in metabolism, a decrease in the resting metabolic rate and an increase in the glucose level in blood serum, which may eventually increase occurrence of obesity, diabetes, cardiovascular disease, gastrointestinal disease, sleep disorders or depression, thus leading to the development of the cardiovascular disease [5–9]. Additionally, vitamin D deficiency may occur among people working night shifts due to limited exposure to the sun [10, 11]. Additional factors that may contribute negatively to the development of cardiovascular disease are stress and low physical activity [12, 13].

Aim

The aim of this study was to assess eating behavior in the groups of women who are working on different, unchanged shifts. Simultaneously, comparison the consumption of selected nutrients which may increase the risk of cardiovascular disease.

Material and Methods

The study was carried out among 300 randomly selected women working in a different shift system, from the Wielkopolska Voivodeship aged between 18 and 61 years. The women participating in the study were divided into three groups, depending on their shift time (morning, afternoon, night).

The dietary intake level was assessed through the 24-hour dietary recall method according to the National Institute of Food and Nutrition (NIFN) guidelines [14]. Each woman was instructed on how to fill in the questionnaire for diet assessment. The 24-h dietary recall interviews were carried out individually (face to face) with each participating woman. Album of Photographs of Food Products and Dishes [15] was used to deter-

mine the amount of consumed foodstuffs. To analyse the qualitative and quantitative composition of daily food rations, databases prepared in the MS Access 2010 program were applied. The assessment of the nutrition was conducted the Standards of Human Nutrition [16].

The anthropometric measurements (body weight, height, waist and hip circumferences) were measured and use it to estimate nutritional status. The body mass index (BMI) was calculated as weight/height squared (kg/m^2) and waist to hip ratio (WHR) as the proportion of waist to hip circumferences.

The dietary intake was completed by dietary questionnaire about selected lifestyle parameters which may contribute to the development of cardiovascular disease.

The statistical analysis was conducted using the statistical program StatSoft, Inc. (2011) STATISTICA (data analysis software system), version 10. Distribution normality of the study groups was determined use the Shapiro-Wilk test.

Analyzing the differences between variables within three groups (for independent variables), for the normal distribution and equal variances, ANOVA test was used. In the absence of normality, the Kruskal-Wallis test was used. In the data analyses carried out, $\alpha = 0.05$ was assumed as the materiality level.

Results

The anthropometric characteristics of the studied groups of women was presented in **Table 1**.

There were no statistically significant differences between the studied groups in the age, body weight, high and BMI value. It is worth noting that the BMI value in all groups was within the adequate. The analysis of the WHR indicated that in the group of women working in the morning and the night shifts the adequate values were slightly exceeded. In the group of women working in the night shift, the WHR value was correct. The differences between the studied groups were statistically significant.

The analysis of food rations pointed out differences between the studied groups (**Table 1**).

Statistically significant differences between the studied groups were observed only in energy value, protein content and in the percentage of energy

Table 1. Characteristics of the studied groups of women depending on the shift work

	Morning shift (N = 100)		Afternoon shift (N = 100)		Night shift (N = 100)		P-value*
	Mean	SD	Mean	SD	Mean	SD	
Demographies							
Age (year)	33.9	10.5	33.3	10.2	32.3	10.1	0.5066**
Height (cm)	166	6.3	166	6.1	165	11.8	0.2741**
Body weight (kg)	60.5	8.7	57.9	5.5	59.1	8.1	0.1249**
BMI (kg/m ²)	21.9	3.1	21.1	2.1	21.7	2.6	0.1944**
Waist circumference (cm)	70.6	12.0	72.2	9.2	76.0	10.8	0.0012**
Hip circumference (cm)	84.7	13.6	90.6	8.4	91.4	10.0	0.0002**
WHR	0.83	0.1	0.79	0.1	0.83	0.1	0.0009**
Diet							
Energy (kcal)	1485	528	1608	423	1547	394	0.0365**
Protein (g)	60.2	23.1	68.5	17.0	67.9	17.3	0.0004**
Protein (%)	16.4	4.3	17.5	4.0	18.0	4.1	0.0124**
Fat (g)	57.8	24.5	62.6	21.5	62.9	22.6	0.1674**
Fat (%)	35.2	10.5	35.4	10.3	36.6	10.4	0.4845**
Carbohydrates (g)	185	79.3	196	79.4	181	67.0	0.4570**
Carbohydrates (%)	49.5	11.2	47.9	10.8	46.4	10.8	0.1882**
Cholesterol (mg)	369	260	331	203	369	260	0.4493*
Dietary fiber (g)	12.8	6.9	12.9	6.2	13.5	6.6	0.7538*
Saccharose (%)	11.1	7.9	10.3	6.2	8.72	5.6	0.0348*
Vitamin D (µg)	1.1	1.7	1.4	1.5	1.7	0.9	0,2525*

* ANOVA test

** Kruskal-Wallis test

SD – standard deviation, P – ns – not significant, BMI – Body mass index, WHR – waist to hip ratio

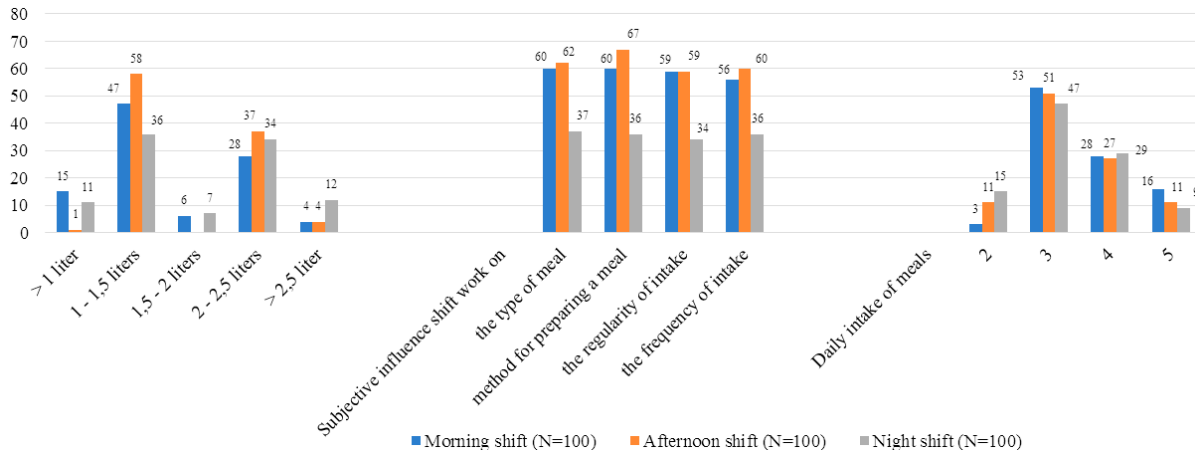


Figure 1. Selected dietary habits of the studied groups of women depending on the shift work

from saccharose. The estimate energy requirement in the all studied groups was insufficient – the average energy value for this group of women should be around 2000 kcal per day. While assessing the percentage of energy derived from saccharose, some insignificant excess of the recommended values was stated in the morning and night shifts. In the third group, this value was correct.

The analysis of energy from fat showed, that in all studied groups, it exceeded the adequate

values. Similar results were obtained in the case of the dietary cholesterol content in the food rations, which in all groups exceeded 300 mg per day. The next analysed parameter was the dietary fiber content. It was revealed that the average content of this component was insufficient in all studied groups, and did not exceed 52% of adequate intake. The average vitamin D content in the studied groups was only 9.5% of adequate intake.

Discussion

The diet plays a significant role in the maintaining health. It can also contribute to the development of cardiovascular disease by influence on many factors such as: blood pressure, anthropometric parameters and lipid profile parameters. It is widely known that shift work affecting the nutrition [17–21]. However, there is still a lack of information about what differences in the nutrition in different shift work and how these differences influence on the risk of cardiovascular disease.

The analysis of the selected anthropometric parameters showed that the BMI value in the studied groups was within the adequate values; however, the highest values of this parameter were stated in the group of the morning and night shifts. It can increase the risk of development of cardiovascular disease in these groups of women. It is also confirmed by research carried out by other authors, which indicated that night shift work correspondents to an increase in body mass and an occurrence of higher BMI values [21–25]. A similar relationship was stated in the case of the WHR, which may prove that people working the morning and night shifts have an increased tendency toward an excessive body mass [22, 23].

According to the American Heart Association guidelines, inadequate nutritional habits may contribute to the development of cardiovascular disease. An increase in the fat intake in the diet, in particular of saturated fatty acids, increased the content of energy from saccharose, decreased the content of fibre or increased dietary cholesterol content and inappropriate content of vitamins and minerals may significantly increase the risk of development of cardiovascular disease [26].

In this studied, there were statistically significant differences between the groups regarding specific parameters of diet assessment. The analysis of the intake level among the groups of women taking part in this studied showed statistically significant differences between energy intake as well as in the protein and saccharose content. The daily food rations did not provide sufficient energy intake. In the morning and night shifts, these values were slightly higher than the Basal Metabolic Rates, which may result from lack of time for preparing and eating meals during the day (frequent meals, but with low energy value). It cannot be ruled out that the participants

undervalued the declared levels. According to the most recent dietary guidelines, the demand for energy among women, taking into account low physical activity level, should reach from 1650 to 2350 kcal per day [16]. Low energy value of the daily food rations as compared to anthropometric values may indicate frequent changes in the diet, which may increase the risk of cardiovascular disease.

The analysis of protein intake and the indicated statistically significant differences between the groups may suggest that female night shift workers consumed so-called 'comfort foods' such as yogurt, cream cheese, kefir, quark, and meat, which are rich in protein more frequently in comparison to the other groups. Further analysis indicated that the highest percentage of energy derived from saccharose, with the adequate value reaching up to 10% of the energy value of the diet, was observed in the morning and night shifts [16]. The daily food rations of these groups were abundant in sweet snacks such as candy bars, cookies, and chocolate, which are the primary sources of saccharose. Moreover, an increased saccharose content could be the reason for a higher WHR values in these groups. Nevertheless, Assis et al. studied presents different results. In this research night shift workers consumed more saccharose as compared to the people working the morning shift, which was due to more frequent consumption of sweets [17]. The differences in the obtained results may be triggered by the diversity of cultural and nutritional habits.

The observed low intake of fiber and excessive intake of dietary cholesterol in all studied group may significantly increase the risk of the cardiovascular disease in the future.

According to the current literature, vitamin D plays a significant role in the prevention of cardiovascular disease. The research results conducted over the last few years reveal an increased risk of the occurrence of vitamin D deficiency among people doing shift work. That applies particularly to the people working the night shift. Therefore, the studied also takes into consideration the assessment of the consumption of vitamin D in the daily food rations. [10, 27]. The vitamin D intake within the diet should reach 15 µg per day, and in the case of women participating in the studied, it constituted about 10% of the demand [16]. However, it should be noted that the

primary source of vitamin D is its production in the skin, and its synthesis depends on exposure to the sun.

Thy analysis of the daily food rations revealed irregularities concerning the intake of specific nutrients within all the examined groups of women. In the group of night shift workers, the daily food rations were characterized by the percentage of energy derived from protein, fats, and carbohydrates that came closest to the standard; however, the percentage of saccharose was the highest in this group. This group had the highest number of meals during a day as compared to the others and consumed the lowest number of fluids. The results comply with the research of other authors. Reeves et al. underline in their research the difference between the number of consumed meals between the groups – the morning group had more meals during a day. What is more, a statistically significant difference in fluid (beverages containing caffeine) intake was observed in the group of women working the night shift [20]. Based on the analysis it was stated that in the case of night shift participants, the content of specific energy components and nutrients was the most deviated from the standard and was characterized by the highest percentage of energy derived from protein and fats and rich in dietary cholesterol. This group had the lowest number of meals per day as compared to the other groups and relatively large amounts of liquids, including a high intake of caffeine-rich beverages. Similar results were obtained in Love et al. [28].

Summing up the obtained results of the studied it should be noted that the shift work system has an impact on eating behaviors among the examined group of women. The impact of the shift work system is particularly visible in the case of night shift, which favours inadequate dietary habits, and its long-term effects may contribute to the occurrence of nutrient deficiency and may aid obesity, arterial hypertension and development of cardiovascular disease.

Acknowledgements

Conflict of interest statement

The authors declare no conflict of interest.

Funding sources

There are no sources of funding to declare.

References

1. Lowden A, Moreno C, Holmbäck U, Lennernäs M, Tucker P. Eating and shift work – effects on habits, metabolism and performance. *Scand J Work Environ Health*. 2010;36(2):150–162.
2. Puttonen S, Härmä M, Hublin C. Shift work and cardiovascular disease – pathways from circadian stress to morbidity. *Scand J Work Environ Health*. 2010; 36(2):96–108.
3. Zhao I, Turner C. The impact of shift work on people's daily health habits and adverse health outcomes. *Aust J Adv Nurs*. 2008;25:8–22.
4. Wang XS, Armstrong ME, Cairns BJ, Key TJ, Travis RC. Shift work and chronic disease: the epidemiological evidence. *Occup Med (Lond)*. 2011;61(2):78–89.
5. Buxton OM, Cain SW, O'Connor SP, Porter JH, Duffy JF, Wang W, et al. Adverse metabolic consequences in humans of prolonged sleep restriction combined with circadian disruption. *Sci Transl Med*. 2012;4(129):129ra43.
6. Antunes LC, Levandovski R, Dantas G, Caumo W, Hidalgo MP. Obesity and shift work: chronobiological aspects. *Nutr Res Rev*. 2010; 23(1):155–168.
7. Brum MC, Filho FF, Schnorr CC, Bottega GB, Rodrigues TC. Shift work and its association with metabolic disorders. *Diabetol Metab Syndr*. 2015;7:45.
8. Proper K, van de Langenberg D, Rodenburg W, Vermeulen R, van der Beek A, van Steeg H, et al. The relationship between shift work and metabolic risk factors – a systematic review of longitudinal studies. *Am J Prev Med*. 2016;50(5):e147–e157.
9. Hall AL, Franche RL, Koehoorn M. Examining exposure assessment in shift work research: A studied on depression among nurses. *Ann Work Expo Health*. 2018;62(2):182–194.
10. Daugaard S, Garde AH, Hansen AM, Vistisen HT, Rejnmark L, Kolstad HA. Indoor, outdoor, and night work and blood concentrations of vitamin D and parathyroid hormone. *Scand J Work Environ Health*. 2018;pii:3745.
11. Alefishat E, Abu Farha R. Determinants of vitamin D status among Jordanian employees: Focus on the night shift effect. *Int J Occup Med Environ Health*. 2016;29(5):859–870.
12. Van Amelsvoort LG, Schouten EG, Kok FJ. Impact of one year of shift work on cardiovascular disease risk factors. *J Occup Environ Med*. 2004;46(7):699–706.
13. Ha M, Park J. Shiftwork and metabolic risk factors of cardiovascular disease. *J Occup Health*. 2005;47(2):89–95.
14. Charzewska J. Instrukcja przeprowadzania wywiadu o spożyciu z 24 godzin. Zakład Epidemiologii Żywienia Instytutu Żywności i Żywienia, Warszawa, 1998.
15. Szponar L, Wolnicka K, Rychlik E. Album Fotografii Produktów i Potraw. IŻŻ, Warszawa, 2000.
16. Jarosz M. Normy żywienia dla populacji Polski. IŻŻ, Warszawa, 2008.
17. De Assis MA, Kupek E, Nahas MV, Bellisle F. Food intake and circadian rhythms in shift workers with a high workload. *Appetite*. 2003;40(2):175–183.

18. Morikawa Y, Miura K, Sasaki S, Yoshita K, Yoneyama S, Sakurai M, et al. Evaluation of the effects of shift work on nutrient intake: a cross-sectional study. *J Occup Health*. 2008;50(3):270–278.
19. Hemiö K, Puttonen S, Viitasalo K, Härmä M, Peltonen M, Lindström J. Food and nutrient intake among workers with different shift systems. *Occup Environ Med*. 2015;72(7):513–520.
20. Reeves SL, Newling-Ward E, Gissane C. The effect of shift-work on food intake and eating habits. *Nutr Food Sci*. 2004;34(5):216–221.
21. Wirth M, Burch J, Shivappa N, Steck S, Hurley T, Vena J, et al. Dietary inflammatory index scores differ by shift work status: NHANES 2005 to 2010. *J Occup Environ Med*. 2014;56(2):145–148.
22. Peplonska B, Bukowska A, Sobala W. Association of rotating night shift work with BMI and abdominal obesity among nurses and midwives. *PLoS One*. 2015;21:10(7):e0133761.
23. Van Amelsvoort LG, Schouten EG, Kok FJ. Duration of shift work related to body mass index and waist to hip ratio. *Int J Obes Relat Metab Disord*. 1999;23(9):973–978.
24. McGlynn N, Kirsh VA, Cotterchio M, Harris MA, Nadalin V, Kreiger N. Shift Work and Obesity among Canadian Women: A cross-sectional study using a novel exposure assessment tool. *PLoS One*. 2015;16;10(9):e0137561.
25. Atkinson G, Fullick S, Grindley C, Maclaren D. Exercise, energy balance and the shift worker. *Sports Med*. 2008;38(8):671–685.
26. Van Horn L, Carson JA, Appel LJ, Burke LE, Economos C, Karmally W. Recommended Dietary Pattern to Achieve Adherence to the American Heart Association/American College of Cardiology (AHA/ACC) Guidelines: A Scientific Statement From the American Heart Association. *Circulation*. 2016;134(22):e505–e529.
27. Coppeta L, Papa F, Magrini A. Are Shiftwork and Indoor Work Related to D3 Vitamin Deficiency? A Systematic Review of Current Evidences. *J Environ Public Health*. 2018;2018:8468742.
28. Love HL, Watters CA, Chang WC. Meal composition and shift work performance. *Can J Diet Pract Res*. 2005;66(1):38–40.

Acceptance for editing: 2019-05-09
Acceptance for publication: 2019-06-29

Correspondence address:
Małgorzata Dobrzyńska
Department of Bromatology
Poznan University of Medical Sciences
42 Marcelinska Street, 60-354 Poznań, Poland
phone: +48 618547198
e-mail: mdobrzyńska@ump.edu.pl



REVIEW PAPERS

DOI: <https://doi.org/10.20883/jms.352>

Causes and mechanisms of peritoneal fibrosis and possible application of NF- κ B inhibitor for prevention and treatment

Andrzej Breborowicz^{1,a}, Kazuo Umezawa²

¹ Department of Pathophysiology, Poznan University of Medical Sciences, Poland

² Department of Molecular Target Medicine, Aichi Medical University, Nagakute, Japan

^a <https://orcid.org/0000-0002-0916-623X>

ABSTRACT

Peritoneal dialysis is an established form of the renal replacement therapy in patients with end stage renal failure. Continuous Ambulatory Peritoneal Dialysis developed by Moncrief and Popovich in 1975 was a revolutionary event, and contributed much to wide application of that form of treatment in uremic patients. On the other hand, the weak point of peritoneal dialysis is relatively short viability of the peritoneum as the dialysis membrane. Two main peritoneal pathologies are observed in patients treated with that form of renal replacement therapy: neovascularization of the membrane what causes increased peritoneal permeability to osmotic solutes and ultrafiltration failure, and fibrosis which results also in ultrafiltration failure due to its decreased hydraulic conductivity and reduced permeability to uremic toxins. Meanwhile, an NF- κ B inhibitor DHMEQ was discovered in 2000 and has been successfully used to suppress various inflammatory and neoplastic disease models. NF- κ B is likely to be involved in the mechanism of peritoneal inflammation and fibrosis. We have studied whether DHMEQ would inhibit cellular model of peritoneal inflammation and fibrosis. It inhibited inflammatory cytokine and collagen productions in primary culture of human peritoneal mesothelial cells, and intraperitoneal administration of NF- κ B inhibitors would be useful to suppress peritoneal fibrosis.

Keywords: fibrosis, NF- κ B, peritoneal dialysis.

Peritoneal membrane fibrosis during dialysis: causes and mechanisms

Peritoneal dialysis is an established form of the renal replacement therapy in patients with end stage renal failure. Development in 1975 by Moncrief and Popovich technique of Continuous Ambulatory Peritoneal Dialysis was a revolutionary event which strongly contributed to wide application of that form of treatment in uremic patients [1]. Peritoneal dialysis is cheaper than hemodialysis and provides better quality of life and results in comparable to hemodialysis survival during first 5 years of treatment [2]. Additio-

nally peritoneal dialysis, better than hemodialysis, preserves residual kidney function what may result in lower amount of systemic complications [3]. Patients treated with peritoneal dialysis have lower risk, than hemodialysis patients, of complications after renal transplantation [4]. In 2008 about 200,000 and in 2012 approximately 300,000 patients were treated with peritoneal dialysis worldwide [5].

The weak point of peritoneal dialysis is relatively short viability of the peritoneum as the dialysis membrane. Approximately 50% of patients treated with chronic peritoneal dialysis for more than 6 years develop ultrafiltration failure what translates into lower efficiency of removal of

water and uremic solutes into the dialysate [6]. Two main peritoneal pathologies are observed in patients treated with that form of renal replacement therapy: neovascularization of the membrane what causes increased peritoneal permeability to osmotic solutes and ultrafiltration failure, and fibrosis which results also in ultrafiltration failure due to its decreased hydraulic conductivity and reduced permeability to uremic toxins [7]. In the extreme situations peritoneal overgrowth of the connective tissue causes encapsulating peritoneal sclerosis, which consequence is not only ultrafiltration failure but also entrapment of intestines in the fibrotic tissue leading to life threatening bowels obstruction [8]. Prevalence of that pathology in peritoneal dialysis patients is proportional to length of the renal replacement therapy and in some studies approaches 18.4% [9].

Besides length of therapy the other factors predisposing to the morphological changes in the peritoneum are diabetes mellitus and uremia, however dialysis related factors are much more important [10]. Episodes of peritonitis may accelerate progression of the dialysis induced changes in the structure and function of the peritoneum leading to ultrafiltration failure [11]. However even without episodes of peritonitis repeated infusion of the dialysis fluid into the peritoneal cavity induces chronic "sterile" inflammatory reaction which contributes both to neovascularization of the peritoneum and its fibrosis [12]. Implantation of the peritoneal catheter and intraperitoneal infusion of the sterile dialysis fluid induce inflammation, simply due to mechanical irritation of the peritoneum [13].

One of the most important factor causing intraperitoneal inflammation and fibrotic changes in the peritoneum is low biocompatibility of the fluids used during peritoneal dialysis. Biocompatibility of the dialysis solutions is related to their low pH, hyperosmolality, high concentration of glucose, presence of glucose degradation products (GDP) and lactate. Exposure of the mesothelial cells in *in vitro* culture to the acidic dialysis fluid which subsequently, to imitate the *in vivo* conditions, was diluted with the effluent dialysate from dialyzed patients resulted in their stimulation reflected by increased synthesis of interleukin 6 [14]. In rats dialyzed during 6 weeks with dialysis fluid with neutral pH and low concentration of GDP, intraperitoneal inflammation

was lower than in animals treated with standard acidic, high GDP dialysis fluid. Additionally effluent dialysate collected from the first group of animals caused weaker *in vitro* synthesis of collagen in mesothelial cells, what was reflected *in vivo* by reduced fibrosis of the peritoneum [15].

Glucose is used in the dialysis fluids in the unphysiologically high concentrations up to 235 mmol/L to create osmotic gradient between bloodstream and dialysate, necessary for induction of the transperitoneal ultrafiltration of fluid. However glucose toxic effect towards the peritoneal mesothelial cells in such scenario depends not only on hyperosmolality [16]. Oxidative stress in mesothelial cells exposed to high glucose concentration induces their senescence [17] apoptosis [18] and epithelial to mesenchymal transformation (EMT) [19]. Mesothelial senescence, apoptosis or mesenchymal transformation may lead to progression of the peritoneal fibrosis [20, 21].

Molecular mechanisms of EMT of mesothelial cells and peritoneal fibrosis are described in various recent publications, but still some details are missing. [22]. Mechanisms of these disorders are not identical in various pathological processes and therefore we should not translate directly observations from studies on various models of fibrosis to the conditions in the peritoneum during chronic peritoneal dialysis. Some mechanisms causing EMT in various experimental models have opposite effect in peritoneal mesothelium. For example, Hepatocyte Growth Factor prevents EMT in mesothelial cells, whereas has opposite effect in hepatocytes [22, 23]. Another example is the role of p38MAPK, which induces synthesis of inflammatory cytokines potentially favoring process of EMT but on the other hand it stimulates E-cadherin expression in mesothelial cells, which prevents their EMT by modulating the TAK1-NF- κ B pathway [24].

An important role in EMT of the mesothelial cells during peritoneal dialysis plays TGF- β 1, which production in these cells is enhanced in presence of high glucose concentration [25]. TGF β cytokines induce mesothelial EMT by Smad-dependent and Smad-independent pathways [26]. TGF β 1 downregulates in mesothelial cells BMP-7 signaling, which determines the maintenance of the epithelial phenotype of these cells [27]. TGF β 1 causes p38 and JNK MAPK activation pathway due to activation of TAK1, which

is an activator of NF- κ B. Inhibition of NF- κ B in mesothelial cells may slow down and even partially reverse their EMT [28]. Activation of JNK MAPK pathway via ligand binding to Toll-like receptor that has a cytoplasmic signaling homologous to IL-1, results in activation of NF- κ B and MAPK. IL-1 is a stronger inducer of NF- κ B activation in mesothelial cells than TGF β 1 but their effects are additive. Inhibition of NF- κ B in mesothelial cells from peritoneal dialysis patients prevents their EMT after treatment with TGF β and IL-1 [29]. These observations prove the role of intraperitoneal inflammation during peritoneal dialysis in progression of the peritoneal fibrosis.

Can we slow down progression of peritoneal fibrosis during chronic peritoneal dialysis?

Bioincompatible dialysis fluids and unphysiological procedure of peritoneal dialysis which result in constant induction of the intraperitoneal inflammatory response are the main causes of the peritoneal pathology in that group of patients. Despite several improvements in the composition of the dialysis fluids such as introduction of dialysis solutions with neutral pH, lower GDP concentrations, alternative to glucose osmotic solutes, problem of peritoneal damage during chronic dialysis still exists. Results from clinical studies are conflicting. In long term study performed in Netherlands, reduced incidence of peritonitis, better transperitoneal ultrafiltration were observed in patients dialyzed with low GDP and neutral pH solutions, as compared to a group treated with standard fluids with high GDP and low pH. However no differences were observed between the two studied groups in peritoneal transport characteristics, or intensity of the intraperitoneal inflammation [30]. In another study from Korea application of a new dialysis fluid with normal pH and low GDP level did not affect the peritoneal permeability to solutes and water but the authors observed reduction in the intensity of the intraperitoneal inflammation [31]. One can say that introduction of new more biocompatible dialysis fluids reduced but not eliminated the negative effect of peritoneal dialysis on the peritoneal structure and function. Problem of the peritoneal damage probable cannot be totally eliminated because pro-

cedure of peritoneal dialysis based on repeated intraperitoneal infusions of the dialysis fluid into the peritoneal cavity is not biocompatible *per se*. An interesting study, supporting that statement was done by Aoki and colleagues, who constructed *in vitro* model of peritoneal cavity lined with mesothelial and endothelial cells. Repeated infusion of physiological solutions (ie. Eagles medium) or dialysis fluids resulted in inhibition of nitric oxide synthase activity both in endothelial and mesothelial cells and EMT of mesothelial cells [32]. These results suggest that repeated infusion of any solution into the peritoneal cavity will trigger EMT of mesothelium. Therefore there is still a big interest in search for mechanisms and agents which can reduce the peritoneal injury during chronic peritoneal dialysis.

Some investigators hypothesized that high glucose induced peritoneal fibrosis is linked with angiotensin II acting via AT1Rs with subsequent activation of the intracellular signaling, such as ie. NF- κ B, leading to fibrosis [33]. Mesothelial cells exposed to high glucose concentration synthesize various elements of the renin-angiotensin system [34]. In addition to high glucose effect, low pH of the dialysis fluid may increase angiotensin receptors expression, what may result in enhancement of fibrosis [35]. In experimental model of chronic peritoneal dialysis in rats use of angiotensin inhibitors valsartan or lisinopril resulted in reduced peritoneal fibrosis caused by repeated exposure to high glucose dialysis fluid [36].

Recently various treatment leading to reduction of peritoneal fibrosis in conditions of peritoneal dialysis were proposed. The final target of these studies was defined as inhibition of the dialysis induced peritoneal fibrosis. Yang and coworkers found that during 4 months peritoneal dialysis performed with high glucose fluid in mice, intraperitoneal supplementation of 1,25(OH) $_2$ D $_3$ at weekly intervals, attenuated dialysis induced mesothelial apoptosis, EMT and fibrosis of peritoneum [37]. In another study Wu and coworkers found increased expression of TGF- β , EMT and autophagy in peritoneal mesothelial cells obtained from the effluent dialysate from patients treated with chronic peritoneal dialysis. In experiments on mesothelial cells in *in vitro* culture they demonstrated that inhibition of the cellular autophagy reduced glucose induced EMT and expression of fibrotic markers [38]. Researchers

from Italy demonstrated that extract from olive leaves blocks in *in vitro* cultured mesothelial cells their TGF- β induced EMT and expression of cellular markers of fibrosis [39]. Cheng and coworkers demonstrated that hydrogen sulfide inhibits EMT of mesothelial cells in *in vitro* culture and reduced peritoneal fibrosis in a rat model of chronic peritoneal dialysis [40]. Inhibition of heparanase blocks glucose induced EMT of the mesothelial cells and changes of their monolayers permeability studied in *in vitro* model [41]. Another approach leading to prevention of peritoneal fibrosis is use of the antioxidants. Wakabayashi and coworkers induced peritoneal fibrosis in rats with chlorhexidine gluconate and simultaneous oral supplementation with the natural antioxidant astaxanthin reduced the peritoneal expression of TGF- β , snail mRNA and type 3 collagen with decrease of the peritoneal thickness [42]. Similar observations with the another antioxidant selenium come from *in vitro* experiments on human mesothelial cells [43]. In another study on rats repeatedly infused with the dialysis fluid and endotoxin to induce peritonitis, inhibition of TAK1-NF- κ B pathway with the PPAR β/δ agonist GW501516 prevented peritoneal fibrosis. Additionally in *in vitro* cultured rat mesothelial cells inhibition of TAK1-NF- κ B pathway reduced glucose induced inflammation [44]. Kitamura and coworkers reported protective effect against the GDP induced peritoneal fibrosis in mice, of a tea polyphenol (-)-epigallocatechin gallate which inhibited NF- κ B pathway [45]. Washida and coworkers injected male rats with chlorhexidine what induced peritoneal thickening with the overgrowth of the connective tissue, macrophage infiltration and angiogenesis [46]. In animals simultaneously treated with Rho-kinase inhibitor fasudil fibrotic changes were significantly reduced and the expression of markers of tissue fibrosis, such as TGF- β , fibronectin and α -smooth muscle cell actin was reduced [46].

Presented above studies show the wide range of possible approaches aimed at inhibition of the dialysis induced peritoneal fibrosis. However most of the results come from acute studies or experiments lasting 3–4 weeks and the used doses of the tested substances sometimes were very high what potentially could induce the negative side effects [45]. Therefore further studies are required to find out/exclude the potential side effects of such a long term treatment. It seems

to be an option to test more than one substance at the same time to evaluate if due to different mechanisms of action they can have synergistic effect preventing the peritoneal fibrosis in conditions of peritoneal dialysis. After verification of these substances in further *in vitro* and *in vivo* experiments on animals, their final suitability for prevention of the peritoneal fibrosis in patients treated with chronic peritoneal dialysis requires the clinical studies.

Discovery and inhibitory mechanism of NF- κ B inhibitor DHMEQ

In the course of our search for NF- κ B inhibitors of low molecular weight, we designed and synthesized new NF- κ B inhibitors based on the structure of epoxyquinomicin C (**Figure 1**). Epoxyquinomicin C was isolated as a weak antibiotic, but it showed no toxicity in animals. Although the structurally related compounds such as panepoxydone [47] and cycloepoxydone [48] were reported to inhibit NF- κ B, epoxyquinomicin C did not inhibit NF- κ B. However, after the removal of the protruding hydroxymethyl moiety, the designed compound, dehydroxymethylepoxyquinomicin (DHMEQ, **Figure 1**), did inhibit NF- κ B activity [49]. We also found that DHMEQ ameliorated inflammation in a collagen-induced rheumatoid arthritis in mice when administered by the IP route [49]. In this way, we found a new NF- κ B inhibitor active in animal experiment.

Racemic DHMEQ can be synthesized from 2,5-dimethoxyaniline in 5 steps [50], and can be separated into each enantiomer practically by lipase [51]. Lipase reacts with racemic dihexanoyl-DHMEQ to give (-)-DHMEQ and monohexanoyl-(+)-DHMEQ that can be easily removed by difference of solubility. (-)-DHMEQ is about 10 times more effective than (+)-DHMEQ in inhibiting NF- κ B [50]. (-)-DHMEQ is mainly used for the cellular experiments, and racemic DHMEQ for the animal experiments. For the development into drugs, racemic DHMEQ is being used.

For the mechanism of DHMEQ, we have firstly reported that it inhibits the nuclear translocation of NF- κ B [52]. However, later, we have found that DHMEQ directly binds to the Rel-family proteins to inhibit their DNA-binding activity [53]. Inhibition of NF- κ B nuclear translocation is likely to be

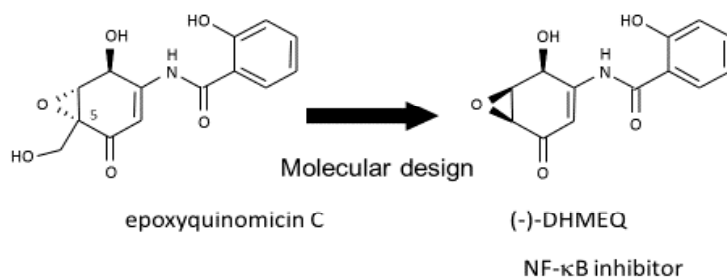


Figure 1. Molecular design of NF-κB inhibitor DHMEQ based on the structure of antibiotic epoxyquinomicin C

a result after the inhibition of DNA binding [54]. Rel family proteins are the constituents of NF-κB molecules including p65, RelB, c-Rel, p50, and p52. (-)-DHMEQ was found to bind to p65 covalently with a 1:1 stoichiometry as revealed by surface plasmon resonance (SPR) and MALDI-TOF mass spectrum (MS) analyses. MS analysis of the chymotrypsin-digested peptide suggested the binding of (-)-DHMEQ to a specific cysteine residue. In the case of p65, DHMEQ only binds to the Cys38 residue, which is located close to the DNA. The binding is specific, since it does not bind to other cysteine residues such as Cys120 in p65. Observation of the adduct in MALDI-TOF MS would indicate that the (-)-DHMEQ-cysteine binding is a covalent one. The formation of DHMEQ-cysteine covalent binding in the protein was supported by chemical synthesis of the conjugate molecule [55]. Since (-)-DHMEQ covalently binds to the cysteine residue in an NF-κB molecule, the inhibitory effect is irreversible. LPS induces NF-κB activation in 30 min in a macrophage-like mouse monocytic leukemia cell line RAW264.7. In our experiment, (-)-DHMEQ was added for only 15 min and then washed out in this experimental system. Even after 8 h of the removal of (-)-DHMEQ, the cells were dormant, and LPS did not activate NF-κB, suggesting that NF-κB would be inhibited irreversibly [56].

All Rel family proteins possess specific cysteine residues essential for their DNA binding. (-)-DHMEQ binds to those cysteine residues of p65, cRel, RelB, and p50, but not of p52. In case of RelB, (-)-DHMEQ inhibits not only DNA-binding of RelB, but also its interaction to importin [57]. It also induces instability of RelB. Thus, (-)-DHMEQ specifically binds to a cysteine residue in both the canonical (p65 and p50) and the noncanonical (RelB) NF-κB components [53, 57]. It is likely that DHMEQ can enter into a specific pocket via

a key and lock mechanism to bind to the limited cysteine residue.

These mechanisms may explain the highly selective NF-κB inhibition and the low toxic effect of DHMEQ in cells and in animals.

Therapeutic activity of DHMEQ in animal models of inflammation and cancer

DHMEQ has been widely used to study the mechanism of diseases, especially to study the role of NF-κB in various disease models in situ and in vivo. The most important transcription factor in osteoclastogenesis is NFATc1. DHMEQ inhibited the expression of NFATc1 in mouse primary culture macrophages to show the involvement of NF-κB in the mechanism of expression [58]. DHMEQ also inhibited the expression of NFATc1 in mouse rheumatoid arthritis model [59]. Cancer stem cell is still a popular topic in cancer research. They say it is important to suppress cancer stem cell activity to eliminate the cancer growth. DHMEQ was used to study the essential factors of cancer stem cells. Goto and coworkers demonstrated that NF-κB and Akt may be essential for the activity of breast cancer cells using DHMEQ [60, 61]. Involvement of NF-κB in the mechanism of early phase [62] and late phase [63] of metastasis was suggested by the experiments using DHMEQ, which was reviewed in [64].

Not only for the mechanistic study, DHMEQ is likely to be useful as new chemotherapeutic agent. Recently reported therapeutic activities of DHMEQ in animal experiments are shown below.

Firstly, topical application to skin of rodents ameliorated atopic dermatitis models. DHMEQ ointment showed anti-inflammatory activity in the mouse genetic atopic dermatitis model. It sho-

wed similar or stronger anti-inflammatory activities compared with betamethasone and tacrolimus ointments [65]. Accumulation of mast cells was inhibited by DHMEQ ointment in this model. Later DHMEQ was found to inhibit MMP-2 expression and cellular invasion of mouse primary culture mast cells treated with DNP antigen and IgE [66]. More recently, DHMEQ ointment was shown to suppress development of chemically induced atopic dermatitis-like lesions in mice [67, 68]. This atopic dermatitis model in BALB/c mice was chronically induced by the repetitive and alternative application of 2,4-dinitrochlorobenzene (DNCB) and oxazolone (OX) on ears, and stratum corneum of the ear skin was additionally stripped off with surgical tapes before each challenge with DNCB/OX. The lesions reaches to peak as well as DHMEQ arrives to its efficacy on day 38. The procedure using adhesive tape in preparation significantly accelerated the skin inflammation. Results showed that the drug reduced the ear thickness, epidermal thickness, mast cell infiltration, and gene expressions of interleukin (IL)-4, IL-13 and interferon (IFN)- γ in ear tissues [68]. Secondly, DHMEQ is being developed for anti-inflammatory and anticancer therapy by intraperitoneal administration, which is discussed later

Secondly, intraperitoneal (IP) administration of DHMEQ ameliorated various inflammatory and neoplastic disease models in animal

experiments. Amniotic apoptosis is essential for the onset of delivery. On the other hand, too early amniotic apoptosis causes baby loss. Activated macrophages around the amniotic epithelial cells are considered to cause amniotic apoptosis producing TNF- α and NO. The TNF- α receptor 1 is expressed in the amniotic epithelial cells. IP administration of DHMEQ inhibited TNF- α and iNOS expressions in pregnant mice to inhibit amniotic apoptosis in this model [69].

Recently, it was reported that IP administration of DHMEQ ameliorates dinitrobenzene sulfonic acid (DNBA)-induced colitis in rats [70]. IP administration of DHMEQ also inhibited dextran-sulfate-sodium-induced colitis in rats [71].

DHMEQ inhibits cancer progression in various animal models. IP administration of DHMEQ inhibited the growth of hormone-insensitive prostate carcinoma [72] and breast carcinoma [73]. It also inhibited thyroid carcinoma [74], regional model of glioma [75], and various lymphomas including adult T-cell leukemia [76], and multiple myeloma [77].

Fluke-induced cholangiocarcinoma is still common in Thailand, and it is one of the most difficult cancers to treat, and there is no effective chemotherapeutic regimen at present. Seubwai and coworkers reported that IP administration of DHMEQ inhibited the growth of cholangiocarcinoma in mice [78]. Normal bile duct epithelia rarely expressed NF- κ B subunits such as p50,

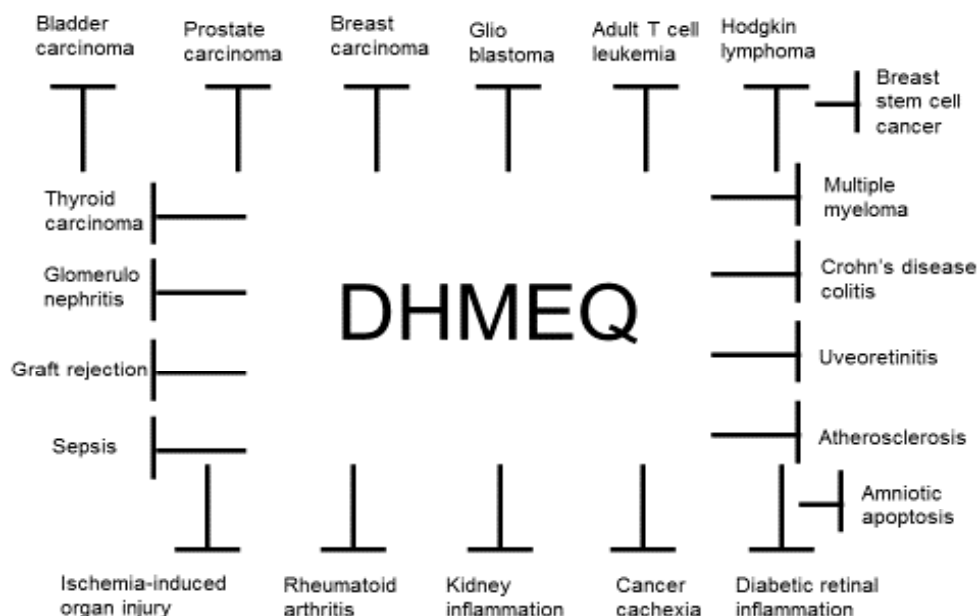


Figure 2. Anti-inflammatory and anticancer activities of DHMEQ in animal experiments. DHMEQ was all administered by intraperitoneal route

p52 and p65, whereas all cholangiocarcinoma patient tissues over-expressed these NF- κ B subunits. DHMEQ increased apoptosis by decreasing the expressions of anti-apoptotic proteins such as Bcl-2 and XIAP in cultured cholangiocarcinoma cells. Moreover, DHMEQ effectively reduced tumor size in cholangiocarcinoma-inoculated mice.

Recently, Ito and coworkers investigated the anticancer effect of DHMEQ in CDDP-resistant bladder cancer cells [79]. Invasive bladder carcinoma cell line T24 and its CDDP-resistant cell line T24PR were used. The NF- κ B activity was stronger in T24PR cells than in T24 cells. DHMEQ alone effectively lowered cell viability and induced apoptosis in T24PR cells. Moreover, using mouse xenograft models, the mean volume of tumors treated with the combination of DHMEQ and paclitaxel was significantly smaller than those treated with paclitaxel alone. Thus, IP administration of DHMEQ showed anticancer activity alone, and also increased the sensitivity to paclitaxel.

Anti-inflammatory and anticancer activities of DHMEQ in animal models are summarized in **Figure 2**, where DHMEQ was given to animals by IP injection in all cases.

Possible application of DHMEQ for the prevention and treatment of peritoneal fibrosis

Thus, IP administration of DHMEQ is quite effective to suppress various inflammatory and neoplastic disease models in animals. No toxicity has been reported so far. For the mechanism of anti-inflammatory and anticancer activity, it is likely

that DHMEQ acts only in the peritoneal cavity [80, 81], because it is easily metabolized in the blood. Because DHMEQ does not enter systemic circulation, IP administration of DHMEQ is considered to be a safe therapy.

Recently, we have demonstrated that DHMEQ inhibits primary cultured human peritoneal cells [82]. We studied the effects of DHMEQ on the functions of human peritoneal mesothelial cells (HPMC) in situ. DHMEQ was not toxic at 1–10 μ g/ml to HPMC. Synthesis of IL-6, MCP-1 and hyaluronan in unstimulated and stimulated with interleukin-1 was measured. DHMEQ at 10 μ g/ml reduced in unstimulated and stimulated HPMC synthesis of IL-6, MCP-1 and hyaluronan (**Figure 3**). The observed effects should be due to the suppression of gene expression responsible for the synthesis of these molecules. DHMEQ also modified the effects of the effluent dialysates from continuous ambulatory peritoneal dialysis (CAPD) patients on the function of HPMC. In the presence of dialysate, DHMEQ inhibited the collagen synthesis by HPMC. These results show that DHMEQ effectively reduces inflammatory response in HPMC and prevents dialysate-induced proliferation and collagen synthesis in these cells. Therefore, IP administration of DHMEQ would be useful for the prevention of progressive dialysis-induced damage to the peritoneum.

Acknowledgements

Conflict of interest statement

The authors declare no conflict of interest.

Funding sources

There are no sources of funding to declare.

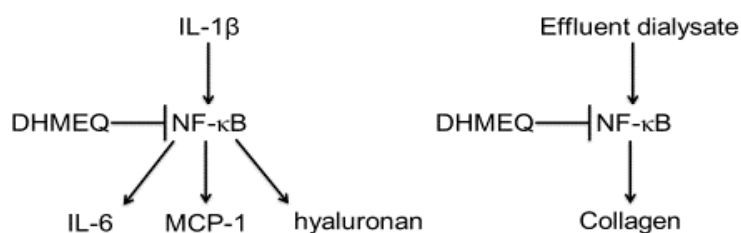


Figure 3. Inhibition of inflammatory cytokine, hyaluronan, and collagen synthesis by DHMEQ in human primary culture peritoneal cells. Human peritoneal mesothelial cells (HPMC) were supplied by the patients with continuous ambulatory peritoneal dialysis (CAPD)

References

1. Popovich RP, Moncrief JW, Decherd JF, Bomar JB, Pyle WK. The definition of a novel portable/wearable equilibrium dialysis technique (abstract). *Trans Am Soc Artif Intern Organs*. 1976;5:64.
2. Struijk DG. Peritoneal Dialysis in Western Countries. *Kidney Dis (Basel)*. 2015; 1:157–164.
3. Krediet RT. Preservation of Residual Kidney Function and Urine Volume in Patients on Dialysis. *Clin J Am Soc Nephrol*. 2017;12:377–379.
4. Jain D, Haddad DB, Goel N. Choice of dialysis modality prior to kidney transplantation: Does it matter? *World J Nephrol*. 2019;8:1–10.
5. Jain AK, Blake P, Cordy P, Garg AX. Global trends in rates of peritoneal dialysis. *J Am Soc Nephrol*. 2012;23:533–544.
6. Davies SJ, Bryan J, Phillips L, Russell GI. Longitudinal changes in peritoneal kinetics: the effects of peritoneal dialysis and peritonitis. *Nephrol Dial Transplant*. 1996;11:498–506.
7. de Lima SM, Otoni A, Sabino AP, Dusse LM, Gomes KB, Pinto SW, et al. Inflammation, neoangiogenesis and fibrosis in peritoneal dialysis. *Clin Chim Acta*. 2013;421:46–50.
8. Danford CJ, Lin SC, Smith MP, Wolf J, Encapsulating peritoneal sclerosis. *World J Gastroenterol*. 2018;24:3101–3111.
9. Brown EA, Bargman J, van Biesen W, Chang MY, Finkelstein FO, Hurst H, Johnson DW, et al. Length of Time on Peritoneal Dialysis and Encapsulating Peritoneal Sclerosis – Position Paper for ISPD: 2017 Update. *Perit Dial Int*. 2017;37:362–374.
10. Honda K, Hamada C, Nakayama M, Miyazaki M, Sherif AM, Harada T, et al. Peritoneal Biopsy Study Group of the Japanese Society for Peritoneal Dialysis. Impact of uremia, diabetes, and peritoneal dialysis itself on the pathogenesis of peritoneal sclerosis: a quantitative study of peritoneal membrane morphology. *Clin J Am Soc Nephrol*. 2008;3:720–728.
11. van Esch S, van Diepen ATN, Struijk DG, Krediet RT. The mutual relationship between peritonitis and peritoneal transport. *Perit Dial Int*. 2016;36:33–42.
12. Di Paolo N, Sacchi G. Atlas of peritoneal histology – in normal conditions and during peritoneal dialysis. *Perit Dial Int*. 2000;20:S5–S10.
13. Flessner MF, Credit K, Henderson K. Peritoneal changes after exposure to sterile solutions by catheter. *J Am Soc Nephrol*. 2007;18:2294–302.
14. Breborowicz A, Rodela H, Karoń J, Martis L, Oreopoulos DG. In vitro simulation of the effect of peritoneal dialysis solution on mesothelial cells. *Am J Kidney Dis*. 1997;29:404–409.
15. Wiczorowska-Tobis K, Polubinska A, Schaub TP, Schilling H, Wisniewska J, Witowski J, et al. Influence of neutral-pH dialysis solutions on the peritoneal membrane: a long-term investigation in rats. *Perit Dial Int*. 2001;21(Suppl 3):S108–S113.
16. Breborowicz A, Rodela H, Oreopoulos DG. Toxicity of osmotic solutes on human mesothelial cells in vitro. *Kidney Int*. 1992;41:1280–1285.
17. Ksiazek K, Breborowicz A, Jörres A, Witowski J. Oxidative stress contributes to accelerated development of the senescent phenotype in human peritoneal mesothelial cells exposed to high glucose. *Free Radic Biol Med*. 2007;42:636–641.
18. Zhang X, Liang D, Guo B, Yang L, Wang L, Ma J. Zinc inhibits high glucose-induced apoptosis in peritoneal mesothelial cells. *Biol Trace Elem Res*. 2012;150:424–432.
19. López-Cabrera M. Mesenchymal Conversion of Mesothelial Cells Is a Key Event in the Pathophysiology of the Peritoneum during Peritoneal Dialysis. *Adv Med*. 2014;2014:473134.
20. Strippoli R, Moreno-Vicente R, Battistelli C, Cicchini C, Noce V, Amicone L, et al. Molecular Mechanisms Underlying Peritoneal EMT and Fibrosis. *Stem Cells Int*. 2016;3543678.
21. Lopez-Anton M, Rudolf A, Baird DM, Roger L, Jones RE, Witowski J, et al. Telomere length profiles in primary human peritoneal mesothelial cells are consistent with senescence. *Mech Ageing Dev*. 2017;164:37–40.
22. Yu MA, Shin KS, Kim JH, Kim YI, Chung SS, Park SH, et al. HGF and BMP-7 ameliorate high glucose-induced epithelial-to-mesenchymal transition of peritoneal mesothelium. *J Am Soc Nephrol*. 2009;20:567–581.
23. Ogunwobi OO, Liu C, Hepatocyte growth factor upregulation promotes carcinogenesis and epithelial-to-mesenchymal transition in hepatocellular carcinoma via Akt and COX-2 pathways. *Clin Exp Metastasis*. 2011;28:721–731.
24. Strippoli R, Benedicto I, Foronda M, Perez-Lozano ML, Sánchez-Perales S, López-Cabrera M, et al. p38 maintains E-cadherin expression by modulating TAK1-NF-kappa B during epithelial-to-mesenchymal transition. *J Cell Sci*. 2010;123:4321–4331.
25. Kokoroishi K, Nakashima A, Doi S, Ueno T, Doi T, Yokoyama Y, et al. High glucose promotes TGF- β 1 production by inducing FOS expression in human peritoneal mesothelial cells. *Clin Exp Nephrol*. 2016;20:30–38.
26. Patel P, Sekiguchi Y, Oh KH, Patterson SE, Kolb MR, Margetts PJ. Smad3-dependent and -independent pathways are involved in peritoneal membrane injury. *Kidney Int*. 2010;77:319–328.
27. Loureiro J, Schilte M, Aguilera A, Albar-Vizcaíno P, Ramírez-Huesca M, Pérez-Lozano ML, et al. BMP-7 blocks mesenchymal conversion of mesothelial cells and prevents peritoneal damage induced by dialysis fluid exposure. *Nephrol Dial Transplant*. 2010;25:1098–1108.
28. Strippoli R, Benedicto I, Perez Lozano ML, Pellinen T, Sandoval P, Lopez-Cabrera M, et al. Inhibition of transforming growth factor-activated kinase 1 (TAK1) blocks and reverses epithelial to mesenchymal transition of mesothelial cells. *PLoS One*. 2012;7:e31492.
29. Strippoli R, Benedicto I, Pérez Lozano ML, Cerezo A, López-Cabrera M, del Pozo MA. Epithelial-to-mesenchymal transition of peritoneal mesothelial cells is regulated by an ERK/NF-kappaB/Snail1 pathway. *Dis Model Mech*. 2008;1:264–274.
30. Farhat K, Douma CE, Ferrantelli E, Ter Wee PM, Beelen RHJ, van Ittersum FJ. Effects of Conversion to a Bicarbonate/Lactate-Buffered, Neutral-pH, Low-GDP PD Regimen in Prevalent PD: A 2-Year Randomized Clinical Trial. *Perit Dial Int*. 2017;37:273–282.

31. Yung S, Lui SL, Ng CK, Yim A, Ma MK, Lo KY, et al. Impact of a low-glucose peritoneal dialysis regimen on fibrosis and inflammation biomarkers. *Perit Dial Int.* 2015;35:147–158.
32. Aoki S, Noguchi M, Takezawa T, Ikeda S, Uchihashi K, Kuroyama H, et al. Fluid dwell impact induces peritoneal fibrosis in the peritoneal cavity reconstructed in vitro. *J Artif Organs.* 2016;19:87–96.
33. Morinelli TA, Luttrell LM, Strungs EG, Ullian ME. Angiotensin II receptors and peritoneal dialysis-induced peritoneal fibrosis. *Int J Biochem Cell Biol.* 2016;77(Pt B):240–50.
34. Kyuden Y, Ito T, Masaki T, Yorioka N, Kohno N. TGF- β 1 induced by high glucose is controlled by angiotensin-converting enzyme inhibitor and angiotensin II receptor blocker on cultured human peritoneal mesothelial cells. *Perit Dial Int.* 2005;25:483–491.
35. Nagami GT, Chang JA, Plato ME, Santamaria R. Acid loading in vivo and low pH in culture increase angiotensin receptor expression: enhanced ammoniagenic response to angiotensin II. *Am J Physiol Renal Physiol.* 2008;295:F1864–F1870.
36. Duman S, Sen S, Duman C, Oreopoulos DG. Effect of valsartan versus lisinopril on peritoneal sclerosis in rats. *Int J Artif Organs.* 2005;28:156–163.
37. Yang L, Fan Y, Zhang X, Huang W, Ma J. 1,25(OH)2D3 treatment attenuates high glucose-induced peritoneal epithelial to mesenchymal transition in mice. *Mol Med Rep.* 2017;16:3817–3824.
38. Wu J, Xing C, Zhang L, Mao H, Chen X, Liang M, et al. Autophagy promotes fibrosis and apoptosis in the peritoneum during long-term peritoneal dialysis. *J Cell Mol Med.* 2018;22:1190–1201.
39. Lupinacci S, Perri A, Totoda G, Vizza D, Puoci F, Parisi OI, et al. Olive leaf extract counteracts epithelial to mesenchymal transition process induced by peritoneal dialysis, through the inhibition of TGF β 1 signaling. *Cell Biol Toxicol.* 2018. doi: 10.1007/s10565-018-9438-9.
40. Cheng S, Lu Y, Li Y, Gao L, Shen H, Song K. Hydrogen sulfide inhibits epithelial-mesenchymal transition in peritoneal mesothelial cells. *Sci Rep.* 2018;8:5863. doi: 10.1038/s41598-018-21807-x.
41. Masola V, Granata S, Bellin G, Gambaro G, Onisto M, Rugiu C, et al. Specific heparanase inhibition reverses glucose-induced mesothelial-to-mesenchymal transition. *Nephrol Dial Transplant.* 2017;32:1145–1154.
42. Wakabayashi K, Hamada C, Kanda R, Nakano T, Ito H, Horikoshi S, et al. Oral Astaxanthin supplementation prevents peritoneal fibrosis in rats. *Perit Dial Int.* 2015;35:506–516.
43. Liu J, Zeng L, Zhao Y, Zhu B, Ren W, Wu C. Selenium suppresses lipopolysaccharide-induced fibrosis in peritoneal mesothelial cells through inhibition of epithelial-to-mesenchymal transition. *Biol Trace Elem Res.* 2014;161:202–209.
44. Su X, Zhou G, Wang Y, Yang X, Li L, Yu R, et al. The PPAR β/δ agonist GW501516 attenuates peritonitis in peritoneal fibrosis via inhibition of TAK1-NF κ B pathway in rats. *Inflammation.* 2014;37:729–737.
45. Kitamura M, Nishino T, Obata Y, Furusu A, Hishikawa Y, Koji T, et al. Epigallocatechin gallate suppresses peritoneal fibrosis in mice. *Chem Biol Interact.* 2012;195:95–104.
46. Washida N, Wakino S, Tonozuka Y, Homma K, Tokuyama H, Hara Y et al. Rho-kinase inhibition ameliorates peritoneal fibrosis and angiogenesis in a rat model of peritoneal sclerosis. *Nephrol Dial Transplant.* 2011;26:2770–2779.
47. Erkel G, Anke T, Sterner O. Inhibition of NF- κ B activation by panepoxydone. *Biochem Biophys Res Commun.* 1996;226:214–221.
48. Gehrt A, Erkel G, Anke T, Sterner OA. Cycloepoxydon: 1-hydroxy-2-hydroxymethyl-3-pent-1-enylbenzene-1-hydroxy-2-hydroxymethyl-3-pent-1, 3-dienylbenzene, new inhibitors of eukaryotic signal transduction. *J Antibiot.* 1998;51:455–463.
49. Matsumoto N, Ariga A, Toe S, Nakamura H, Agata N, Hirano S, et al. Synthesis of NF- κ B activation inhibitors derived from epoxyquinomicin C. *Bioorg Med Chem Lett.* 2000;10:865–869.
50. Suzuki Y, Sugiyama C, Ohno O, Umezawa K. Preparation and biological activities of optically active dehydroxymethylepoxyquinomicin, a novel NF- κ B inhibitor. *Tetrahedron.* 2004;60:7061–7066.
51. Hamada M, Niitsu Y, Hiraoka C, Kozawa I, Higashi T, Shoji M. et al. Chemoenzymatic synthesis of (2S,3S,4S)-form, the physiologically active stereoisomer of dehydroxymethylepoxyquinomicin (DHMEQ), a potent inhibitor on NF- κ B. *Tetrahedron.* 2010;66:7083–7087.
52. Ariga A, Namekawa J, Matsumoto N, Inoue J, Umezawa K. Inhibition of TNF- α -induced nuclear translocation and activation of NF- κ B by dehydroxymethyl-epoxyquinomicin. *J Biol Chem.* 2002;277:27625–27630.
53. Yamamoto M, Horie R, Takeiri M, Kozawa I, Umezawa K. Inactivation of nuclear factor kappa B components by covalent binding of (-)-dehydroxymethylepoxyquinomicin to specific cysteine residues. *J Med Chem.* 2008;51:5780–5788.
54. Horie K, Ma J, Umezawa K. Inhibition of canonical NF- κ B nuclear localization by (-)-DHMEQ via impairment of DNA binding. *Oncology Res.* 2015;22:105–115.
55. Kozawa I, Kato K, Teruya T, Suenaga K, Umezawa K. Unusual intramolecular N \rightarrow O acyl group migration occurring during conjugation of (-)-DHMEQ with cysteine. *Bioorg Med Chem Lett.* 2009;19:5380–5382.
56. Shimada C, Ninomiya Y, Suzuki E, Umezawa K. Efficient cellular uptake of the novel NF- κ B inhibitor (-)-DHMEQ and irreversible inhibition of NF- κ B in neoplastic cells. *Oncology Research.* 2010;18:529–535.
57. Takeiri M, Horie K, Takahashi D, Watanabe M, Horie R, Simizu S, et al. Involvement of DNA binding domain in the cellular stability and importin affinity of NF- κ B component RelB. *Org Biomol Chem.* 2012;10:3053–3059.
58. Takatsuna, H, Asagiri M, Kubota T, Oka K, Osada T, Sugiyama C, et al. Inhibition of RANKL-induced osteoclastogenesis by (-)-DHMEQ, a novel NF- κ B inhibitor, through downregulation of NFATc1. *J. Bone Mineral Res.* 2005;20:653–661.
59. Kubota T, Hoshino M, Aoki K, Ohya K, Komano Y, Nanki T, et al. NF- κ B inhibitor DHMEQ suppresses osteoclastogenesis and expression of NFATc1 in mouse arthritis without affecting expression of RANCL, OPG or

- M-CSF. Arthritis Research & Therapy. <http://arthritis-research.com/content/9/5//R97>, 2007.
60. Murohashi M, Hinohara K, Kuroda M, Isagawa T, Tsuji S, Kobayashi S, et al. Gene set enrichment analysis provides insight into novel signaling pathways in breast cancer stem cells. *British J Cancer*. 2010;102:206–212.
 61. Hinohara K, Kobayashi S, Simizu S, Tada K, Tsuji E, Nishioka K, et al. ErbB receptor tyrosine kinase/NF- κ B signaling controls mammosphere formation in human breast cancer. *Proc Natl Acad Sci USA*. 2012;109:6584–6589.
 62. Ukaji T, Lin Y, Okada S, Umezawa K. Inhibition of MMP-2-mediated cellular invasion by NF- κ B inhibitor DHMEQ in 3D culture of breast carcinoma MDA-MB-231 cells: A model for early phase of metastasis. *Biochem Biophys Res Commun*. 2017;485:76–81.
 63. Suzuki K, Aiura K, Matsuda S, Itano O, Takeuchi O, Umezawa K, et al. Combined effect of dehydroxymethylepoxyquinomicin and gemcitabine in a mouse model of liver metastasis of pancreatic cancer. *Clinical & Experimental Metastasis*. 2013;30:381–392.
 64. Lin Y, Ukaji T, Koide N, Umezawa K. Inhibition of late and early phases of cancer metastasis by NF- κ B inhibitor DHMEQ derived from microbial bioactive metabolite epoxyquinomicin: A review. *Int J Mol Sci*. 2018;19:729. doi: 10.3390/ijms19030729.
 65. Hamasaka A, Yoshioka N, Abe R, Kishino S, Umezawa K, Ozaki M, et al. Topical application of DHMEQ improves allergic inflammation via NF- κ B inhibition. *Journal of Allergy and Clinical Immunology*. 2010;126:400–403.
 66. Noma N, Asagiri M, Takeiri M, Ohmae S, Takemoto K, Iwaisako K, et al. Inhibition of MMP-2-mediated mast cell invasion by NF- κ B inhibitor DHMEQ in mast cells. *International Archives of Allergy and Immunology*. 2015;166:84–90.
 67. Jiang X, Wei B, Lan Y, Dai C, Gu Y, Ma J, et al. External application of NF- κ B inhibitor DHMEQ suppresses development of atopic dermatitis-like lesions induced with DNCB/OX in BALB/c mice. *Immunopharmacology and Immunotoxicology*. 2017;39:157–164.
 68. Jiang X, He H, Xie Z, Wen H, Li X, Ma J, et al. Dehydroxymethylepoxyquinomicin suppresses atopic dermatitis-like lesions in a stratum corneum-removed murine model through NF- κ B inhibition. *Immunopharmacology and Immunotoxicology*. doi: 10.1080/08923973.2018.1510962.
 69. Kobayashi K, Umezawa K, Yasui M. Apoptosis in mouse amniotic epithelium is induced by activated macrophages through the TNF receptor type 1/TNF pathway. *Biology of Reproduction*. 2011;84:248–254.
 70. El-Salhy M, Umezawa K. Effects of AP-1 and NF- κ B inhibitors on colonic endocrine cells in rats with TNBS-induced colitis. *Molecular Medicine Reports*. 2016;14:1515–1522.
 71. El-Salhy M, Umezawa K. Anti-inflammatory effects of novel AP-1 and NF- κ B inhibitors in dextran-sulfate-sodium-induced colitis in rats. *International J Mol Med*. 2016;37:1457–1464. doi: 10.3892/ijmm.
 72. Kikuchi, E, Horiguchi Y, Nakashima J, Kuroda K, Oya M, Ohigashi T, et al. Suppression of hormone-refractory prostate cancer by a novel nuclear factor κ B inhibitor in nude mice. *Cancer Res*. 2003;63:107–110.
 73. Matsumoto G, Namekawa J, Muta M, Nakamura T, Bando H, Tohyama K, et al. Targeting of NF- κ B pathways by DHMEQ, a novel inhibitor of breast carcinomas: Anti-tumor and anti-angiogenic activity in vivo. *Clin Cancer Res*. 2005;11:1287–1293.
 74. Starenki DV, Namba H, Saenko VA, Ohtsuru A, Maeda S, Umezawa K, et al. Induction of thyroid cancer cell apoptosis by a novel nuclear factor kappaB inhibitor, DHMEQ. *Clin. Cancer Res*. 2004;10:6821–6829.
 75. Fukushima T, Kawaguchi M, Yorita K, Tanaka H, Umezawa K, Kataoka H. Antitumor effect of dehydroxymethylepoxyquinomicin (DHMEQ), a small molecule inhibitor of nuclear factor- κ B, on glioblastoma. *Neuro-Oncology*. 2012;14:19–28.
 76. Watanabe M, Ohsugi T, Shoda M, Ishida T, Aizawa S, Maruyama-Nagai M, et al. Dual targeting of transformed and untransformed HTLV-1-infected T-cells by DHMEQ, a potent and selective inhibitor of NF- κ B, as a strategy for chemoprevention and therapy of adult T cell leukemia. *Blood*. 2005;106:2462–2471.
 77. Tatetsu H, Okuno Y, Nakamura M, Matsuno F, Sonoki T, Taniguchi I, et al. A novel nuclear factor-kappa B inhibitor induced apoptosis of multiple myeloma cells. *Mol. Cancer Ther*. 2005;4:1114–1120.
 78. Seubwai W, Kraiklang R, Vaeteewoottacharn K, Umezawa K, Okada S, Wongkham S. Aberrant expression of NF- κ B in liver fluke associated cholangiocarcinoma: implications for targeted therapy. *PLOS ONE*. 2014;9 (8), e106056. DOI:10.1371/journal.pone.0106056.
 79. Ito Y, Kikuchi E, Tanaka N, Kosaki T, Suzuki E, Mizuno R, et al. Down-regulation of NF-kappa B activation is an effective therapeutic modality in acquired platinum-resistant bladder cancer. *BMC Cancer*. 2015;15:324. doi: 10.1186/s12885-015-1315-9.
 80. Umezawa K. Possible role of peritoneal NF- κ B in peripheral inflammation and cancer: Lessons from the inhibitor DHMEQ. *Biomedicine & Pharmacotherapy*. 2011;65:252–259.
 81. Umezawa K. Peritoneal NF- κ B as a Possible molecular target for suppression of various cancers and inflammation. (Review) *Forum of Immunopathological Diseases and Therapeutics*. 2013;4:63–77.
 82. Sosinska P, Mackowiak B, Staniszewski R, Umezawa K, Breborowicz A. Inhibition of NF- κ B with dehydroxypoxyquinomicin modifies function of human peritoneal mesothelial cells. *American Journal of Translational Research*. 2016;8:5756–5765.

Acceptance for editing: 2019-05-09
 Acceptance for publication: 2019-06-29.

Correspondence address:

Andrzej Bręborowicz
 Department of Pathophysiology
 Poznan University of Medical Sciences
 60-806 Poznań, Poland
 e-mail: abreb@ump.edu.pl



REVIEW PAPERS

DOI: <https://doi.org/10.20883/jms.339>

Spirometry in selected clinical situations

Piotr Szczechowiak^a, Tomasz Piorunek^b

Chair and Clinic of Pulmonology, Allergology and Pulmonary Oncology, Poznan University of Medical Sciences, Poland

^a  <https://orcid.org/0000-0003-0424-8823>

^b  <https://orcid.org/0000-0002-2257-4967>

ABSTRACT

Spirometry is the most frequently performed functional test of the respiratory system. In pulmonological practice it is a basic tool used to diagnose ventilation disorders and to monitor treatment. The results obtained during the test are compared to predicted values, that is, assumed parameter values, computed on the basis of anthropometrical data such as: age, gender and height, with the use of complex equations. The use of additional variables including, e.g. an ethnic group or a race as well as corrective factors, enables a more exact determination of their values. Spirometry can be conducted in a sitting or standing position; however, for the subject safety reasons it is usually performed in a sitting position. It allows to eliminate the risk of fall as a result of syncope or impaired balance. Spirometry in a standing position should be considered in measurably obese patients or in patients with a wide abdominal circumference caused by other reasons. Patients with normal body weight obtain equivalent or slightly higher spirometric values in a standing position. In the selected clinical situations some problems with the measurement of the actual height of patients in a standard way (measurement without shoes, feet together, upright position, eyes straight ahead) and with correct calculation of predicted values occur. They are, among others, silhouette-disturbing disorders or diseases causing changes in body proportions, from the less often occurring, like Marfan syndrome or achondroplasia, to more frequent posture defects and mobility impairments. These diseases influence the change of the predictive functional parameter values which are used to compare with the obtained results. The aim of the study is to demonstrate the methods of height and predicted values determination on the basis of measurements of ranges between different body points with the use of simple and complex equations in a group of patients in whom the application of standard measurement methods is impossible.

Keywords: spirometry.

Introduction

Spirometry is the most frequently performed functional test of the respiratory system. In pulmonological practice it is a basic tool used to diagnose ventilation disorders and to monitor treatment. The results obtained during the test are compared to predicted values, that is, assumed parameter values, computed on the basis of anthropometrical data such as: age, gender and height, with the use of complex equations. The use of additional variables including,

e.g. an ethnic group or a race as well as corrective factors, enables a more exact determination of their values [1]. Spirometry can be conducted in a sitting or standing position; however, for the subject safety reasons it is usually performed in a sitting position [2]. It allows to eliminate the risk of fall as a result of syncope or impaired balance. Spirometry in a standing position should be considered in measurably obese patients or in patients with a wide abdominal circumference caused by other reasons. Patients with normal

body weight obtain equivalent or slightly higher spirometric values in a standing position [3].

In the selected clinical situations some problems with the measurement of the actual height of patients in a standard way (measurement without shoes, feet together, upright position, eyes straight ahead) and with correct calculation of predicted values occur. They are, among others, silhouette-disturbing disorders or diseases causing changes in body proportions, from the less often occurring, like Marfan syndrome or achondroplasia, to more frequent posture defects and mobility impairments [4]. These diseases influence the change of the predictive functional parameter values which are used to compare with the obtained results.

Aim

The aim of the study is to demonstrate the methods of height and predicted values determination on the basis of measurements of ranges between different body points with the use of simple and complex equations in a group of patients in whom the application of standard measurement methods is impossible.

Height determination on the basis of rigid body proportions

A simple method of patient's height determination allowing to minimize errors in the determination of predicted spirometric values, is to determine averaged, rigid body proportions in healthy subjects in a particular population [5]. Knowing the proportions, predicted height of a person can be estimated with the help of selected body parts' measurements [6]. It is a simple and fast method used in practice, however burdened with a margin of error due to non-consideration of other factors, such as age or an ethnic group [7]. In the group of patients with achondroplasia or Marfan syndrome the margin of error may be even bigger due to impaired body proportions [8]. This method may be successfully used in screening examination of patients with skeletal malformations, mobility problems or faulty postures. There are numerous formulas for the prediction of height with the use of proportional equations, the

most frequent employ: arm span measurement (height in a standing position = arm span/1.06), measurement of height in a sitting position (height in a standing position = height in a sitting position/0.52), measurement of feet-navel range (height in a standing position = feet-navel range x 1.618). The arm span is measured between the tips of middle fingers, the height of a sitting position is determined from the top of the head to the base on which the patient is sitting, the feet-navel range is measured in a standing position [9].

Height determination based on regression equations

The inadequacy of the method of height determination on the basis of rigid body proportions caused the search for better solutions in the form of regression equations based on anthropometric parameters and different variables, which enable more exact estimation of patients' height.

Based on a group of 5415 healthy adults and 13,821 healthy children Cameron developed the regression equation which allows to compute the predicted height of patients with mobility and psychophysical impairments. During the development of the equations he considered parameters like: age, gender, ethnic group, absolute height, height in a sitting position, height from the ground to knees, range from the buttock to knees. The most credible regression equation estimating proper height of women, men and children whose measurement was impossible with a standard method included the knee height. The expansion of the margin of error in the calculated height was connected with posture impairment intensification [10].

Based on arm span measurements, Miller developed similar regression equations, which predicted the height of patients with chest deformations equally well [11].

Arm span as an independent predictor of lung function parameters

Golshan created equations of pulmonary system function parameters based directly on arm span measurements in a group of 1865 healthy, non-smoking subjects [12]. He performed height

measurements in a standing position, arm span measurements and pulmonary function tests. Then, he compared the obtained results of spirometry with the predicted values computed with the use of different methods. He demonstrated that the predicted values computed with the use of a prediction equation, based on the arm span, are the most exact ones when it comes to the prediction of values obtained during spirometry of healthy subjects. Slightly bigger discrepancies between the estimated and the obtained results were observed in the case of the predicted values computed with the use of the height of subjects. However, the predicted values determined for height, which were computed with a regression equation based on the arm span, did not correspond to the spirometric results [13].

The determination of the values of the pulmonary functional parameters with the use of prediction equations, based on the arm span, is equally reliable as the use of equations based on height measurements in a standing position. It is an effective method in patients in whom standard measurement methods are not possible [14].

Chest deformations and lack of limbs

Inborn and acquired skeletal abnormalities such as profound kyphosis (syringomyelia, muscular atrophy) or kyphoscoliosis disable standard height measurements. In these cases, an estimation of height is possible with the use of the above-mentioned equations: patient's height = arm span/1.06, patient's height = range from the top of the head to the base which the patient is sitting on/0.52 or patient's height = feet-navel range x 1.618 [15].

The application of the above-mentioned equations causes some uncertainty when it comes to the accuracy of the calculated predicted values of the functional parameters and the measured to predicted value ratio. It especially concerns extreme cases such as: significant chest deformations or problems with proper arm spreading. A possible outcome of the determination of predicted values in this way is a misdiagnosis or a false exclusion of ventilation disorders [16]. A more precise method of height estimation is the use of developed by Parker regression equations

including the measurement of the arm span, race, age and patient's gender. A standard estimation error in height measurement is within 3.0 to 3.7 cm [17]. The application of similar equations using knee height in a patient's height estimation is also possible. Such equations were developed in 1994 by Chumlea [18].

Regression equations and the above-mentioned formulas may be used in a height estimation in patients with no lower limbs (congenital abnormalities, post-amputation condition). In exceptional situations when a patient is also deprived of one upper limb, the measurement is taken from the middle of a body to the tip of a middle finger with a wide-open arm and the obtained value is multiplied x2 and is used in the chosen formula [2].

Marfan syndrome

Marfan syndrome is a genetic disorder of connective tissues caused by a mutation in the FBN1 gene, resulting in abnormalities in the creation of elastic fibres, elastin and the ground substance of connective tissues. This disease is inherited in an autosomal dominant fashion and its *de novo* mutation frequency is estimated at about 25%. In a general population the frequency of the disorder occurrence is estimated at 10–20:100 000. The clinical picture includes: tallness (average final height for men: 191 cm, for women: 175 cm), body proportion abnormalities – including limb prolongation, degenerative spine arthritis, chest deformations, eyesight, nervous system and cardiovascular defects [19].

One of the first reports regarding the necessity to use in Marfan syndrome patients separate predicted values to evaluate spirometric results, is a study by Streeten [20]. The author of the publication analysed the results of 79 patients with diagnosed Marfan syndrome. He demonstrated that patients without significant chest deformations had lower values of forced vital capacity (FVC) than the predicted values determined on the basis of a standard height measurement (83 percentile). However, when prediction equations were used in prediction value calculations with the use of sitting position height, the obtained values were higher (FVC: 105 percentiles, FEV1: 92 percentiles). In the case of significant chest

deformations, lower FVC and forced expiratory volume in 1-st second (FEV1) were demonstrated regardless of the predicted value determination method [10].

Giske performed spirometry tests in a group of 17 Marfan syndrome patients at the age of 18–30. He demonstrated normal or slightly lowered FVC and FEV1/FVC values. Nevertheless, the results of functional tests were based on predicted values calculated with a standard height measurement method [21].

Achondroplasia

Achondroplasia is a genetically conditioned disorder with an autosomal dominant inheritance pattern, caused by a mutation of a gene responsible for a receptor synthesis for the fibroblast growth factor. The origin of the disorder is abnormal endochondral ossification leading to osteochondral dysplasia with long bones and spine growth impairments, which result in dwarfism. Clinical picture includes, among others, short stature (average height: 125 cm) and limb size reduction with a normal length of torso (ratio of height in a sitting position is 0.66 with the norm of 0.52–0.53 for healthy population) [22].

Dennis conducted spirometry tests in 102 subjects at the age of 7–60 who suffered from achondroplasia. Then, on the basis of the obtained results, he developed prediction equations which may be used to calculate proper predicted values for this group of patients. They included sitting position height and age and referred to FEV1 and FVC (Table 1) [23].

The author additionally compared the obtained spirometric results with the predicted values obtained with the use of other methods, e.g.: he used the predicted values for height, calculated with a regression equation including sitting position height. The obtained in the regres-

sion equation values did not correspond to the predicted values calculated with the prediction equations [24].

Acknowledgements

Conflict of interest statement

The authors declare no conflict of interest.

Funding sources

There are no sources of funding to declare.

References

1. Boros P, Franczuk M, Wesołowski S. Zalecenia polskiego towarzystwa chorób płuc dotyczące wykonywania badań spirometrycznych. *Pneumonologia i Alergologia Polska*. 2006.
2. Boros P, Franczuk M, Wesołowski S. Zalecenia polskiego towarzystwa chorób płuc dotyczące wykonywania badań spirometrycznych. *Pneumonologia i Alergologia Polska*. 2006.
3. Miller MR, Crapo R, Hankinson J, Brusasco V, Burgos F, Casaburi R, Coates A, Enright P, van der Grinten CPM, Gustafsson P, Jensen R, Johnson DC, MacIntyre N, McKay R, Navajas D, Pedersen OF, Pellegrino R, Viegi G, Wanger J. General considerations for lung function testing. *European Respiratory Journal*. 2005;26:153–161.
4. Cameron Chumlea WM, Guo SS, Steinbaugh ML. Prediction of stature from knee height for black and white adults and children with application to mobility-impaired or handicapped persons. *Journal of the American Dietetic Association*. 1994;94:1385–1391.
5. Haeuslerab M, McHenry HM. Body proportions of *Homo habilis* reviewed. *Journal of Human Evolution*. 2004;46:433–465.
6. Bogin B, Varela-Silva MI. Leg Length, Body Proportion, and Health: A Review with a Note on Beauty. *Int J Environ Res Public Health*. 2010;7:1047–1075.
7. Bogin B, Varela-Silva MI. Leg Length, Body Proportion, and Health: A Review with a Note on Beauty. *Int J Environ Res Public Health*. 2010;7:1047–1075.
8. Ng BKW, Hung VWY, Cheng JCY, Lam TP. Limb Lengthening for Short Stature: A 10-year Clinical Experience. *J Paediatr*. 2003;8:307–317.
9. Bogin B, Varela-Silva MI. Leg Length, Body Proportion, and Health: A Review with a Note on Beauty. *Int J Environ Res Public Health*. 2010;7:1047–1075. Haeuslerab M, McHenry HM. Body proportions of

Table 1. Examples of prediction equations for the predicted FVC values. Source: own elaboration based on D.C. Stokes, R.E. Pyeritz, R.A. Wise, D.L. Fairclough, E.A. Murphy, Spirometry and Chest Wall Dimensions in Achondroplasia, *Chest* 1988;93:364–369

Men under the age of 25	$FVC(L) = -3.56 + 0.162 \cdot \text{height in a sitting position (in)} + 0.067 \cdot \text{age (in years)}$
Men over the age of 25	$FVC(L) = -0.73 + 0.162 \cdot \text{height in a sitting position (in)} + 0.047 \cdot \text{age (in years)}$
Women under the age of 20	$FVC(L) = -3.56 + 0.150 \cdot \text{height in a sitting position (in)} + 0.067 \cdot \text{age (in years)}$
Women over the age of 20	$FVC(L) = -1.92 + 0.150 \cdot \text{height in a sitting position (in)} + 0.016 \cdot \text{age (in years)}$

in – inch.

- Homo habilis reviewed. *Journal of Human Evolution*. 2004;46:433–465.
10. Cameron Chumlea WM, Guo SS, Steinbaugh ML. Prediction of stature from knee height. *Journal of the American Dietetic Association*. 1994;94:1385–1391.
 11. Miller MR, Crapo R, Hankinson J, Brusasco V, Burgos F, Casaburi R, Coates A, Enright P, van der Grinten CPM, Gustafsson P, Jensen R, Johnson DC, MacIntyre N, McKay R, Navajas D, Pedersen OF, Pellegrino R, Viegi G, Wanger J. General considerations for lung function testing. *European Respiratory Journal*. 2005;26:153–161.
 12. Golshan M, Crapo RO, Amra B, Jensen RL, Golshan R. Arm span as an independent predictor of pulmonary function parameters: validation and reference values. *Respirology*. 2007;12:361–366.
 13. Golshan M, Crapo RO, Amra B, Jensen RL, Golshan R. Arm span as an independent predictor of pulmonary function parameters: validation and reference values. *Respirology*. 2007;12:361–366.
 14. Golshan M, Crapo RO, Amra B, Jensen RL, Golshan R. Arm span as an independent predictor of pulmonary function parameters: validation and reference values. *Respirology*. 2007;12:361–366.
 15. Haeuslerab M, McHenry HM. Body proportions of Homo habilis reviewed. *Journal of Human Evolution*. 2004;46:433–465.
 16. Aggarwal AN, Grupa D, Jindal SK. Interpreting spirometric data: impact of substitution of arm span for standing height in adults from North India. *Chest*. 1999;115:557–562.
 17. Parker JM, Dillard TA, Phillips YY. Arm span-height relationship in patients referred for spirometry. *Am J Respir Crit Care Med*. 1996;154:533–536.
 18. Cameron Chumlea WM, Guo SS, Steinbaugh ML. Prediction of stature from knee height for black and white adults and children with application to mobility-impaired or handicapped persons. *Journal of the American Dietetic Association*. 1994;94:1385–1391.
 19. Chiu HH, Wu MH, Chen HC, Kao FY. Epidemiological profile of Marfan syndrome in a general population: a national database study. Elsevier Inc. 2014.
 20. Streeten EA, Murphy EA, Pyeritz RE. Pulmonary Function in the Marfan Syndrome. *Chest*. 1987;91:408–412.
 21. Giske L. Pulmonary Function, Working Capacity and Strength in Young Adults with Marfan Syndrome. *J Rehabil Med*. 2003;35:221–228.
 22. Giudicelli MD, Serazin V, Le Sciellour CR, Albert M. Increased achondroplasia mutation frequency with advanced age and evidence for G1138A mosaicism in human testis biopsies. *Fertil Steril*. 2008;89:1651–1656.
 23. Stokes DC, Pyeritz RE, Wise RA, Fairclough DL, Murphy EA. Spirometry and Chest Wall Dimensions in Achondroplasia. *Chest*. 1988;93:364–369.
 24. Stokes DC, Wohl ME, Wise RA, Pyeritz RE, Fairclough DL. The Lungs and Airways in Achondroplasia: Do Little People Have Little Lungs? *Chest*. 1990;98:145–152.

Acceptance for editing: 2019-05-09
Acceptance for publication: 2019-06-29

Correspondence address:

Piotr Szczechowiak
Chair and Clinic of Pulmonology
Allergology and Pulmonary Oncology
Poznan University of Medical Sciences
84 Szamarzewskiego Street, 60-569 Poznań, Poland
e-mail: p.szczechowiak@gmail.com



THOUSAND WORDS ABOUT...

DOI: <https://doi.org/10.20883/jms.349>

A thousand words about the cardiopulmonary exercise test in respiratory system diseases


Jacek Tarchalski^{1,a}, Tomasz Piorunek^{2,b}, Przemyslaw Guzik^{1,c}

¹ Department of Cardiology-Intensive Therapy, Poznan University of Medical Sciences, Poland

² Department of Pulmonology, Allergology and Respiratory Oncology, Poznan University of Medical Sciences, Poland

^a  <https://orcid.org/0000-0002-7433-4236>

^c  <https://orcid.org/0000-0001-9052-5027>

^b  <https://orcid.org/0000-0002-2257-4967>

ABSTRACT

The cardiopulmonary exercise test (CPET) is designed to measure some physiological variables related to the function of the cardiovascular and respiratory systems during exercise. Usually, the CPET is performed either on a treadmill or a cycle ergometer. In this mini-review, we describe a set of parameters which are most commonly used to quantify CPET. We also summarize clinical indications for this test and interpretation of the obtained results in patients with respiratory system diseases. The CPET, if made appropriately, may deliver valuable information helpful in the diagnosis, e.g., of unexplained dyspnea, and prognosis, e.g., in chronic obstructive pulmonary disease, pulmonary hypertension, or interstitial lung diseases.

Keywords: respiratory diseases, cardiopulmonary exercise test, VCO_2 , VO_2 .

Cardiopulmonary exercise test (CPET) is a non-invasive method that combines progressive exercise stress with measures of the function of the cardiovascular and respiratory system [1–3]. During this test, a set of signals is continuously monitored, for instance: ECG, arterial blood pressure, oxygen saturation (sO_2), breathing rate, tidal volume, carbon dioxide output (VCO_2) or oxygen uptake (VO_2) [1–9]. The complex information delivered by CPET goes beyond the lungs, airways, and heart. CPET results also depend on the neuropsychological factors, hemoglobin concentration (e.g., anemia) and quality (e.g., thalassemia), peripheral circulation, the function of leg muscles and even mitochondria [1–3, 5–7]. For these reasons, it is believed that CPET gives an insight into integrative responses of several systems involved in the exercise physiology.

Many patients with respiratory or cardiac diseases complain about dyspnea which starts,

evolves or exacerbates on exertion. Employing diagnostic tests performed at rest is misleading in such individuals. Therefore, using a controlled exercise in clinical conditions to provoke and reproduce patient's symptoms is commonly accepted. In contrast to the standard exercise test with ECG, the CPET provides much more useful physiological and clinical information [1–3, 5–10]. This test permits to evaluate a patient at the submaximal or even maximal exercise, until limiting symptoms or exhaustion appear.

During the CPET, patients either walk or run on a treadmill or sit and ride a cycle ergometer [3]. A set of ECG electrodes, a sO_2 sensor, a brachial cuff for blood pressure monitoring, and a mouthpiece or mask with a system measuring breathing rate, gas volumes and exchange are attached to a patient before the test [1–3]. Exercise during the CPET initiates after a short warm-up, followed by

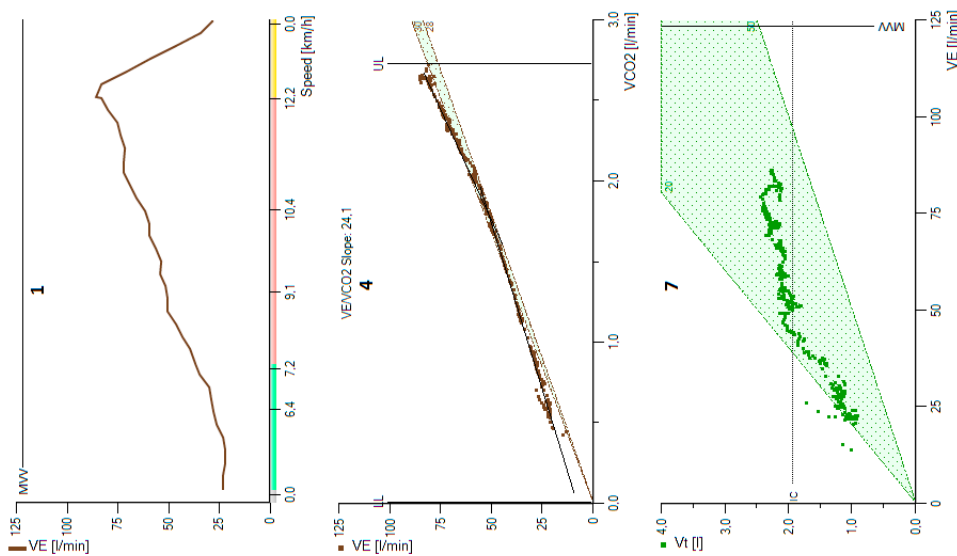


Figure 1. Nine-panel plot graphical display with results of the CPET in a 25-year old female patient with obesity (body mass – 94 kg, body mass index – 31.1 kg/m²) complaining about exertional dyspnea of unknown origin. The test was terminated when the dyspnea became a limiting symptom; the perceived exhaustion by the 10-grade Borg scale was 9/10 [12]. The maximal value of VO_{2max} was 2.5 l/min but normalized to body mass VO_{2max}/kg was 26.6 ml/kg/min what corresponded to 73% of the predicted VO_{2max}/kg . There was no drop in sO_2 . The CPET results were within normal range (with the exception of VO_{2max}), neither cardiac nor pulmonary dysfunction was observed. The patient reached nearly maximal predicted heart rate. There was a short increase of pulse O_2 (Panel 2), mainly during the warm-up and the early phase of the exercise, which then flattened into a plateau. After the premature increase of RER above 1 (due to initial hyperventilation), there was a rapid normalization and RER reached the value of 1 again in the second half of exercise. Neither ST-segment changes suggestive of myocardial ischemia nor cardiac arrhythmias were observed. The final CPET result was normal. Other pulmonary and cardiac tests, including echocardiography and spirometry, were normal as well. Finally, a mildly reduced exercise tolerance due to a sedentary life and obesity was diagnosed. Upper panels: panel 1: VE plotted over time (or treadmill speed); panel 2: heart rate (HR) and oxygen pulse (VO_2/HR) plotted over time; panel 3: VCO_2 and VO_2 plotted over time. Middle panels: panel 4: VE plotted over VCO_2 to determine the change in the VE/VCO_2 slope; panel 5: HR and VCO_2 plotted over time; panel 6: ventilatory equivalents VE/VCO_2 and VE/VO_2 plotted over time. Lower panels: panel 7: VT plotted over VE; panel 8: RER and breathing reserve (BR) plotted over time; panel 9: end-tidal partial pressures of O_2 ($PETO_2$) and CO_2 ($PETCO_2$) plotted over time. For panels with speed on the X-axis, i.e., 1, 2, 3, 6, 8 and 9, different phases of CPET are marked with colors: warm-up with green, exercise with red, and recovery with yellow

a gradually increasing exercise and ending with post-exercise recovery. A list of directly measured or indirectly derived parameters acquired during the CPET is shown in **Table 1**.

The CPET can be used in healthy people, athletes for fitness evaluation or to determine their training loads. In clinical practice, this test is applied in a number of patients suffering from heart and pulmonary diseases such as heart failure or chronic respiratory failure or other dis-

eases of the respiratory system [1–10]. The CPET may be used to distinguish cardiac from pulmonary causes of dyspnea, to assess the response to applied therapy both in cardiac and pulmonary patients, to perform pre-rehabilitation or pre-surgery evaluation in high-risk patients [5, 6]. This test can also be applied in individuals with heart or respiratory failure who are potential candidates for heart or lung transplantation, respectively [1–3, 5–10].



Figure 2. The nine-panel diagram used to describe the results of the CPET. Panels mainly applied for the evaluation of the function of the respiratory system are 1 & 7 (yellow) for the ventilation and 4, 6 & 9 (blue) for the ventilation efficiency. Panels for the cardiovascular function are 2 and 5 (green). Panel 8 (red) is used to determine metabolic abnormalities, and panel 3 (orange) depends on the function of the respiratory system, cardiovascular system, and metabolic factors [1, 11]

Table 1. Typical signals and parameters measured or derived during a standard CPET [1–9]

Measured Signals	
HR	Heart rate from ECG in beats/minute
Vt	Tidal volume of each breath in ml
BF	Breathing frequency or rate in breaths/minute
VCO ₂	The volume of carbon dioxide output in ml/minute
VO ₂	The volume of oxygen uptake in ml/minute. An index of aerobic exercise capacity
PETO ₂	Peak end-tidal oxygen partial pressure in mmHg
PETCO ₂	Peak end-tidal carbon dioxide partial pressure in mmHg. An index of the ventilation-perfusion matching in the lung and the level of arterial PCO ₂
sO ₂	Peripheral arterial oxygen saturation in %
Treadmill speed	The speed of the treadmill in km/h
Watt	The workload for cycle ergometer in Watt
Derived parameters	
VE	Minute ventilation – accumulative volume of all tidal volumes during one minute in l/minute
RER	Respiratory exchange ratio, i.e., the ratio of VCO ₂ to VO ₂ – it shows the balance between VCO ₂ and VO ₂
Pulse O ₂	The ratio of VO ₂ to heart rate in ml/beat – it shows how much oxygen is delivered to tissues during one cardiac beat and is proportional to the stroke volume
VE/VCO ₂	The ventilatory equivalent for CO ₂ – it shows the amounts of air in ml ventilated in a minute (VE) needed to exhale and remove 1 ml of CO ₂ (VCO ₂) or efficiency for CO ₂ pulmonary clearance. It reflects a proper matching of pulmonary ventilation to perfusion
VE/VO ₂	The ventilatory equivalent for O ₂ – it shows the amounts of air in ml ventilated in a minute (VE) needed to deliver with inhalation 1 ml of oxygen (VO ₂) or ventilatory efficiency for oxygen delivery
BR	Breathing reserve, i.e., the difference between the predicted maximal VE and peak VE measured during the CPET
VO _{2peak}	The peak or highest oxygen uptake during CPET – it corresponds to the patient's aerobic capacity
VO _{2max}	The highest VO ₂ value that can be attained by the patient regardless of still increasing treadmill speed or workload on a cycle ergometer
VO _{2max} /kg	VO _{2max} divided by body weight in kilograms
AT or VT1	Anaerobic threshold (AT) or the first ventilatory threshold – the point during a CPET beyond which the aerobic metabolism is supplemented with anaerobic metabolism
RCP or VT2	Respiratory compensation point (RCP) or the second ventilatory threshold – the point beyond which there is respiratory compensation for metabolic acidemia generated during an extensive exercise with anaerobic metabolism. After this point, the acidemia becomes an additional (to CO ₂) stimulus (through chemoreceptors) for increased ventilation

There are many different reasons to order CPET in patients with respiratory system diseases or symptoms. A list of clinical indications for CPET in such patients is presented in **Table 2**.

Parameters measured during CPET are presented in a graphical display [1–3, 5, 6, 9, 11]. Typically, results of the CPET are presented in 9 separate panels (**Figure 1**) showing either changes of values of measured parameters (e.g. VO_2 , pulse O_2 , VCO_2 , VE/VCO_2 , PETO_2 , RER) during the CPET or mutual relations between different parameters (e.g. VT and VE, VO_2 and VCO_2).

The nine-panel plot was first proposed by Wasserman et al. in 1977, and, with some modifications, is still in use. Each of the nine plots can be assigned to mainly evaluate the respiratory system, circulatory system, their mutual interaction or some features of body metabolism relat-

ed to energy production [1, 11]. An example of the nine-panel graph with results of a CPET performed in a 25-year old woman with unexplained exertional dyspnea is shown in **Figure 1**. The general rule for reading and interpretation of such nine-panel graphs is given in **Figure 2** – a set of different panels is used to estimate the ventilation, ventilatory efficiency, heart and circulation, or their combined effects. Panel number with RER is used to describe body metabolism related to O_2 and CO_2 . The RER shows the balance between O_2 consumption and the total amount of CO_2 which first comes from burning fats and carbohydrates, and later when anaerobic processes also begin from buffering lactic acid by bicarbonate [1, 2, 8, 9, 11].

In practice, out of many possible parameters, only some have earned special attention for their usefulness in the diagnostic and prognostic eval-

Table 2. The most common clinical indications for CPET in patients with confirmed or suspected respiratory system disease or involvement of the respiratory system in other diseases [1–3, 5–10]

Clinical indication	Explanation
Dyspnea of unknown origin	<ul style="list-style-type: none"> – Diagnostic assessment of possible causes of dyspnea – Differentiation between potential cardiac and respiratory causes of dyspnea
COPD	<ul style="list-style-type: none"> – Diagnostic assessment of COPD – Prognostic stratification of a patient with COPD – Determination of exercise capacity and its limitation – Monitoring of treatment and therapeutic interventions – Evaluation of the disease progression – Screening for secondary pulmonary hypertension
Pulmonary hypertension (PAH)	<ul style="list-style-type: none"> – Diagnostic assessment of patients with a higher risk of PAH – Differentiation between the primary and secondary PAH – Prognostic stratification of a patient with PAH – Guiding and monitoring of the applied treatment – Evaluation of the disease progression
Pulmonary surgery	<ul style="list-style-type: none"> – Pre-operative assessment for risk quantification in moderate- and high-risk patients with cardiac and pulmonary diseases – more accurate than standard pulmonary functional testing – Prediction of postoperative pulmonary complications – Prediction of exercise limitation in patients undergoing lung volume reduction surgery
Interstitial Lung Disease (ILD)	<ul style="list-style-type: none"> – Diagnostic assessment of ILD – Prognostic stratification of a patient with ILD – Screening for secondary pulmonary hypertension – Detection of pulmonary gas exchange abnormalities – Determination of the O_2 concentration value in the treatment – Evaluation of the disease progression
Exercise-Induced Bronchospasm (EIB)	<ul style="list-style-type: none"> – Diagnostic assessment of EIB. Pulmonary function tests must be performed before and after the CPET to determine FEV1 and PEF. If FEV1 drops more than 10% compared with the pre-exercise level, then EIB is diagnosed – Evaluation of the disease progression
Cystic Fibrosis	<ul style="list-style-type: none"> – Prognostic stratification of a patient with cystic fibrosis – Evaluation of the effectiveness of the applied treatment – Guiding and monitoring of the applied treatment – Evaluation of the progression of respiratory system involvement
Heart failure	<ul style="list-style-type: none"> – Assessment of the contribution of lung disease to the severity of HF – Detection of pulmonary gas exchange abnormalities accompanying HF – Evaluation of the clinical effects of secondary PAH due to HF on the function of the respiratory system

Table 3. Summary of the most common CPET parameters used for the evaluation of the respiratory system with clinical interpretation [1–3, 5–9]

Parameter	CPET result	Interpretation related to pulmonary diseases
VO _{2max}	Low	Lung or airway disease with low capacity of getting O ₂ into the lungs or from the lungs into the blood. An unfit patient who cannot reach maximum exercise capacity; The degree of the impairment of the cardiorespiratory function based on VO _{2max} : < 20 ml/kg/min – minor < 15 ml kg/min – moderate; < 10 ml kg/min – severe.
	Normal/high	No lung disease; VO _{2max} >80% of predicted value – low probability of clinically significant pathology of either the cardiovascular or respiratory systems.
HR	Low	Not reaching predicted value with dyspnea or exhaustion suggests lung disease; unfit patient; Bradyarrhythmias (e.g., sick sinus syndrome, 2 nd -degree atrioventricular block); Effect of drugs slowing heart rate, e.g., beta-blockers, verapamil, diltiazem.
	Normal/high	Does not suggest lung disease; HR >80% of the predicted maximal HR at peak exercise equals a low HR reserve; A fast increase in HR in patients with heart failure or unfit individuals; Well preserved or high HR reserve if exercise is limited by other than cardiac causes, for example by lung disease.
VE	Low/normal	Excludes lung disease; Should not reach 80% of the predicted value during a CPET in a healthy individual.
	High	Suggests a lung disease, particularly when VE reaches 80% of predicted value (a low ventilatory reserve) and VO _{2max} is low. A flatter Vt/VE slope with a visible plateau in patients with lung disease; Poor or no Vt increase during a CPET suggests a lung disease.
Pulse O ₂	Low	A plateau in the O ₂ pulse at a low value and during low workload or treadmill speed suggests a limited cardiac output or presence of anemia or pathology within pulmonary circulation;
	Normal/high	O ₂ pulse of at least 10 ml/beat at peak exercise should be observed in healthy people;
VCO ₂	Low	High VE with low VCO ₂ suggests a lung disease
	High	Exclusion of lung disease as CO ₂ is effectively eliminated from the blood.
VE/VCO ₂	Low	A lack of fall of VE/QCO ₂ below 30 suggests an impaired gas exchange in the lungs – usually in pulmonary vascular disease.
	High	High VE/VCO ₂ (>30) suggests poor perfusion of some lung areas not participating in the gas exchange and increased dead space in the respiratory system. Most commonly it translates to the presence of pulmonary vascular disease. In patients with HF indicates a poor prognosis.
RER	Low < 1.0	< 1.0 only in the early and middle part of a CPET. The exercise phase should be near or cross 1 at the end. If CPET ends with RER < 1, then exercise intensity was too low.
	Normal/high > 1.0	If in the latter part of CPET then submaximal or maximal exercise capacity is reached; If at the beginning then probably due to hyperventilation and agitated emotional status; Erratic RER behavior during a CPET (falls and increases) suggests dysfunctional breathing. Value > 1 indicate an intense effort and >1.1 corresponds to exhaustion or near-exhaustion level reached during CPET.
VE/VO ₂	Low	Suggests a lung disease or pulmonary vascular disease.
	Normal/high	Excludes a lung disease.
PETCO ₂	Low	Acute or chronic hyperventilation
	High	Increase by 3–8 mm Hg suggests pulmonary vascular disease
RCP	Not visible or uncertain	Presence of lung disease or poor ventilation is a limiting factor of exercise capacity, and a patient is unable able to exercise until academia develops.
	Normal/high	A clear RCP is a marker of acidemia developed during exercise (an expected physiological response to maximal physical effort). If RCP is present, then ventilation is not a limiting factor of exercise and excludes a lung disease.
BR	Low	When accompanied by low VO ₂ then typical for COPD. When accompanied by normal/high VO ₂ then typical for people with high cardiovascular capacity, e.g., endurance athletes.
	Normal/High	In patients with cardiac disease, for example, HF.
SpO ₂	Low	A fall of more than 4% during CPET suggests a disease of the lungs or the pulmonary circulation accompanied by impaired gas exchange. It may also be present in patients with right-to-left cardiac or aortic-pulmonary shunts.
	Normal	Usually in patients with cardiac diseases and no right-to-left shunts. Should exclude lung disease

uation of a patient with respiratory diseases. For example, VO_{2max} is the most commonly measured single parameter during CPET. When VO_{2max} is less than 80% of the predicted value, then it may indicate some lung pathology [1–3, 5–11]. However, a reduced VO_{2max} can also be found in patients with heart failure, ischemic heart disease, some cardiomyopathies, anemia or unfit individuals. It is worth mentioning that typically VO_{2max} gradually declines with aging. Although VO_{2max} is the most popular parameter in the CPET description, it is not sufficient to describe and diagnose all pathologies responsible for exertional dyspnea or other pathologies from the respiratory system.

Unfortunately, there is no single variable exclusively characteristic for the respiratory system diseases. For this reason, a set of different parameters, including HR, VE, pulse O_2 , VE/VCO_2 , sO_2 , must always be reviewed in concert to make an appropriate clinical decision. **Table 3** summarizes such CPET parameters with their clinical interpretation.

It is worth mentioning that CPET is useful not only as a confirmatory but also in ruling out respiratory diseases and pathologies as causes of exertional dyspnea or poor exercise capacity [2, 3, 5–8]. The probability that dyspnea originates in the respiratory system is low if a patient has achieved at least predicted value of VO_2 , HR, pulse O_2 , VE/VO_2 , and RCP with low to normal VE, no or irrelevant (< 4%) drop in sO_2 and a distinct RCP during this test.

The CPET is a valuable method in the diagnosis and risk stratification of patients with dyspnea, suspected and confirmed respiratory system diseases. It is also helpful in monitoring the progress of respiratory diseases and guiding the applied therapy. This test quantifies an integrative response of the cardiovascular and respiratory systems combined with metabolic factors (hemoglobin concentration, aerobic and anaerobic metabolism) to a controlled exercise. The examination of patients with respiratory diseases during exercise reveals new and clinically significant information which, in another case, might be inaccessible with resting measurements.

Acknowledgements

Conflict of interest statement

The authors declare no conflict of interest.

Funding sources

There are no sources of funding to declare.

References

1. Wasserman K, Hansen JE, Sue DY, Stringer WW, Sietsema KE, Sun X-G. Principles of Exercise Testing and Interpretation: Including Pathophysiology and Clinical Applications. Fifth Edition; LWW; 2011.
2. Kinnear W, Blakey J. A Practical Guide to the Interpretation of Cardiopulmonary Exercise Tests. Oxford University Press; 2014.
3. ATS/ACCP Statement on cardiopulmonary exercise testing. *Am J Respir Crit Care Med.* 2003;167:211–77.
4. Kowalska M, Fehlau M, Cymerys M, Guzik P. A thousand words about running fitness tests. *JMS.* 2019. Ahead of print, doi: <https://doi.org/10.20883/jms.344>.
5. Guazzi M, Adams V, Conraads V, Halle M, Mezzani A, Vanhees L, et al. Clinical recommendations for cardiopulmonary exercise testing data assessment in specific patient populations. *Eur Heart J.* 2012;33:2917–2927.
6. Guazzi M, Arena R, Halle M, Piepoli MF, Myers J, Lavie CJ. 2016 focused update: clinical recommendations for cardiopulmonary exercise testing data assessment in specific patient populations. *Circulation.* 2016;133:e694–e711.
7. Guazzi M. How to interpret cardiopulmonary exercise tests. *Heart Metab.* 2014;64:31–36.
8. Arena R, Sietsema KE. Cardiopulmonary exercise testing in the clinical evaluation of patients with heart and lung disease. *Circulation.* 2011;123: 668–680.
9. Herdy AH, Ritt LE, Stein R, Araújo CG, Milani M, Meneghelo RS, et al. Cardiopulmonary exercise test: background, applicability and interpretation. *Arq Bras Cardiol.* 2016;107:467–481.
10. Farina S, Correale M, Bruno N, Paolillo S, Salvioni E, Badagliacca R, et al. The role of cardiopulmonary exercise tests in pulmonary arterial hypertension. *Eur Respir Rev.* 2018;27:170134.
11. Dumitrescu D, Rosenkranz S. Graphical data display for clinical cardiopulmonary exercise testing. *Ann Am Thorac Soc.* 2017;14(Suppl 1):S12–21.
12. Borg GA. Psychophysical bases of perceived exertion. *Med Sci Sports Exerc.* 1982;14:377–381.

Acceptance for editing: 2019-05-09
Acceptance for publication: 2019-06-29

Correspondence address:

Przemysław Guzik, MD, PhD, FESC, ISHNE Fellow
Department of Cardiology-Intensive Therapy
Poznan University of Medical Sciences
49 Przybyszewskiego Street, 60-355 Poznań, Poland
phone: +48 618691391, fax: +48 618691689
e-mail: pguzik@ptkardio.pl



THOUSAND WORDS ABOUT...

DOI: <https://doi.org/10.20883/jms.350>

A thousand words about the imaging in cardiac amyloidosis

Rafał Dankowski^{1,a}, Marek Leszniewski^{1,b}, Małgorzata Pyda^{2,c}, Andrzej Szyszka^{1,d}


¹ Second Department of Cardiology, Poznan University of Medical Sciences, Poland

² Cardiac Magnetic Resonance Unit, First Department of Cardiology, Poznan University of Medical Sciences, Poland

^a  <https://orcid.org/0000-0003-0843-5378>

^c  <https://orcid.org/0000-0002-9963-0533>

^b  <https://orcid.org/0000-0002-0458-4934>

^d  <https://orcid.org/0000-0003-0471-7001>

ABSTRACT

Cardiac amyloidosis is an infiltrative disease which usually occurs under the form of restrictive cardiomyopathy. Advances in the treatment have changed the unfavorable outcomes of this disease. Thus, early diagnosis is essential. Recent advances in echocardiography and cardiac magnetic resonance have provided new modalities for the detection of cardiac amyloidosis. This summary discusses the role of imaging techniques in the diagnosis of cardiac amyloidosis.

Keywords: amyloidosis, echocardiography, myocardial strain imaging, cardiac magnetic resonance.

Introduction

Amyloidosis is characterized by the extracellular deposition of a structurally abnormal protein called 'amyloid' [1]. Cardiac amyloidosis (CA), or amyloid cardiomyopathy, refers to a group of inherited and acquired forms of amyloidosis involving the heart. Current classification of amyloidosis is based on a biochemical characteristic of amyloid fibrils [2]. Nomenclature includes a capital letter 'A', which denotes amyloid fibril protein, followed by a suffix that is an abbreviation of the parent or precursor protein name [3]. For example, for AL-type amyloidosis, the letter 'A' is a common index for amyloid and letter 'L' refers to an immunoglobulin light chain or light chain fragment.

CA occurs in two main forms, which accounts for 98% of clinical cases. The most common type (80% of cases) is AL-type amyloidosis, where the amyloid protein derives from misfolded immunoglobulin light chains.

The second most common type is transthyretin (ATTR) amyloidosis, resulting from the accumulation of the protein transthyretin. Transthyretin acts as a transport protein for thyroxine and retinol, and it is produced primarily in the liver. About 120 mutations in the TTR gene have been found to cause transthyretin amyloidosis. The most common mutation in patients with ATTR amyloidosis replaces valine with methionine at position 30 in the transthyretin protein (Val30-Met or V30M). V122I variant is another common mutation, mainly present in black Americans (3 to 4% of the population) or West African populations [4, 5]. ATTR amyloidosis accounts approximately for 18% of diagnosed cases of amyloidosis. This type of amyloidosis is further sub-divided into two types of disease: wild-type ATTR (ATTRwt) and hereditary (or mutant) ATTR (ATTRm) CA. Since the estimated survival from the onset of heart failure in patients with CA is of 3–4 years, early recognition is essential. These three most common forms of CA are described in **Table 1**.

Table 1. Characteristics of main types of cardiac amyloidosis

	AL amyloidosis	Acquired ATTR amyloidosis (wild type; senile amyloidosis)	Hereditary ATTR amyloidosis
Underlying reason	Plasma cell dyscrasia	Senile deposition of amyloid in myocardium	mutations in transthyretin gene (>100)
Precursor protein	Immunoglobulin light chains	Transthyretin, wild type (non-mutated, otherwise normal)	Mutated transthyretin (or prealbumin)
Percentage of cardiac amyloidosis (%)	80	18	
Age at manifestation (years)	> 40	> 60 (> 70)	30 to 70
Population	No specific population, both sexes	Older black men (mainly)	Afro-American, Afro-Caribbean, Portugal, Sweden, Japan
Course of disease	Poor prognosis, depending on specific organ involvement	Better prognosis, slower progression (compared to AL type)	
Organ involvement	One or more organs; In 50% of patients cardiac involvement	Mainly cardiomyopathy; Carpal tunnel syndrome; Involvement of other organs absent	Depending on mutation; cardiomyopathy, neuropathy, vitreous amyloidosis
Specific treatment	Chemotherapy (Bortezomib); Autologous bone marrow transplantation	Liver transplant, heart transplant Tafamidis	

The diagnosis of CA remains challenging due to its non-specific presentation. CA is considered a rare disease [6], which could also be the reason for misdiagnosis. Indeed, in the study by González-López et al. [7], the percent of the previous misdiagnosis was as high as 35%. Furthermore, ATTR amyloidosis seems also to be underdiagnosed [8]. Even if the majority of cases show a characteristic hypertrophic pattern, the full range of morphological findings in CA is more diverse. ATTR amyloidosis has been diagnosed in older patients with aortic stenosis [9] or patients with previously diagnosed hypertrophic cardiomyopathy [10]. No marked hypertrophy could also be observed [11]. Currently, noninvasive cardiac imaging including echocardiography and cardiac magnetic resonance are the first line modalities in the diagnosis of CA.

Echocardiography in the diagnosis of CA

Echocardiography is the first-line screening tool, and virtually every patient with unexplained cardiac hypertrophy should be suspected of amyloidosis. Before harmonic imaging was commonly used, the echocardiographic pattern of sparkling myocardium was considered to be diagnostic for CA. However, myocardial speckling in amyloidosis has been shown to have low diagnostic sensi-

tivity and specificity [12]. This echocardiographic phenomenon could also be found in hypertrophic cardiomyopathy, myocarditis, as well as in other infiltrative diseases of the myocardium. Most common echocardiographic representation of CA is the thickening of the left and right ventricular wall, thickening of the heart valves, and enlarged atria [13, 14] (**Figure 1, Video 1** – online). Extracellular deposition of amyloid fibrils contributes to ventricular stiffening and left ventricular diastolic dysfunction. Doppler analysis of mitral inflow reveals a restrictive pattern with a high E wave velocity and E/A ratio (**Figure 1**). Elevated E/e' ratio reflects the high filling pressures.

Although all these echocardiographic features are typical for CA, none of them are specific enough to be diagnostic.

Introduction of myocardial deformation analysis with the use of speckle tracking echocardiography significantly expanded the diagnostic potential of echocardiography. This technique utilizes the speckle pattern of two-dimensional gray-scale echocardiographic images. By grouping of the speckles into blocks and tracing it frame-by-frame, it allows measuring myocardial deformation in the longitudinal, circumferential and radial axis (**Figure 2**). During the last ten years, this modality has become a recognized method in the assessment of the left ventricular systolic function [15]. It has also been shown to be a valuable tool in the diagnosis of CA – the

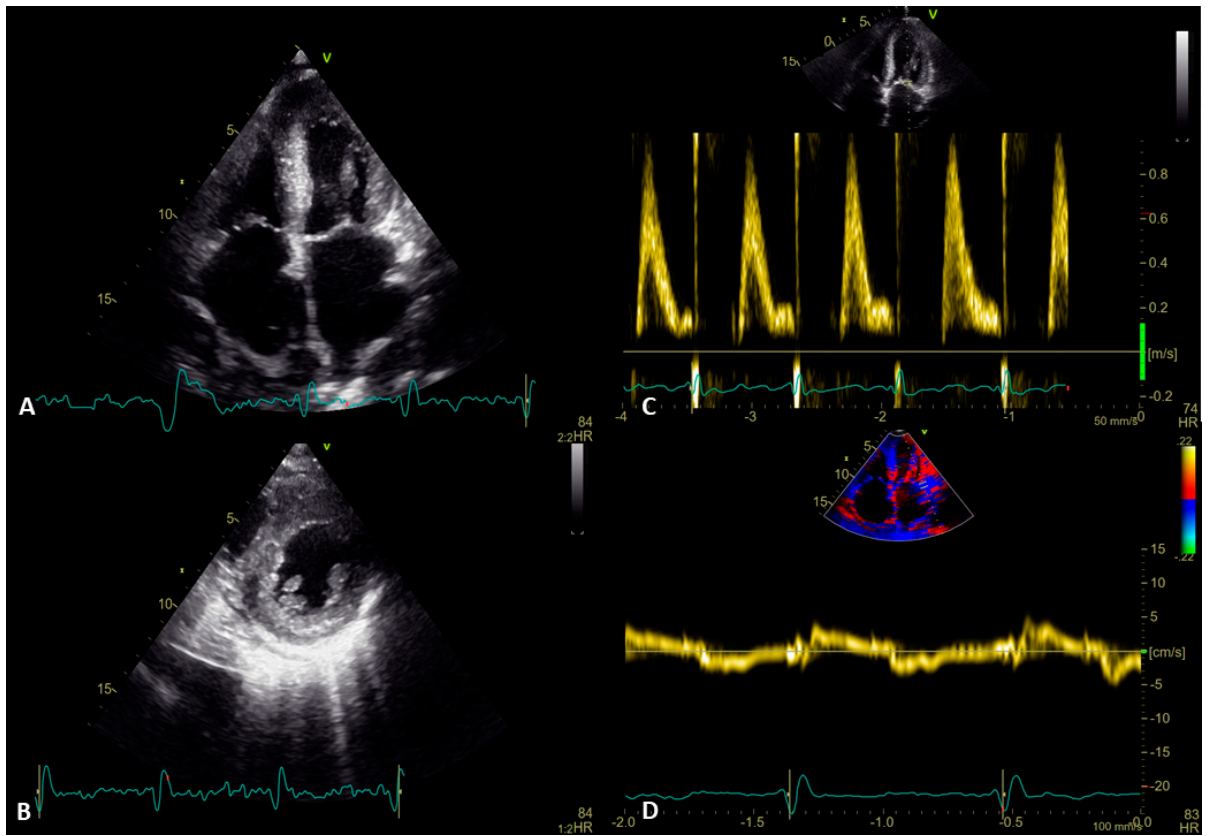


Figure 1. Echocardiographic image of cardiac amyloidosis. Panel A: apical four chamber view; thickening of the left ventricular wall, thickening of the heart valves, and enlarged atria thickened interatrial septum and pericardial effusion. Panel B: Parasternal short axis view: small, hypertrophied left ventricle. Panel C: Doppler inflow of the mitral valve, high velocity of E-wave, no A-wave (atrial fibrillation) showing restrictive pattern of the mitral inflow. Panel D: Tissue Doppler echocardiography – decreased velocities of the myocardium

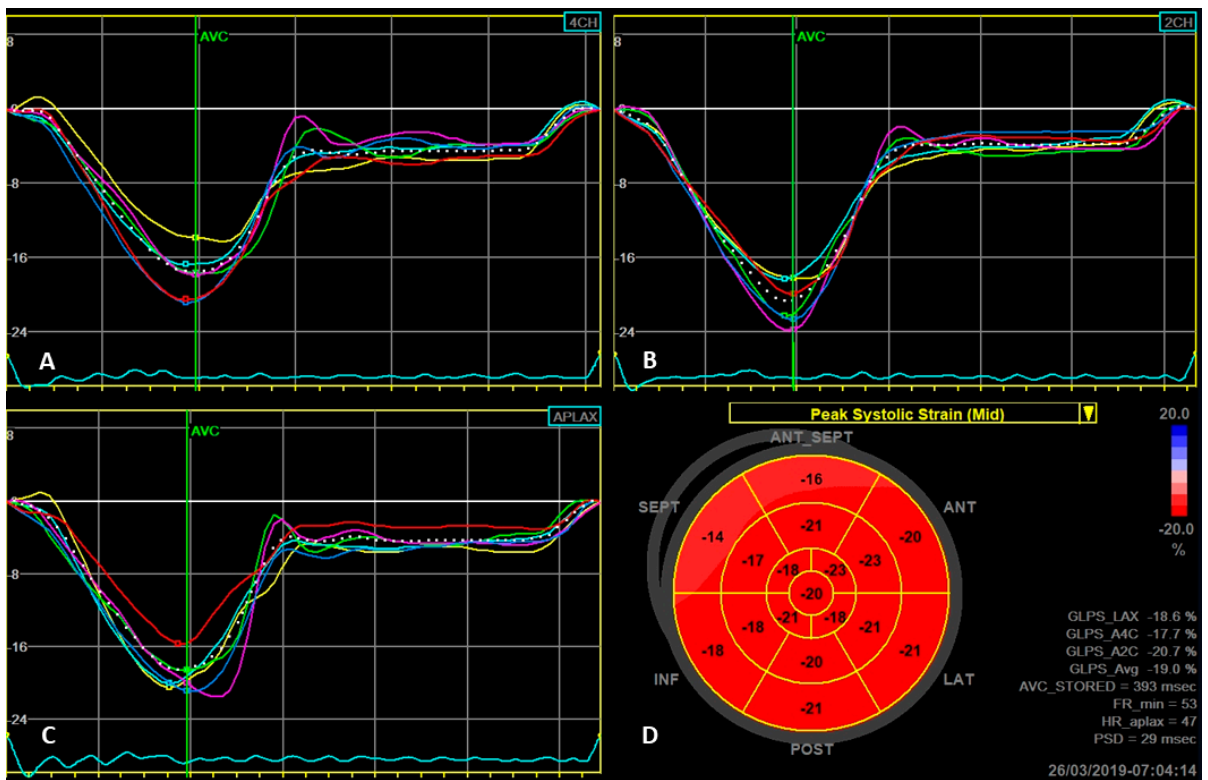


Figure 2. Normal values of longitudinal strain. Panels A, B and C show strain curves for left ventricular segments in apical four chamber-, two chamber and three chamber view, respectively. Dotted with line shows average value. Panel D – planar map of the peak systolic strain values for 17 segments of the left ventricle. Global longitudinal strain is – 19%.

global longitudinal strain (GLS) is impaired early in the course of the disease, even when left ventricular ejection fraction is preserved [16]. Importantly, the segmental longitudinal strain has an unusual and typical for CA pattern, with greater reduction of strain values in basal and mid segments of the left ventricle with relative sparing of apical segments (**Figure 3**). This phenomenon of 'apical sparing' is clearly visible on planar maps (so-called "bullseye") of segmental myocardial strain, and it is sensitive and specific for the diagnosis of CA [17].

ducible and accurate index to differentiate CA from other causes of LV thickening [20].

Cardiac magnetic resonance imaging

Cardiac magnetic resonance (CMR) is a very sensitive and specific tool for the diagnosis of CA. The main advantage of CMR over echocardiography is the ability of tissue characterization. The myocardial deposition of amyloid increases extracellular volume, which results in the accu-

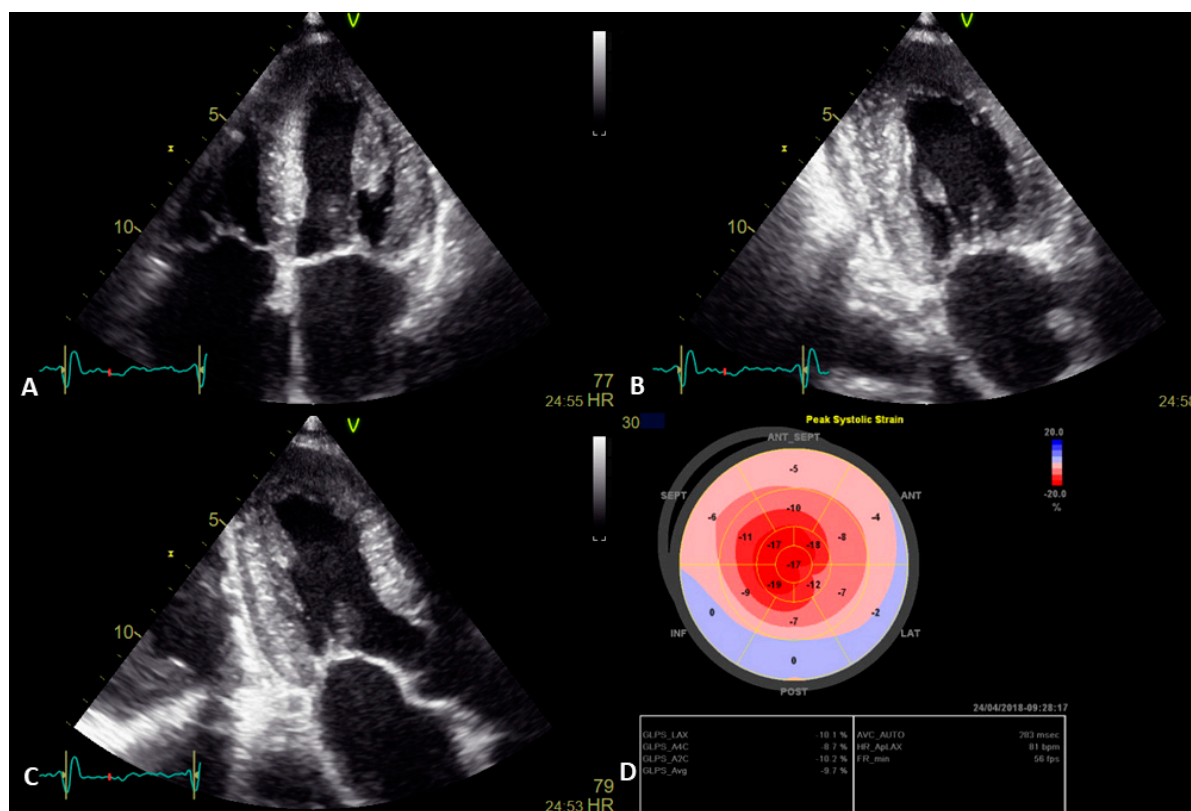


Figure 3. Global longitudinal strain in cardiac amyloidosis. Panels A, B, C show 2-dimensional apical four chamber-, two chamber, and three chamber view, respectively. In panel D, the strain map shows particular patterns suggestive of amyloidosis with relative preserved strain in apical segments and decreased on mid and basal level (apical sparing pattern).

Apical sparing could be expressed with the use of the formula: average longitudinal apical strain/(average basal longitudinal strain+average mid longitudinal strain). Furthermore, echocardiographic measurement of myocardial strain parameters can discriminate CA from the other causes of cardiac hypertrophy [18, 19]. Most recently, the dissociation between preserved left ventricular ejection fraction and reduced GLS (LVEF/GLS ratio), has been reported as a repro-

duction of gadolinium contrast. For this reason, late gadolinium enhancement (LGE) imaging has been proven to be effective in identifying CA [21]. Although the typical pattern for CA is diffuse subendocardial LGE in a non-coronary artery territory distribution, transmural or focal patchy LGE could also be observed [22]. **Figure 4** shows common LGE patterns that may be encountered in patients with CA. Another promising technique is non-contrast T1 CMR. Of note, it is safe

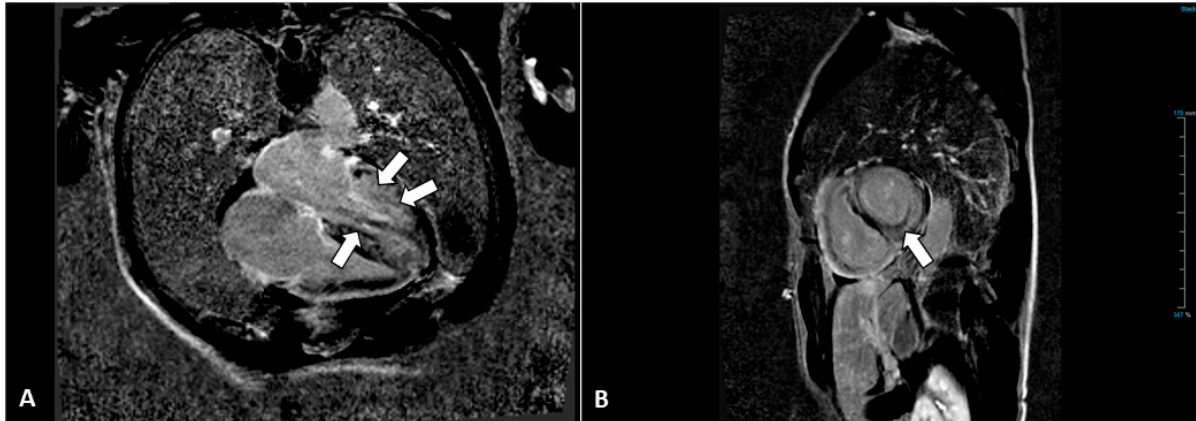


Figure 4. Cardiac magnetic resonance. Panel A: 4-chamber view. LGE image. Diffuse amyloid infiltration with interstitial fibrosis of interventricular septum and lateral wall of left ventricle (arrows). Panel B: short axis view. LGE image. Subendocardial amyloid infiltration in mid segment of left ventricle (arrow)

in patients with renal failure, which is a common problem in this group of patients. In this technique, the direct quantitative myocardial signal is measured before and after the application of contrast. It has been found that native myocardial T1 mapping has a high diagnostic accuracy for both types of CA (AL and ATTR), and is more sensitive for detecting early disease in gene mutation carriers than LGE imaging [23]. Furthermore, CMR allows differentiating between ATTR and AL amyloidosis [24].

The diagnosis of CA remains a diagnostic challenge. Reduced GLS with the unique regional deformation pattern is used for the initial diagnosis and differentiation from other types of cardiac hypertrophy. CMR with the LGE assessment could be applied for the confirmation of diagnosis.

Acknowledgements

Conflict of interest statement

The authors declare no conflict of interest.

Funding sources

There are no sources of funding to declare.

References

- Maleszewski JJ. Cardiac amyloidosis: pathology, nomenclature, and typing. *Cardiovasc Pathol.* 2015;24(6):343–50.
- Benson MD, Buxbaum JN, Eisenberg DS, Merlini G, Saraiva MJM, Sekijima Y, et al. Amyloid nomenclature 2018: recommendations by the International Society of Amyloidosis (ISA) nomenclature committee. *Amyloid.* 2018;25(4):215–9.
- Sipe JD, Benson MD, Buxbaum JN, Ikeda S-i, Merlini G, Saraiva MJM, et al. Nomenclature 2014: Amyloid fibril proteins and clinical classification of the amyloidosis. *Amyloid.* 2014;21(4):221–4.
- Jacobson DR, Pastore RD, Yaghoubian R, Kane I, Gallo G, Buck FS, et al. Variant-sequence transthyretin (isoleucine 122) in late-onset cardiac amyloidosis in black Americans. *N Engl J Med.* 1997;336(7):466–73.
- Rapezzi C, Quarta CC, Obici L, Perfetto F, Longhi S, Salvi F, et al. Disease profile and differential diagnosis of hereditary transthyretin-related amyloidosis with exclusively cardiac phenotype: an Italian perspective. *Eur Heart J.* 2013;34(7):520–8.
- Pinney JH, Smith CJ, Taube JB, Lachmann HJ, Verner CP, Gibbs SD, et al. Systemic amyloidosis in England: an epidemiological study. *Br J Haematol.* 2013;161(4):525–32.
- González-López E, Dominguez F, Alonso-Pulpon L, Cobo-Marcos M, Garcia-Pavia P, Lara-Pezzi E, et al. Clinical characteristics of wild-type transthyretin cardiac amyloidosis: disproving myths. *European Heart Journal.* 2017;38(24):1895–904.
- Mohammed SF, Mirzoyev SA, Edwards WD, Dogan A, Grogan DR, Dunlay SM, et al. Left ventricular amyloid deposition in patients with heart failure and preserved ejection fraction. *JACC Heart Fail.* 2014;2(2):113–22.
- Castano A, Narotsky DL, Hamid N, Khaliq OK, Morgenstern R, DeLuca A, et al. Unveiling transthyretin cardiac amyloidosis and its predictors among elderly patients with severe aortic stenosis undergoing transcatheter aortic valve replacement. *Eur Heart J.* 2017;38(38):2879–87.
- Morner S, Hellman U, Suhr OB, Kazzam E, Waldenström A. Amyloid heart disease mimicking hypertrophic cardiomyopathy. *J Intern Med.* 2005;258(3):225–30.
- Falk RH. Tafamidis for transthyretin amyloid cardiomyopathy: the solution or just the beginning of the end? *European Heart Journal.* 2019;40(12):1009–12.
- Picano E, Pinamonti B, Ferdeghini E, Landini L, Slavich G, Orlandini A, et al. Two-Dimensional Echocardi-

- ography in Myocardial Amyloidosis. *Echocardiography*. 1991;8(2):253–9.
13. Cacciapuoti F. The role of echocardiography in the non-invasive diagnosis of cardiac amyloidosis. *J Echocardiogr*. 2015;13(3):84–9.
 14. Di Nunzio D, Recupero A, de Gregorio C, Zito C, Carerj S, Di Bella G. Echocardiographic Findings in Cardiac Amyloidosis: Inside Two-Dimensional, Doppler, and Strain Imaging. *Curr Cardiol Rep*. 2019;21(2):7.
 15. Lang RM, Badano LP, Mor-avi V, Afilalo J, Armstrong A, Ernande L, et al. Recommendations for Cardiac Chamber Quantification by Echocardiography in Adults: An Update from the American Society of Echocardiography and the European Association of Cardiovascular Imaging. *Journal of the American Society of Echocardiography*. 2015;28(1):1–39.e14.
 16. Bellavia D, Abraham TP, Pellikka PA, Al-Zahrani GB, Dispenzieri A, Oh JK, et al. Detection of left ventricular systolic dysfunction in cardiac amyloidosis with strain rate echocardiography. *J Am Soc Echocardiogr*. 2007;20(10):1194–202.
 17. Phelan D, Collier P, Thavendiranathan P, Popovic ZB, Hanna M, Plana JC, et al. Relative apical sparing of longitudinal strain using two-dimensional speckle-tracking echocardiography is both sensitive and specific for the diagnosis of cardiac amyloidosis. *Heart*. 2012;98(19):1442–8.
 18. Marwick TH, Shah SJ, Thomas JD. Myocardial Strain in the Assessment of Patients With Heart Failure: A Review. *JAMA Cardiol*. 2019.
 19. Sun JP, Stewart WJ, Yang XS, Donnell RO, Leon AR, Felner JM, et al. Differentiation of hypertrophic cardiomyopathy and cardiac amyloidosis from other causes of ventricular wall thickening by two-dimensional strain imaging echocardiography. *Am J Cardiol*. 2009;103(3):411–5.
 20. Pagourelas ED, Duchenne J, Mirea O, Vovas G, Van Cleemput J, Delforge M, et al. The Relation of Ejection Fraction and Global Longitudinal Strain in Amyloidosis: Implications for Differential Diagnosis. *JACC: Cardiovascular Imaging*. 2016;9(11):1358–9.
 21. Maceira AM, Joshi J, Prasad SK, Moon JC, Perugini E, Harding I, et al. Cardiovascular magnetic resonance in cardiac amyloidosis. *Circulation*. 2005;111(2):186–93.
 22. Syed IS, Glockner JF, Feng D, Araoz PA, Martinez MW, Edwards WD, et al. Role of Cardiac Magnetic Resonance Imaging in the Detection of Cardiac Amyloidosis. *JACC: Cardiovascular Imaging*. 2010;3(2):155–64.
 23. Fontana M, Banyersad SM, Treibel TA, Maestrini V, Sado DM, White SK, et al. Native T1 mapping in transthyretin amyloidosis. *JACC Cardiovasc Imaging*. 2014;7(2):157–65.
 24. Dzungu JN, Valencia O, Pinney JH, Gibbs SD, Rowczenio D, Gilbertson JA, et al. CMR-based differentiation of AL and ATTR cardiac amyloidosis. *JACC Cardiovasc Imaging*. 2014;7(2):133–42.

Acceptance for editing: 2019-05-09
 Acceptance for publication: 2019-06-29

Correspondence address:

Rafał Dankowski
 2nd Department of Cardiology
 Poznan University of Medical Sciences
 194 28 Czerwca 1956 r. Street, 61-485 Poznań, Poland
 phone: +48 612274160
 e-mail: rafaldan@ump.edu.pl



THE RATIONALE, DESIGN AND METHODS OF NEW STUDIES

DOI: <https://doi.org/10.20883/jms.328>

Characterization of the selected honeybee products based on omics techniques

Eliza Matuszewska^{1,a}, Paweł Dereziński^{1,b}, Agnieszka Klupczyńska^{1,c},
Agata Światły-Błaszkiwicz^{1,d}, Szymon Plewa^{1,e}, Jan Lubawy^{2,f}, Arkadiusz Urbański^{2,g},
Grzegorz Rosiński^{2,h}, Zenon J. Kokot^{1,i}, Jan Matysiak^{1,j}

¹ Department of Inorganic and Analytical Chemistry, Poznan University of Medical Sciences, Poland

² Faculty of Biology, Department of Animal Physiology and Development, Adam Mickiewicz University in Poznan, Poland

^a  <https://orcid.org/0000-0002-5765-2603>

^b  <https://orcid.org/0000-0002-6066-1260>

^c  <https://orcid.org/0000-0002-5028-1408>

^d  <https://orcid.org/0000-0002-3603-0207>

^e  <https://orcid.org/0000-0002-9600-3980>

^f  <https://orcid.org/0000-0003-4030-3471>

^g  <https://orcid.org/0000-0003-4875-4541>

^h  <https://orcid.org/0000-0001-6686-7254>

ⁱ  <https://orcid.org/0000-0003-4950-9759>

^j  <https://orcid.org/0000-0002-9993-1504>

ABSTRACT

The research project "Characterization of the selected honeybee products based on omics techniques" is to comprehensively characterize honeybee venom, royal jelly, propolis, and pollen, by applying advanced analytical and bioinformatics methodologies. Honeybee products (HBP) contain many bioactive components with both beneficial and harmful effects on the human organism. Nevertheless, the overall composition of the HBP remains not fully investigated. Thus, this research is focused on complementary proteomic and metabolomic characterization of biologically active compounds derived from HBP, regarding their toxicological and pharmacological properties. The objectives of the study will be achieved by the application of up to date mass spectrometry techniques. Due to increasing interest in using of HBP in medicine, this project will contribute to improving the safety of HBP-derived dietary supplements and drugs.

Keywords: honeybee products, proteomics, metabolomics, mass spectrometry.

General Information

The research project entitled „Characterization of the selected honeybee products based on omics techniques" was awarded by the Polish National Science Center (NCN) in the SONATA12 competition under grant number 2016/23/D/NZ7/03949. The project is run by Department of Inorganic and Analytical Chemistry at Poznan University of Medical Sciences, Poland. The principal investigator is Jan Matysiak (Ph.D.). The duration of the grant is 36 months, from 29th August 2017 to 28th August 2020.

This proposed study will contribute to broadening the knowledge of the honeybee products (HBP), such as honeybee venom, royal jelly, propolis, and pollen. It is known, that HBP contain many bioactive components with potential biological, toxic or allergic properties [1–3]. Because of their beneficial effects on the human organism, HBP have been used in medicine since ancient times. The present-day medical field utilizing HBP in the treatment of various diseases is termed apitherapy and is gaining popularity [4]. Nevertheless, despite increasing interest in natural honeybee-derived products, the composition and

the molecular basis of HBP activities remain not fully characterized. This project, using innovative approaches with the most modern LC-MS (mass spectrometry-liquid chromatography) techniques, will result in the discovery of new biologically and pharmacologically active compounds. Moreover, it will contribute to the evaluation of the biological activity of HBP. This is of great significance for assessing the quality and safety of HBP-based products (dietary supplements and drugs). Thus, this research will positively affect healthcare, improving human wellness.

Finance

This project is mainly financed by a grant from the NCN Life Science Panel in the SONATA12 competition. The total grant value is 1,199,810 Polish Zloty. Grant funds were earmarked to purchase new laboratory instrumentation, disposable laboratory equipment and reagents for the conducting of proposed research. In particular, MALDI Imaging Equipment is planned to be purchased for MALDI imaging studies. Also, grant funds were designed to cover personnel costs of project participants and costs associated with the promotion of research results and publications in reviewed journals.

Research project objectives

This research is focused on complementary proteomic and metabolomic characterization of biologically active compounds derived from HBP (honeybee venom, royal jelly, propolis, and pollen). There are three main hypotheses in this project:

- › Proteomic and metabolomic study of HBP will lead to the discovery of new compounds with biological activity.
- › HBP contain compounds with toxic properties (their presence and concentration are related to environmental contamination in HBP sampling locations) that impact on the specific biological activity of HBP.
- › The applied bioanalytical methods will allow gaining detailed knowledge of the biological activity of the studied compounds. That will

contribute to the explanation of the influence of HBP on the human organism.

The objectives of the study will be achieved by the application of up to date mass spectrometry techniques supported by advanced bioinformatics tools. Mass spectrometry is a modern technique that deals with the identification and studying of the structure of the chemical compound. In this proposed research, novel methodologies based both on nanoLC-MALDI-TOF-MS (nano-liquid chromatography-matrix assisted laser desorption/ionization-time of flight mass spectrometry) and LC-ESI-QTOF-MS (liquid chromatography-electrospray ionization-hybrid quadrupole-time of flight mass spectrometry) will be developed. Mass spectrometry coupled with liquid chromatography allows for detection and identification of thousands of low-abundance molecules in biological matrices. Thus, applying complex targeted and untargeted proteomic and metabolomic approach will lead to the discovery of new biologically active HBP components. Moreover, the proposed strategy will enable to assess the variability of the composition of HBP. Factors responsible for that variability will be pointed out, as a biological activity of HBP depends on their constituents.

Quality of HBP is not only associated with their composition. The contaminants (i.e., pesticides, organic pollutants, pharmaceutical residues, and heavy metals) may significantly weaken the properties of bee-derived products. In particular, accumulation of pesticides in HBP should be examined in terms of their toxic effect both on humans and on bees [5]. Therefore, this study aims to evaluate the impact of the contaminants on HBP and to assess exposure of honeybees to various chemicals. The multi-compound screening methods enabling simultaneous analysis of miscellaneous groups of pollutants will be developed.

As mentioned before, the constituents of HBP, due to different biological properties, may affect the functioning of the human organism. To investigate the mechanism of HBP activity and effects on live organisms, the bioassay analysis will be performed. According to the literature, the insect model was successfully applied in the characterization of the mechanism underlying human diseases [6–8]. Therefore, in this study insect tissues will be used instead of those

derived from humans, as the insect tissues' physiology is considered to be similar to the human organism. Therefore, the aim of this project is to explore potential pharmacological and toxic properties of HBP and their constituents by complementary use of bioassay and mass spectrometry analysis. The alternative to the classical MS techniques is mass spectrometry imaging (MSI). MSI coupled with matrix assisted laser desorption/ionization (MSI-MALDI) has been previously reported in honeybee venom compounds monitoring in envenomed tissues [9]. Thus, in this project, novel MSI-MALDI procedures will be implemented.

Research plan and basic concept

The main goal of this project is to comprehensively characterize natural HBP by applying advanced analytical and bioinformatics methodologies. The HBP may be a valuable source of components with potential biological activity. Proteomic and metabolomic techniques will allow for detection of novel low molecular compounds (including amino acids), peptides and proteins which can be used in medicine. To date, most of the reported studies were focused on honeybee venom investigations [1, 2, 10]. Therefore, in order to extend knowledge of HBP, within this project, large-scale omics research will be conducted. In particular, the study will focus on:

- › Collecting of HBP and bee samples and creation of biorepository in which the samples and data will be stored. Materials and data retained in biorepository could be used for future investigations.
- › Development of innovative methods based on modern analytical techniques. These methodologies may be implemented to the characterization of HBP as well as other natural products.
- › Compilation of data obtained from proteomic, metabolomic, toxicological and bioassay analyses.
- › Creation of a database of HBP and their constituents. This database will consider biological, toxicological and pharmacological properties of the HBP. It will collect the results of this research and could be extended by results obtained from other projects.

Research methodology

The research will be conducted using HBP samples collected from 4 apiaries located in Poland. During three years, from each apiary, three samples of each HBP type will be collected within four months of each year. Samples will be stored at -80°C in a newly created biorepository. In order to perform comprehensive analyses, two mass spectrometers coupled with liquid chromatography systems will be used: nanoLC-MALDI-TOF-MS and LC-ESI-QTOF-MS. The combination of multiple strategies will ensure the complete insight into HBP. Thus, in this study, the application of both targeted and untargeted mass spectrometry-based methodologies is planned. The project is planned for 36 months, and the main assumptions include the following tasks:

- › Development of toxicological methods and study of toxicology. To isolate the HBP compounds, different sample preparation strategies will be tested, such a lyophilization, solid phase extraction (SPE), homogenization, liquid-liquid extraction (LLC) and QuEChERS method (Quick, Easy, Cheap, Effective, Rugged and Safe). The targeted analysis will be performed using LC-ESI-QqQ-MS (hybrid triple quadrupole-linear ion trap mass spectrometer) system. For untargeted analysis, LC-ESI-QTOF-MS will be used.
- › Development of bioassay methods and study of bioassays. Different isolation methods (isoelectric focusing, liquid chromatography, gel electrophoresis, capillary electrophoresis) for HBP components will be tested. Studied substances derived from HBP will be injected into insect samples. The mass spectrometry analyses will be performed using MSI-MALDI system.
- › Development of proteomic methods and proteomic studies. To achieve proteomics purposes of this project, for the protein-peptide profiling of HBP compounds, MALDI-TOF-MS and ESI-QTOF-MS systems will be used. New protocols for HBP analysis will be developed. Moreover, because of the sensitivity of mass spectrometry analyses, various sample pretreatment strategies will be tested, like SPE, isoelectric focusing, two-dimensional gel electrophoresis, and combinatorial ligand library. Additionally, isobaric labeling for semi-quantitative analysis will be implemented.

- › Development of metabolomic methods and metabolomic studies. Untargeted and targeted metabolomic studies will be performed by using the hyphenated LC-MS techniques. LC-ESI-QTOF-MS and nanoLC-MALDI-TOF-MS platforms will be used for investigation of HBP components.
- › Data analysis and omics data compilation. The results obtained from HBP investigations will be statistically analyzed by univariate and multivariate approaches. Correlation analyses between the obtained results and pathway analyses will be performed. The data will be interpreted using various databases. Statistical analysis will enable to assess the variability in HBP composition and the responsible factors.
- › HBP database constitution. Creation of a new open access database of HBP and their constituents, regarding their biological, toxicological and pharmacological properties is planned. This database could be used in future HBP studies.

Measurable effects and expected results

This project will result in the deep characterization of HBP. We expect, that applying combined proteomic and metabolomic strategies, including mass spectrometry techniques, allows to significantly extend the knowledge of HBP composition and their biological properties. Due to increasing interest in using of HBP in medicine, this project will contribute to improving the safety of HBP-derived dietary supplements and drugs. Moreover, a compilation of the obtained data will result in a better understanding of the molecular mechanism of HBP activities. The impact of the contaminants (in particular pesticides) on the HBP properties will also be assessed. In addition, the development of novel advanced omics strategies and creation of unique HBP database will allow to comprehensively investigate the HBP and other natural products in the future.

Acknowledgements

Conflict of interest statement

The authors declare no conflict of interest.

Funding sources

This paper is a part of the project "Characterization of the selected honeybee products based on omics techniques" supported by the Polish National Science Centre (grant number 2016/23/D/NZ7/03949).

References

1. Matysiak J, Hajduk J, Mayer F, Hebel R, Kokot ZJ. Hyphenated LC-MALDI-ToF/ToF and LC-ESI-QToF approach in proteomic characterization of honeybee venom. *J Pharm Biomed Anal.* 2016;121:69–76.
2. Matysiak J, Hajduk J, Pietrzak Ł, Schmelzer CEH, Kokot ZJ. Shotgun proteome analysis of honeybee venom using targeted enrichment strategies. *Toxicol.* 2014;90:255–64.
3. Matysiak J, Schmelzer CEH, Neubert RHH, Kokot ZJ. Characterization of honeybee venom by MALDI-TOF and nanoESI-QqTOF mass spectrometry. *J Pharm Biomed Anal.* 2011;54(2):273–8.
4. Kim CMH. Apitherapy – Bee Venom Therapy. In: Grassberger M, Sherman RA, Gileva OS, Kim CMH, Mumcuoglu KY, editors. *Biotherapy – History, Principles and Practice.* Dordrecht: Springer Netherlands; 2013. p. 77–112.
5. Sánchez-Bayo F, Goulson D, Pennacchio F, Nazzi F, Goka K, Desneux N. Are bee diseases linked to pesticides? – A brief review. *Environ Int.* 2016;89–90:7–11.
6. Ugur B, Chen K, Bellen HJ. *Drosophila* tools and assays for the study of human diseases. *Dis Model Mech.* 2016;9(3):235–44.
7. Alfa RW, Kim SK. Using *Drosophila* to discover mechanisms underlying type 2 diabetes. *Dis Model Mech.* 2016;9(4):365–76.
8. Tabunoki H, Bono H, Ito K, Yokoyama T. Can the silkworm (*Bombyx mori*) be used as a human disease model? *Drug Discov Ther.* 2016;10(1):3–8.
9. Francese S, Lambardi D, Mastrobuoni G, la Marca G, Moneti G, Turillazzi S. Detection of Honeybee Venom in Envenomed Tissues by Direct MALDI MSI. *J Am Soc Mass Spectrom.* 2009;20(1):112–23.
10. Kokot ZJ, Matysiak J, Urbaniak B, Dereziński P. New CZE-DAD method for honeybee venom analysis and standardization of the product. *Anal Bioanal Chem.* 2011;399(7):2487–94.

Acceptance for editing: 2019-05-09
Acceptance for publication: 2019-06-29

Correspondence address:

Jan Matysiak
Department of Inorganic and Analytical Chemistry
Poznan University of Medical Sciences
6 Grunwaldzka Street, 60-780 Poznań, Poland
phone: +48 618546611, fax: +48 618546609
e-mail: jmatysiak@ump.edu.pl

Journal of Medical Science (JMS) is a PEER-REVIEWED, OPEN ACCESS journal that publishes original research articles and reviews which cover all aspects of clinical and basic science research. The journal particularly encourages submissions on the latest achievements of world medicine and related disciplines. JMS is published quarterly by Poznan University of Medical Sciences.

ONLINE SUBMISSION:

Manuscripts should be submitted to the Editorial Office by an e-mail attachment: nowinylekarskie@ump.edu.pl. You do not need to mail any paper copies of your manuscript.

All submissions should be prepared with the following files:

- Cover Letter
- Manuscript
- Tables
- Figures
- Supplementary Online Material

COVER LETTER: Manuscripts must be accompanied by a cover letter from the author who will be responsible for correspondence regarding the manuscript as well as for communications among authors regarding revisions and approval of proofs. The cover letter should contain the following elements: (1) the full title of the manuscript, (2) the category of the manuscript being submitted (e.g. Original Article, Brief Report), (3) the statement that the manuscript has not been published and is not under consideration for publication in any other journal, (4) the statement that all authors approved the manuscript and its submission to the journal, and (5) a list of at least two referees.

MANUSCRIPT: Journal of Medical Science publishes Original Articles, Brief Reports, Review articles, Mini-Reviews, Images in Clinical Medicine and The Rationale and Design and Methods of New Studies. From 2014, only articles in English will be considered for publication. They should be organized as follows: Title page, Abstract, Introduction, Materials and Methods, Results, Discussion, Acknowledgments, Conflict of Interest, References and Figure Legends. All manuscripts should be typed in Arial or Times New Roman font and double spaced with a 2,5 cm (1 inch) margin on all sides. They should be saved in DOC, DOCX, ODT, RTF or TXT format. Pages should be numbered consecutively, beginning with the title page.

Ethical Guidelines

Authors should follow the principles outlined in the Declaration of Helsinki of the World Medical Association (www.wma.net). The manuscript should contain a statement that the work has been approved by the relevant institutional review boards or ethics committees and that all human participants gave informed consent to the work. This statement should appear in the Material and Methods section. Identifying information, including patients' names, initials, or hospital numbers, should not be published in written descriptions, illustrations, and pedigrees. Studies involving experiments with animals must be conducted with approval by the local animal care committee and state that their care was in accordance with institution and international guidelines.

Authorship:

According to the International Committee on Medical Journal Ethics (ICMJE), an author is defined as one who has made substantial contributions to the conception and development of a manuscript. Authorship should be based on all of the following: 1) substantial contributions to conception and design, data analysis and interpretation; 2) article drafting or critical advice for important intellectual content; and 3) final approval of the version to be published. All other contributors should be listed as acknowledgments. All submissions are expected to comply with the above definition.

Conflict of Interest

The manuscript should contain a conflict of interest statement from each author. Authors should disclose all financial and personal relationships that could influence their work or declare the absence of any conflict of interest. Author's conflict of interest should be included under Acknowledgements section.

Abbreviations

Abbreviations should be defined at first mention, by putting abbreviation between brackets after the full text. Ensure consistency of abbreviations throughout the article. Avoid using them in the title and abstract. Abbreviations may be used in tables and figures if they are defined in the table footnotes and figure legends.

Trade names

For products used in experiments or methods (particularly those referred to by a trade name), give the manufacturer's full name and location (in parentheses). When possible, use generic names of drugs.

Title page

The first page of the manuscript should contain the title of the article, authors' full names without degrees or titles, authors' institutional affiliations including city and country and a running title, not exceeding 40 letters and spaces. The first page should also include the full postal address, e-mail address, and telephone and fax numbers of the corresponding author.

Abstract

The abstract should not exceed 250 words and should be structured into separate sections: Background, Methods, Results and Conclusions. It should concisely state the significant findings without reference to the rest of the paper. The abstract should be followed by a list of 3 to 6 Key words. They should reflect the central topic of the article (avoid words already used in the title).

The following categories of articles can be proposed to the Journal of Medical Science:

ORIGINAL RESEARCH

Original articles: Manuscripts in this category describe the results of original research conducted in the broad area of life science and medicine. The manuscript should be presented in the format of Abstract (250-word limit), Keywords, Introduction, Material and Methods, Results, Discussion, Perspectives, Acknowledgments and References. In the Discussion section, statements regarding the importance and *novelty of the study* should be presented. In addition, the limitations of the study should be articulated. The abstract must be structured and include: Objectives, Material and Methods, Results and Conclusions. Manuscripts cannot exceed 3500 words in length (excluding title page, abstract and references) and contain no more than a combination of 8 tables and/or figures. The number of references should not exceed 45.

Brief Reports: Manuscripts in this category may present results of studies involving small sample sizes, introduce new methodologies, describe preliminary findings or replication studies. The manuscript must follow the same format requirements as full length manuscripts. Brief reports should be up to 2000 words (excluding title page, abstract and references) and can include up to 3 tables and/or figures. The number of references should not exceed 25.

REVIEW ARTICLES

Review articles: These articles should describe recent advances in areas within the Journal's scope. Review articles cannot exceed 5000 words length (excluding title page, abstract and references) and contain no more than a combination of 10 tables and/or figures. Authors are encouraged to restrict figures and tables to essential data that cannot be described in the text. The number of references should not exceed 80.

A THOUSAND WORDS ABOUT... is a form of Mini-Reviews. Manuscripts in this category should focus on *latest achievements of life science and medicine*. Manuscripts should be up to 1000 words in length (excluding title page, abstract and references) and contain up to 5 tables and/or figures and up to 25 most relevant references. The number of authors is limited to no more than 3.

OTHER SUBMISSIONS

Invited Editorials: Editorials are authoritative commentaries on topics of current interest or that relate to articles published in the same issue. Manuscripts should be up to 1500 words in length. The number of references should not exceed 10. The number of authors is limited to no more than 2.

Images in Clinical Medicine: Manuscripts in this category should contain one distinct image from life science or medicine. Only original and high-quality images are considered for publication. The description of the image (up to 250 words) should present relevant information like short description of the patient's history, clinical findings and course, imaging techniques or molecular biology techniques (e.g. blotting techniques or immunostaining). All labeled structures in the image should be described and explained in the legend. The number of references should not exceed 5. The number of authors is limited to no more than 5.

The Rationale, Design and Methods of New Studies: Manuscripts in this category should provide information regarding the grants awarded by different founding agencies, e.g. National Health Institute, European Union, National Science Center or National Center for Research and Development. The manuscript should be presented in the format of Research Project Objectives, Research Plan and Basic Concept, Research Methodology, Measurable Effects and Expected Results. The article should also contain general information about the grant: grant title, keywords (up to five), name of the principal investigator and co-investigators, founding source with the grant number, *Ethical Committee permission number*, code in clinical trials (if applicable). Only grant projects in the amount over 100,000 Euro can be presented. Manuscripts should be up to 2000 words in length (excluding references) and can include up to 5 tables and/or figures. The abstract should not exceed 150 words. The number of authors is limited to the Principal Investigator and Co-investigators.

Acknowledgements

Under acknowledgements please specify contributors to the article other than the authors accredited. List here those individuals who provided help during the research (e.g., providing language help, writing assistance or proof reading the article, etc.). Also acknowledge all sources of support (grants from government agencies, private foundations, etc.). The names of funding organizations should be written in full.

References

All manuscripts should use the 'Vancouver' style for references. References should be numbered consecutively in the order in which they appear in the text **and listed at the end of the paper.** References cited only in Figures/Tables should be listed in the end. Reference citations in the text should be identified by Arabic numbers in square brackets. Some examples:

This result was later contradicted by Smith and Murray [3].

Smith [8] has argued that...

Multiple clinical trials [4–6, 9] show...

List all authors if there are six or fewer; if there are seven or more, list first six followed by "et al.". Journal names should be abbreviated according to Index Medicus.

Some examples

Standard journal articles

1. Fassone E, Rahman S. Complex I deficiency: clinical features, biochemistry and molecular genetics. *J Med Genet.* 2012 Sep;49(9):578–590.
2. Pugh TJ, Morozova O, Attiyeh EF, Asgharzadeh S, Wei JS, Auclair D et al. The genetic landscape of high-risk neuroblastoma. *Nat Genet.* 2013 Mar;45(3):279–284.

Books

Personal author(s)

1. Rang HP, Dale MM, Ritter JM, Moore PK. *Pharmacology.* 5th ed. Edinburgh: Churchill Livingstone; 2003.

Editor(s) or compiler(s) as authors

2. Beers MH, Porter RS, Jones TV, Kaplan JL, Berkwitz M (editors). *The Merck manual of diagnosis and therapy.* 18th ed. Whitehouse Station (NJ): Merck Research Laboratories; 2006.

Chapter in the book

1. Phillips SJ, Whisnant JP. Hypertension and stroke. In: Laragh JH, Brenner BM, editors. *Hypertension: pathophysiology, diagnosis, and management.* 2nd ed. New York: Raven Press; 1995. p. 465–478.

TABLES: Tables should be typed on sheets separate from the text (each table on a separate sheet). They should be numbered consecutively with Arabic numerals. Tables should always be cited in text (e.g. table 2) in consecutive numerical order. Each table should include a compulsory, concise explanatory title and an explanatory legend. Footnotes to tables should be typed below the table body and referred to by superscript lowercase letters. No vertical rules should be used. Tables should not duplicate results presented elsewhere in the manuscript (e.g. in figures).

FIGURES: All illustrations, graphs, drawings, or photographs are referred to as figures and must be uploaded as separate files when submitting a manuscript. Figures should be numbered in sequence with Arabic numerals. They should always be cited in text (e.g. figure 3) in consecutive numerical order. Figures for publication must only be submitted in high-resolution TIFF or EPS format (*minimum 300 dpi resolution*). Each figure should be self-explanatory without reference to the text and have a concise but descriptive legend. All symbols and abbreviations used in the figure must be defined, unless they are common abbreviations or have already been defined in the text. Figure Legends must be included after the reference section of the Main Text.

Color figures: Figures and photographs will be reproduced in full colour in the online edition of the journal. In the paper edition, all figures and photographs will be reproduced as black-and-white.

SUPPLEMENTARY ONLINE MATERIAL: Authors may submit supplementary material for their articles to be posted in the electronic version of the journal. To be accepted for posting, supplementary materials must be essential to the scientific integrity and excellence of the paper. The supplementary material is subject to the same editorial standards and peer-review procedures as the print publication.

Review Process

All manuscripts are reviewed by the Editor-in-Chief or one of the members of the Editorial Board, who may decide to reject the paper or send it for external peer review. Manuscripts accepted for peer review will be blind reviewed by at least two experts in the field. After peer review, the Editor-in-Chief will study the paper together with reviewer comments to make one of the following decisions: accept, accept pending minor revision, accept pending major revision, or reject. Authors will receive comments on the manuscript regardless of the decision. In the event that a manuscript is accepted pending revision, the author will be responsible for completing the revision within 60 days.

Copyright

The copyright to the submitted manuscript is held by the Author, who grants the Journal of Medical Science (JMS) a nonexclusive licence to use, reproduce, and distribute the work, including for commercial purposes.